1072

~~Gift~~
~~ROD~~
report file
subject — connections
— bracing, bldg

GUSSET PLATE DESIGN UTILIZING BLOCK-SHEAR CONCEPTS

by

Steve G. Hardash
Reidar Bjorhovde — author

The Department of Civil Engineering
and Engineering Mechanics
THE UNIVERSITY OF ARIZONA
Tucson, Arizona 85721

August 1984

GUSSET PLATE DESIGN UTILIZING

BLOCK-SHEAR CONCEPTS

by

Steve G. Hardash

and

Reidar Bjorhovde

Department of Civil Engineering
and Engineering Mechanics
THE UNIVERSITY OF ARIZONA
Tucson, Arizona 85721

August 1984

ACKNOWLEDGMENTS

This report was funded by a grant from the American Institute of Steel Construction, for which the authors are sincerely appreciative. Also, the interaction with Dr. R. M. Richard is appreciated.

Special thanks are due Messrs. Mun-Foo Leong and A. E. Moussa for the laboratory assistance, and to our shop personnel, Messrs. W. D. Lichtenwalter and L. Lujan, for their skills rendered.

TABLE OF CONTENTS

TABLE OF CONTENTS -- Continued

LIST OF ILLUSTRATIONS

LIST OF ILLUSTRATIONS -- Continued

LIST OF ILLUSTRATIONS -- Continued

LIST OF TABLES

ABSTRACT

The prime object of this study is to develop an ultimate strength design procedure for gusset plates loaded in tension. Twenty-eight gusset plates, reflecting different strength parameters, were tested to failure, and the results are presented in this study.

Utilizing the results from these tests along with the results from previous ultimate strength tests, a block-shear model incorporating tensile ultimate stress on the net area between the last row of bolts and an effective uniform shear stress on the gross area along the outside bolt lines is shown to be the most realistic ultimate strength model. The effective uniform shear stress is shown to be a linear function of the total connection length.

A value for the resistance factor, ϕ, of 0.85 is determined using the proposed strength model. Design curves for A36 steel are presented, along with a sample gusset plate design problem.

CHAPTER 1

INTRODUCTION

Gusset plates are common fastening elements used in fabricated steel structures such as trusses or braced-frame structures. In the latter case, their primary purpose is to transfer either tensile or compressive loads from a bracing member to a beam and column joint.

Current gusset plate design is based primarily on elastic analyses for determining critical sections and stresses. No known failures or adverse behavior have been noted, but substantial differences in the factor of safety against ultimate load exist because of the assumptions involved [1]. It is therefore important to develop an improved design method, with the goal of providing economy of design by means of a consistent factor of safety.

The ultimate strength approach would fulfill this requirement for a consistent design and analysis method. To date, a few experimental studies have been conducted to determine the behavior and ultimate strength of gusset plate connections. However, additional tests are needed to develop a design method based on ultimate strength behavior.

With the above in mind, a series of gusset plate tests were conducted at the University of Arizona. The results of these and previous ultimate strength tests are presented in this study, from which a practical design method is developed.

CHAPTER 2

SCOPE OF INVESTIGATION

The development of a design and analysis procedure for gusset plates, based on ultimate strength, will be accomplished by the following:

1. Test to failure in tension 28 simple gusset plate models, to determine failure modes and ultimate loads. Each plate will reflect different strength parameters, consisting of gage between lines of bolts, edge distance to first bolt, bolt pitch in bolt lines, and number of bolts in a line.
2. Propose various block-shear models and compare the theoretical results to the actual ultimate loads for the tests conducted in this study and previous studies. Select the block-shear model, with modifications if necessary, that most accurately predicts the ultimate strength of the tested gusset plates.
3. Develop a design and analysis procedure for tensile gusset plate connections, based on the Load and Resistance Factor Design (LRFD) format.

The behavior of gusset plate connections is very complex. However, considering the behavior of these connections at ultimate load will assist in the development of a design procedure which incorporates elastic as well as ultimate strength considerations.

CHAPTER 3

PREVIOUS STUDIES

Plate connections have been an area of research since 1837. At that time, riveted flat-plate joints, such as those used in tanks and boilers, were considered.

Since the late 1800's, long span structures have been common, and these incorporated truss-type members; hence, truss-type plate connections became an important topic of study up to the mid 1960's. The first detailed studies of gusset plate behavior only considered elastic response, and these will be described briefly.

One of the first significant elastic experimental analyses was conducted by Whitmore on a Warren truss joint [2]. Analyses showed that the maximum tensile and compressive stresses were located in a region of the plate at the ends of the tension and compression diagonals, respectively. It was determined that the "effective width", found by drawing 30° lines from the first line of rivets to intersect the line through the row of rivets at the end of the connected member, as shown in Figure 3.1, could be used to define the section subjected to maximum normal stress.

Irvan [3] and Hardin [4] studied the elastic behavior of truss joints and found that the area of large tensile stress in the gusset plates was also found in a region near the end of the tension diagonal.

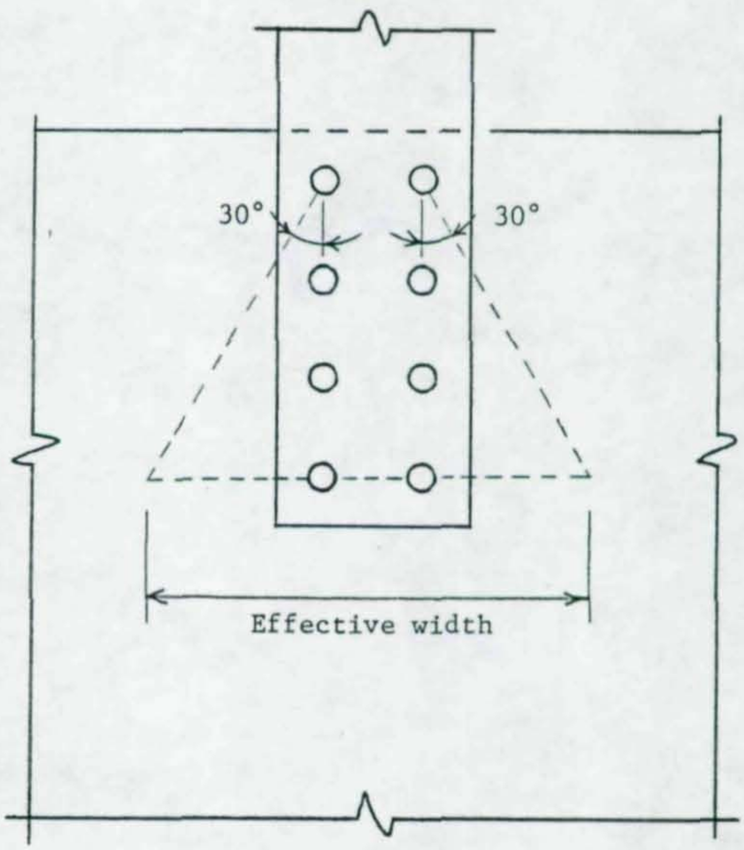

Figure 3.1 Whitmore Criterion for Determining Effective Width

Birkemoe, Eubanks, and Munse [5] conducted analytical and experimental work on simple steel gusset plates, and Figure 3.2 shows the details of the gusset plates used in the study. It was found that removing material from the corners caused little change in the results until the net cross-sectional area across the last bolt was reduced. Also, it was observed that a very large transverse stress developed at the free edge of the line of bolts which tends to split the plate apart along the line of fasteners.

In tests of steel gusset plates, Vasarhelyi [6] observed that the maximum stresses determined by the various elastic methods were only slightly different; the major difference was in the locations of these maxima.

There have been relatively few ultimate strength tests of gusset plate connections. The probable reason is that behavior beyond the elastic range was beyond the scope of analyses before the advent of finite element techniques. Chesson and Munse [7] conducted ultimate strength tests of 16 large truss-type connections. Only one of these failed at the gusset, which exhibited tearing across and on the outer lines of bolts. Further work by the same investigators [8] provided ultimate strength data for 30 truss-type tensile connections. In this study, ten (10) connections failed by tearing in the vicinity of the bolted or riveted connection to the gusset plate.

More recently, tests were conducted at the University of Alberta [9] to determine the ultimate strength of gusset plates

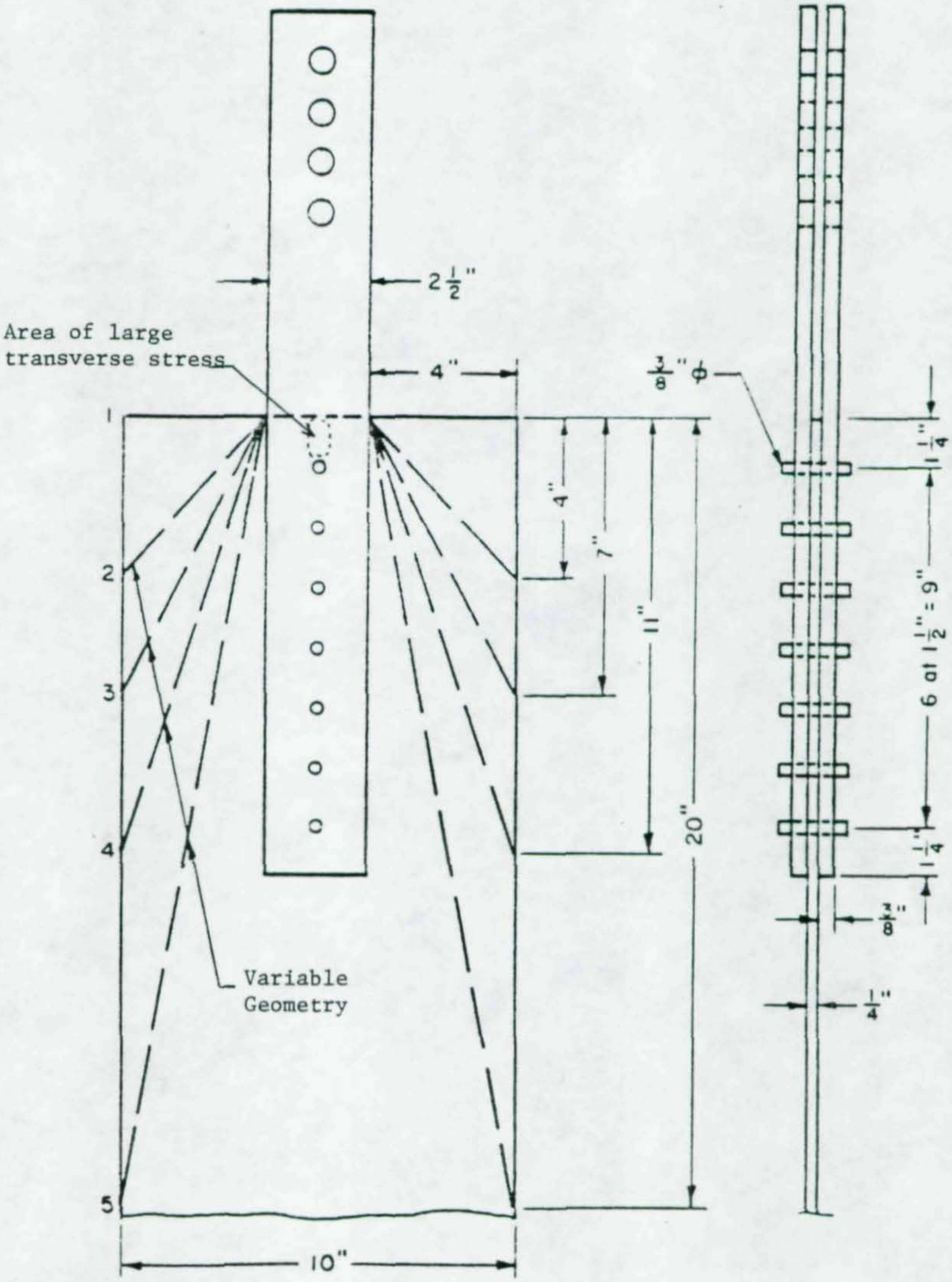

Figure 3.2 Gusset Plate Detail [5]

utilized in diagonal bracing connections. The three gusset plates that were tested to failure were full-size; tearing was observed across the last row of bolts and also in boundary connections, along with plate buckling. Among other things, this work demonstrated the importance of the type and size of the connection between the gusset plate and the other members in the joint, as well as the influence of secondary deformations.

Non-linear finite element analyses of gusset plate behavior have been conducted in recent years [10, 11]. The results confirm that the locations of maximum normal stresses are located in a region near the end of the gusset plate connection.

CHAPTER 4

THE BLOCK-SHEAR CONCEPT

In 1976, the Research Council on Riveted and Bolted Structural Joints increased the allowable bearing stress in high-strength bolted joints from $1.35F_y$ to $1.5F_u$ [12], where F_y and F_u are the yield and ultimate tensile stresses of the material in the connected parts, respectively. This was a radical alteration that prompted significant changes in the connection design and detailing practices that had been used previously. For example for ASTM A36, the most commonly used grade of steel for construction purposes, the increase in the bearing stress amounted to approximately 80 percent (from 48.6 ksi to 87.0 ksi).

Around the time when the changes in the bearing stress criteria were being implemented, research was being conducted at the University of Toronto on the shear force capacity of coped beam webs. This work had been undertaken in order to verify the shear design criteria of the new Canadian limit states design code [13]. The research involved a series of full-scale tests on uncoped and coped double-angle beam-to-column connections, loaded in as close to pure shear conditions as possible [14]. Beam action therefore did not enter into the overall behavior of the connection.

It was discovered that the coped web failed in a mode that involved a combination of a horizontal splitting of the beam web at the lower bolt hole, along with an elongation of all bolt holes in the direction parallel to the applied shear force. This produced a shearing out of a block of the web, as illustrated in Figure 4.1, leading to the development of the concept of a block-shear ultimate strength model. In the block-shear model, the strength is developed by the shear resistance of the web along line 1-1 (see Figure 4.1), in addition to the tensile resistance of the web along line 2-2.

As a result of the above studies, the AISC Specification [12] incorporated design criteria for connections that aimed at covering the block-shear problem. The allowable strength is thus given by Equation 4.1 as:

$$R_a \leq 0.30\, A_v F_u + 0.50\, A_t F_u \qquad (4.1)$$

where:

R_a = Allowable resistance to block-shear, kips

A_v = Net shear area along line 1-1, in.^{2}

A_t = Net tension area along line 2-2, in.^{2}

F_u = Specified minimum tensile strength, ksi.

This equation is based on a factor of safety against tension failure of 2.0 (hence, 0.5 F_u), and against shear failure of approximately 2.0. It is implied that the ultimate shear stress is related to the ultimate tensile stress as 0.6 F_u.

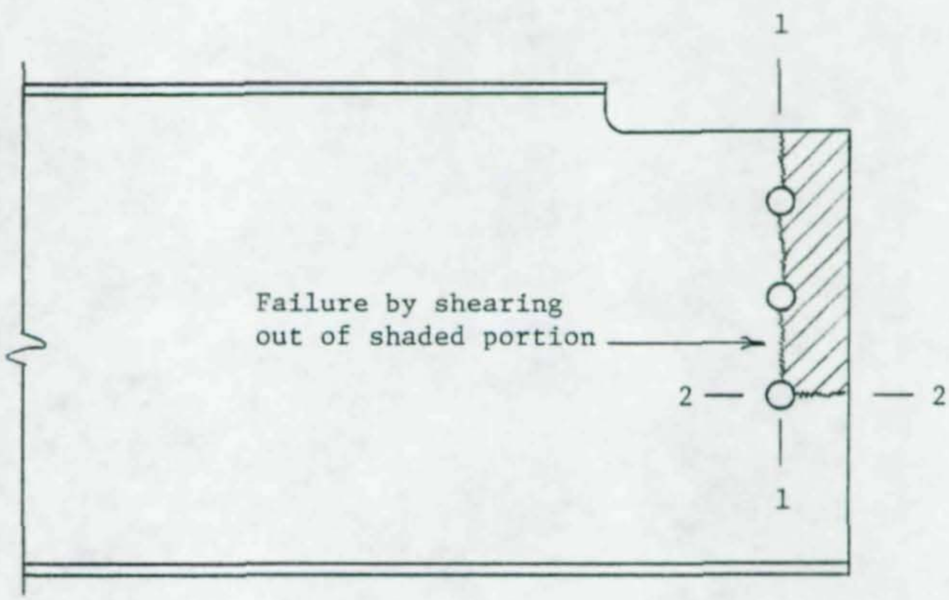

Figure 4.1 Block-Shear Model of Failure for a Coped Beam Web

Further testing of coped beam connections was conducted at the University of Texas at Austin [15]. Eight different coped beam connections were tested, and those that failed exhibited tensile fractures along line 2-2 of Figure 4.1. However, it was noted that the AISC equation given in Equation 4.1 overestimates the allowable capacity. Seven additional coped beam connections with two rows of bolts were then tested [16], and all of the connections failed in the block-shear mode. It was noted after testing that the vertical plane of the connection exhibited gross yielding, but no shear fracture. Also, from a linear finite element analysis it was found that the tensile stresses along the bottom row of bolts varied approximately linearly. A modified block-shear model was therefore proposed, and is illustrated in Figure 4.2. The block-shear capacity for double-row coped beam connections can be expressed by the following equation, based on the modified model:

$$R_f = 0.6F_y(A_v)_g + 0.50\ F_u(A_t)_n \qquad (4.2)$$

where:

R_f = ultimate block-shear capacity, kips

$(A_v)_g$ = gross shear area along line 1-1, in.^{2}

$(A_t)_n$ = net tension area along line 2-2, in.^{2}

F_y = static yield stress, ksi

F_u = static ultimate tensile stress, ksi

This equation has been found to predict the ultimate strength of the connections with an error of a few percent.

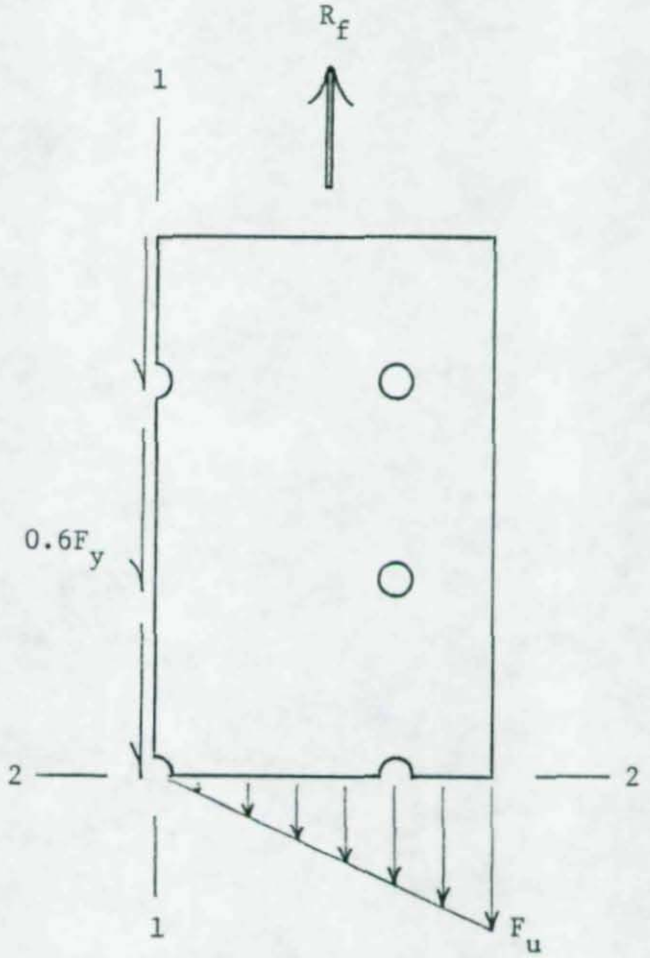

Figure 4.2 Modified Block-Shear Model of Failure for a Coped Beam Web

Based on the work with coped beam-to-column connections, the block-shear failure mode has been considered for application to gusset plates loaded in tension. One such suggestion was advanced by the AISC Commentary [12]; subsequent evaluations of full-size gusset plate tests [9, 17] suggested a model in which the ultimate shear resistance was developed along the outside line of bolts, and the ultimate tensile resistance was developed along the last row of bolts, as shown in Figure 4.3. The agreement between tests and theory was good; a maximum error of 7 percent was recorded.

Since this initial application of the block-shear concept to gusset plates only involved a diagonal bracing gusset plate, it would appear to be necessary to further modify the model to take into account various strength parameters, such as connection length, distance between outside bolt lines, plate thickness, bolt diameter, material yield strength, material ultimate strength, and plate geometry. If successful, this will make the model generally applicable to tension-loaded connections. This has been the basic premise of the study that is presented here.

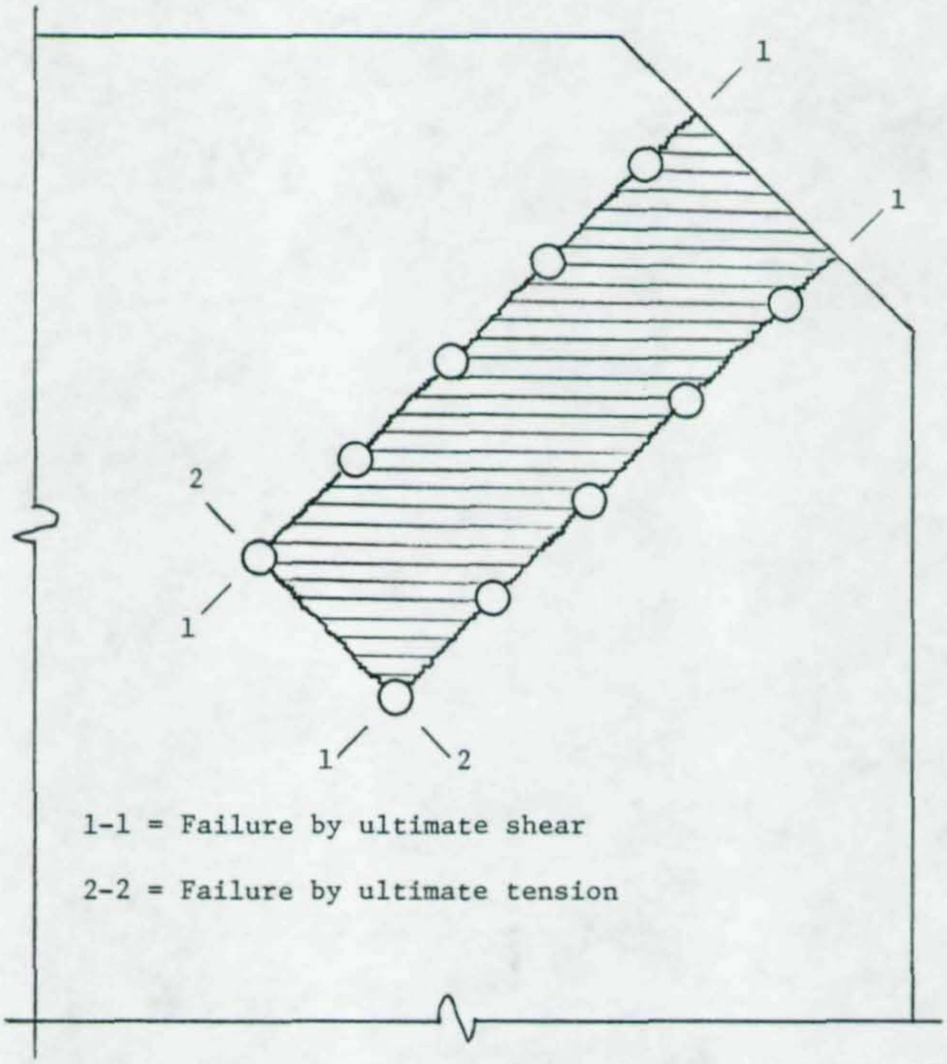

Figure 4.3 Proposed Block-Shear Model for Gusset Plates

0026

CHAPTER 5

DESCRIPTIONS OF TESTS

5.1 Design of Test Specimens

For the purpose of testing the application of the block-shear concept to gusset plate design, it was decided to test simple gusset plates loaded in tension by two lines of bolts. The intent was to isolate the tested joint in order to observe its behavior, and Figure 5.1 shows the general configuration of the gusset plate.

As indicated in the figure, the following were considered as the strength parameters which were to be varied in the specimens: 1) gage between lines of bolts, S; 2) edge distance, e; 3) bolt pitch, s; and 4) number of bolts. The total connection length, ℓ, depends on the edge distance and the total number of bolts in line.

A Tinius Olsen universal testing machine with a capacity of 200 kips was to be used in the testing program. With this limit on capacity, 1/4 inch nominal thickness A36 steel plate and 1/2 inch diameter A325 bolts were chosen for the test gusset plate connections. The preliminary design of the tested connection was based on: 1) the block-shear model for ultimate strength, and 2) allowable bolt shear. From these considerations, 28 test plates were designed, having a range of 2, 3, and 4 inches for S, 1 and 1-1/2 inches for e,

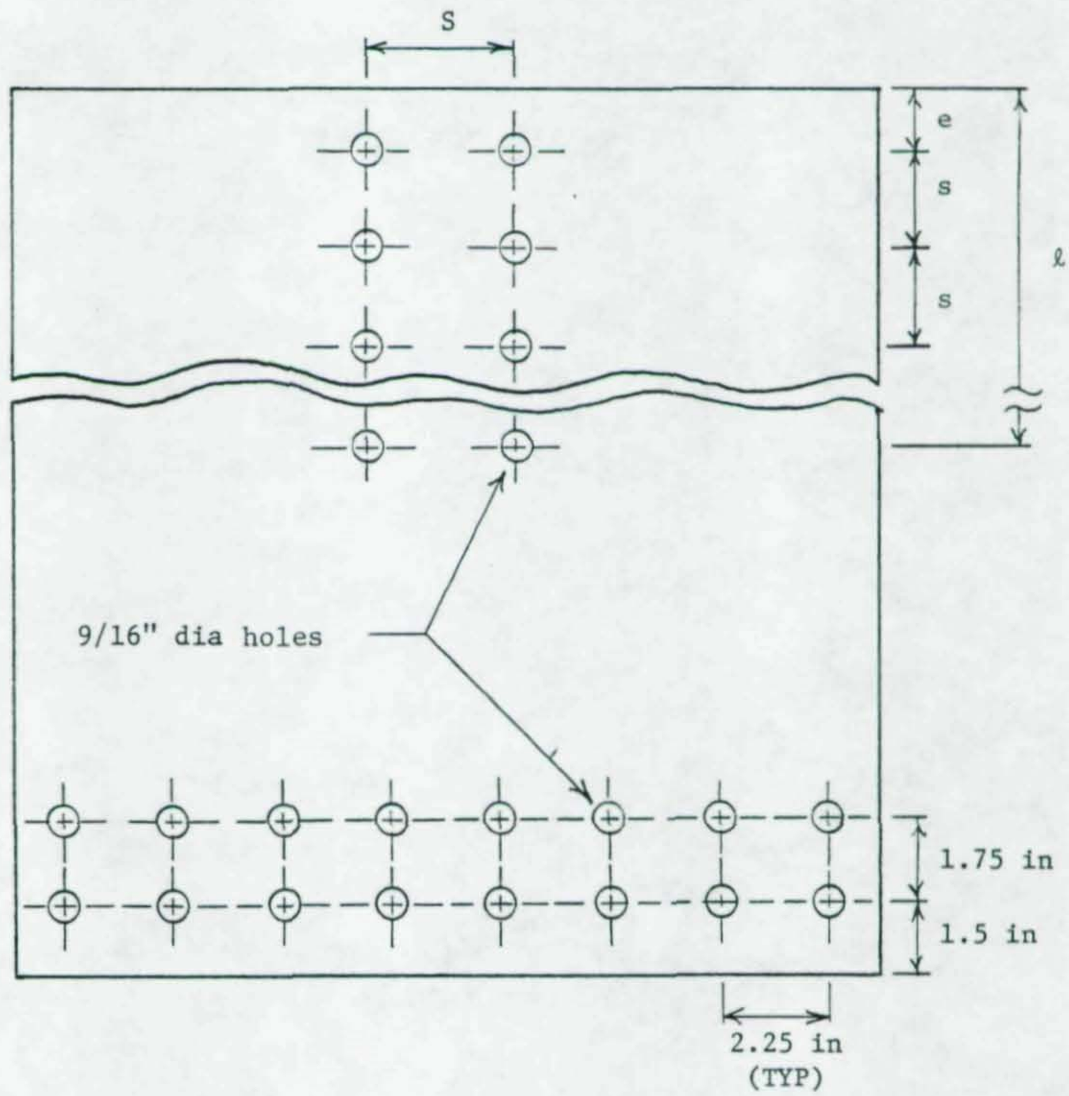

Figure 5.1 General Gusset Test Plate Configuration

and 1-1/2 and 2 inches for s. The total number of bolts in a line ranged from 2 to 5. Details of the various test connections are given in Table 5.1.

In order to fix the far end of the gusset plate, to obtain plates that would fail in the connection region, two rows of bolts with as many lines of bolts as were necessary to transfer the expected load were designed. The final gusset plate width was based on the minimum of $0.9F_u$ on the net area across the fixed base end, or $0.9F_y$ on the gross cross-sectional area. The gusset plate length was typically twice the tested connection length, plus the length necessary for the fixed base connection.

5.2 Description of Fabricated Test Specimens and Materials

Fabrication of the gusset plate test specimens and necessary splice plates and bearing assemblies was performed by the company Willis Steel of Tucson. The test plates were cut to size by shearing, and the holes were punched to a final diameter of 9/16 inch. Slight fabrication errors in test plates nos. 16, 20, and 26 required that the test connection holes be redrilled to a diameter of 11/16 inch (3/16 inch oversize).

All but one test plate were cut from the same steel plate. This one test plate, no. 18, was cut from a different steel plate because it was noticed, following the original shipment, that one test plate was missing; hence, it was fabricated separately. Dimensions and hole sizes for all the test plates are given in Appendix A.

Table 5.1 Test Connection Details for the Present Study

Test No.	Total No. of Bolts	S (in.)	e (in.)	s (in.)	ℓ (in.)
1	4	2.00	1.10	1.50	2.60
2	4		1.50		3.00
3	6		1.00		4.00
4			1.00	2.00	5.00
5			1.50	1.50	4.50
6			1.50	2.00	5.50
7		3.00	1.00	1.50	4.00
8			1.00	2.00	5.00
9			1.50	1.50	4.50
10			1.50	2.00	5.50
11		4.00	1.00	1.50	4.00
12		4.00	1.60		4.60
13	8	2.00	1.00		5.50
14			1.00	2.00	7.00
15			1.50	1.50	6.00
16			1.50	2.00	7.50
17		3.00	1.00	1.50	5.50
18			1.00	2.00	7.00
19			1.50	1.50	6.00
20			1.50	2.00	7.50
21		4.00	1.00	1.50	5.50
22			1.00	2.00	7.00
23			1.50	1.50	6.00
24			1.65	2.00	7.65
25	10	3.00	1.00	1.50	7.00
26			1.00	2.00	9.00
27			1.50	1.50	7.50
28			1.50	2.00	9.50

Tension test specimens were cut to full plate thickness from both steel plate materials, and were tested according to the procedures of ASTM A370 [18]. The central width of these test specimens was 0.50 inch and the gage length was 2.00 inches; the average thickness of test plates nos. 1 to 17 and nos. 19 to 28 was 0.237 inch, and the average thickness of test plate no. 18 was 0.253 inch. A 10,000 lb. capacity Instron universal testing machine was used for the tension tests, and since the results were very consistent, only three tension specimens were tested for the material in plates nos. 1 to 17 and 19 to 28, and two were tested for the material in plate no. 18.

The average mechanical properties for the material in plates nos. 1 to 17 and nos. 19 to 28 were as follows:

Yield stress, F_y = 33.2 ksi

Tensile strength, F_u = 46.9 ksi

Elongation in 2 inch gage length = 37 percent.

These properties correspond to A283, Grade A, mild structural steel [18]. For the material in plate no. 18, the average mechanical properties of the test specimen was as follows:

Yield stress (0.2% offset), F_y = 49.5 ksi

Tensile strength, F_u = 64.5 ksi

Elongation in 2 inch gage length = 27 percent.

These properties correspond to A611, Grade D, cold-rolled sheet structural steel [18].

5.3 Test Set-Up and Instrumentation

To insure accurate load measurements, the 200 kip capacity Tinius Olsen universal testing machine was calibrated with a registered load cell; it was found to be in agreement to within 0.6 percent throughout the entire loading range (0.4 kips maximum deviation).

The splice plates used to connect the gusset plate test specimens were designed to fit through the grip holes in the top and bottom testing machine crossheads. Since the minimum width of these grip holes was 4 inches, all splice plates were made 1-1/4 inches in thickness in order to develop the necessary capacity. The splice plates were secured to the testing machine by bolting a bearing assembly, consisting of a channel section with a plate welded across one end, to the splice plates once they had passed through the crossheads. All splice plates and bearing assemblies used for the testing program were of A36 steel and are shown in Figures 5.2 and 5.3. By drilling the test connection splice plates with multiple holes, it was possible to design only three different sets of plates to accommodate all the test specimens. The fixed end splice plates fit all the test plates and, therefore, remained in the testing machine for the duration of the testing program.

Prior to installing a gusset test plate into the test jig, the test plate was cleaned, and whitewash was applied to the surface not covered by the splice plates. The whitewash consisted of eight parts type S lime to one part table salt by dry proportion. Water was added until the mix acquired the consistency of paint.

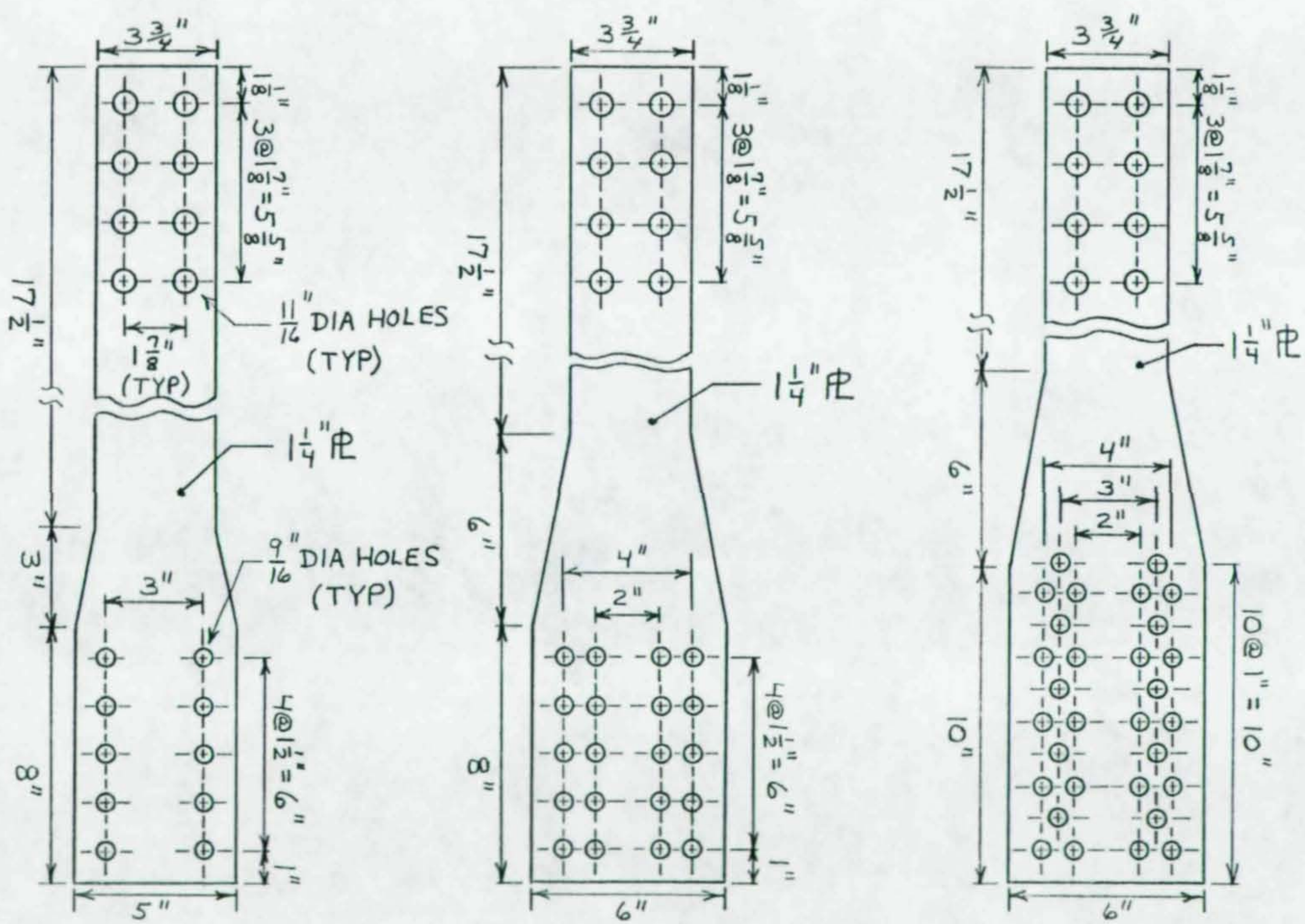

Figure 5.2 Fabrication Details for the Test Connection Splice Plates.

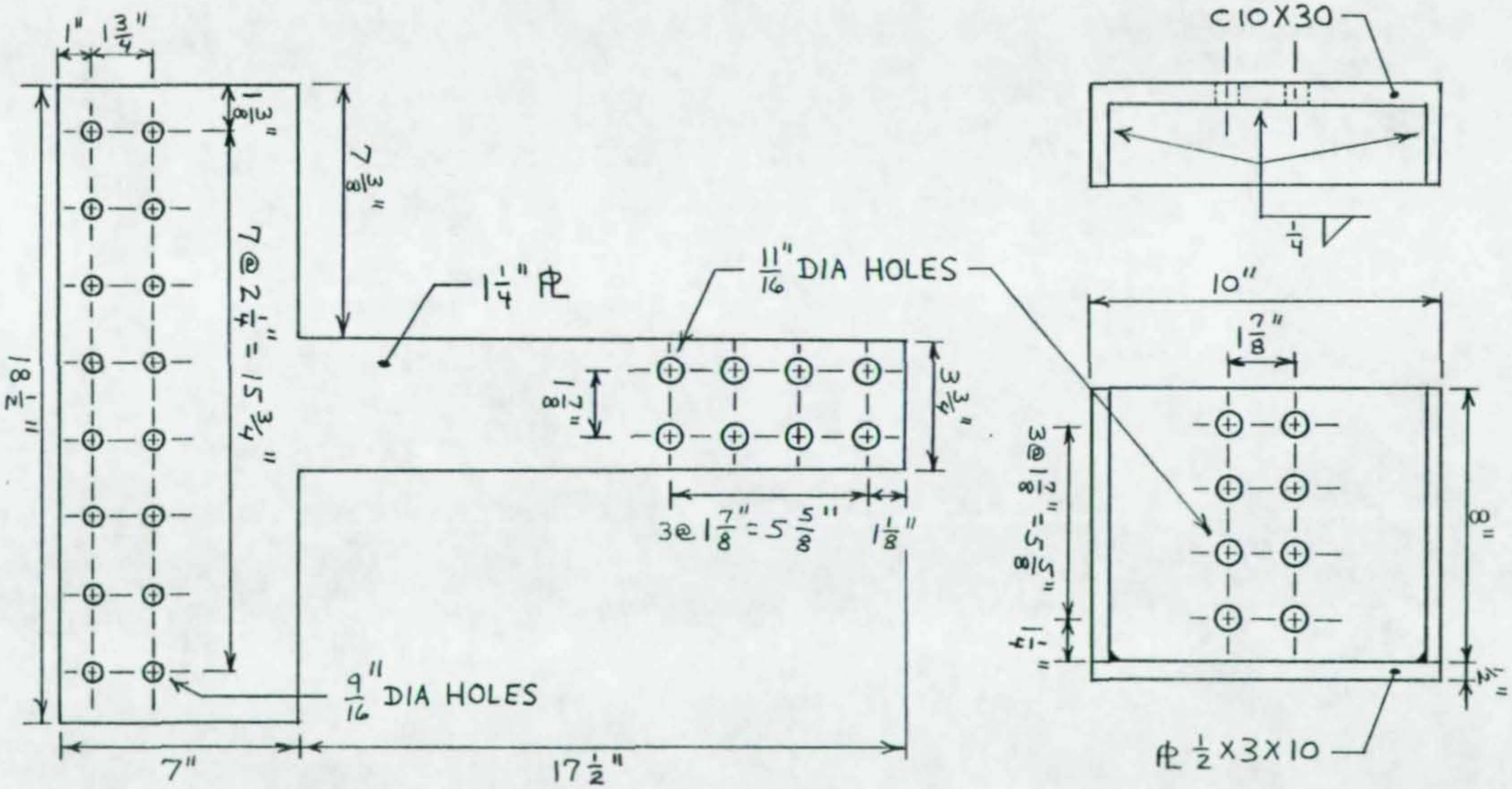

Figure 5.3 Fabrication Details for the Fixed End Splice Plates and Bearing Assemblies

The bolts that were used to fasten the test plate to the splice plates were 1/2 inch diameter A325 bolts of length 3-1/2 inches, and threads were excluded from all shear planes. The first shipment of these bolts which was received was galvanized. It was decided to use these bolts for test plates nos. 1 to 13, 15, 17, and 23, since research has shown that the behavior of a connection is not influenced if galvanized instead of ungalvanized bolts are used, provided that proper pretension is reached before bolt failure [1]. To reduce friction, the threads were lubricated with machine oil, and in many instances, it was possible to reuse the bolts once more before the threads began to gall.

The remainder of the plates were fastened using ungalvanized A325 bolts. It will be shown later that there is no distinguishable difference in the gusset plate results that can be attributed to the use of galvanized A325 bolts.

Both types of bolts were used without hardened washers, and the turn-of-the-nut method was used to give the necessary pretension. With a grip length of 2-3/4 inches, 1/2 turn of the nut from the finger tight position was consistently used for all test plate fastening bolts. The 5/8 inch SAE Grade 8 bolts that were used in the upper and lower bearing connections were finger tightened only; these bolts were used instead of the A490 grade, because the latter could not be obtained in the length desired.

In order to record the load-deformation characteristics of each plate, dial gages were used. Initially, for the first three test plates, bars were clamped at the top and bottom of the test connection, and dial gages with an accuracy of 0.0001 inch were then placed between the bottom testing machine crosshead and the bars, as depicted in Figure 5.4. It was reasoned that the connection deformation could be found by subtracting the deformation recorded by gage no. 2 from the deformation recorded by gage no. 1. However, it was found that the net deformation results were not consistent, due to probable rotation of the clamped bars. Therefore, test plates nos. 4 to 28 were tested using the instrumentation set-up shown in Figure 5.5. One dial gage with an accuracy of 0.001 inch was placed between the test machine crossheads. Although this set-up included any deformations occurring in the test plate, splice plates, and bearing connections, the major deformations would occur at the tested connection, and would be affected very little by the other sources of deformation. The final test set-up is shown schematically in Figure 5.6, and an actual photograph of an installed and instrumented gusset test plate is shown in Figure 5.7.

5.4 Test Procedure

In order to achieve consistency, each gusset plate was tested in the following manner. All bolts were installed in the test specimen under no load conditions. After all bolts were properly pretensioned, the test plate was preloaded to 10 kips, and then the load was reduced to 1 kip. At this point, the dial gage reading was recorded as zero. Load was then applied at a slow rate, while load and dial gage readings were taken at convenient intervals. The

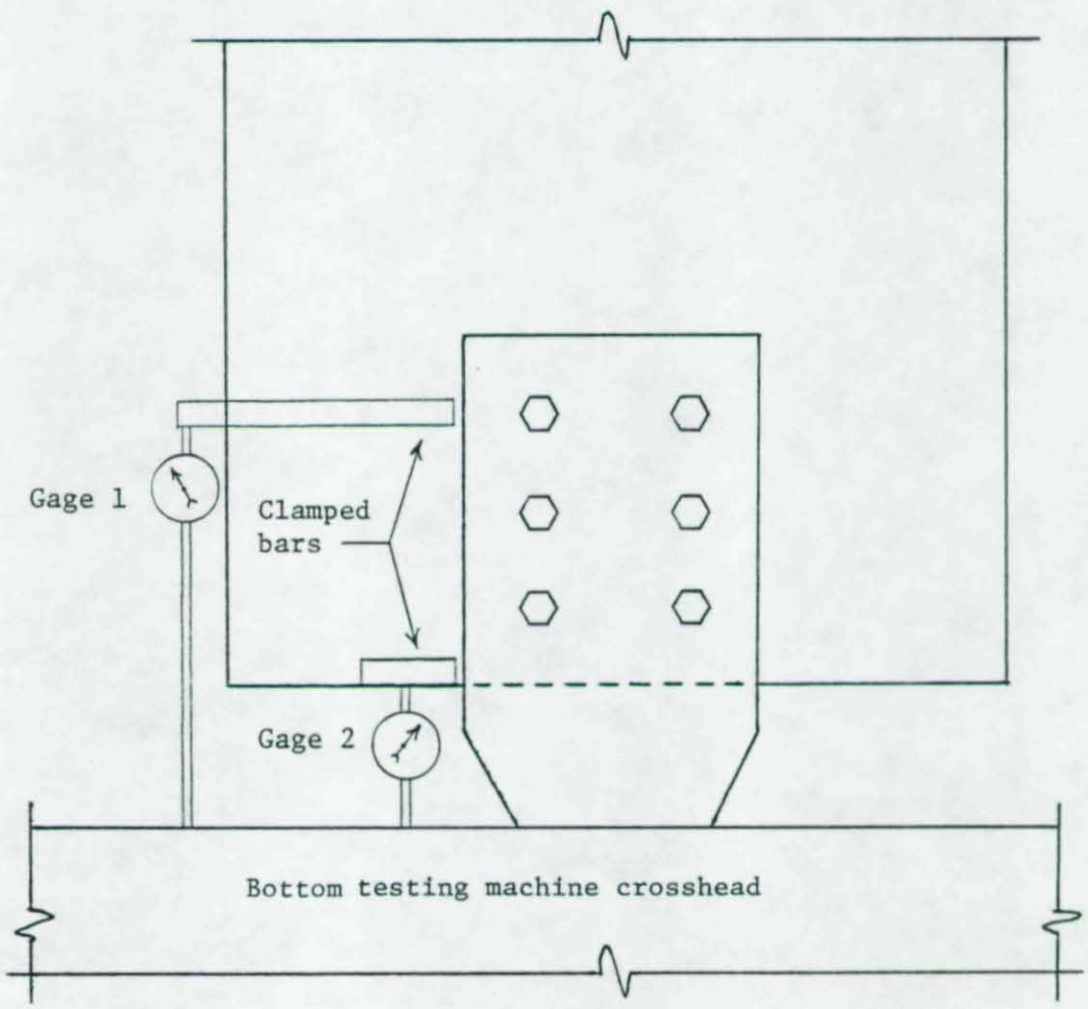

Figure 5.4 Instrumentation for Test Plates Nos. 1, 2, and 3

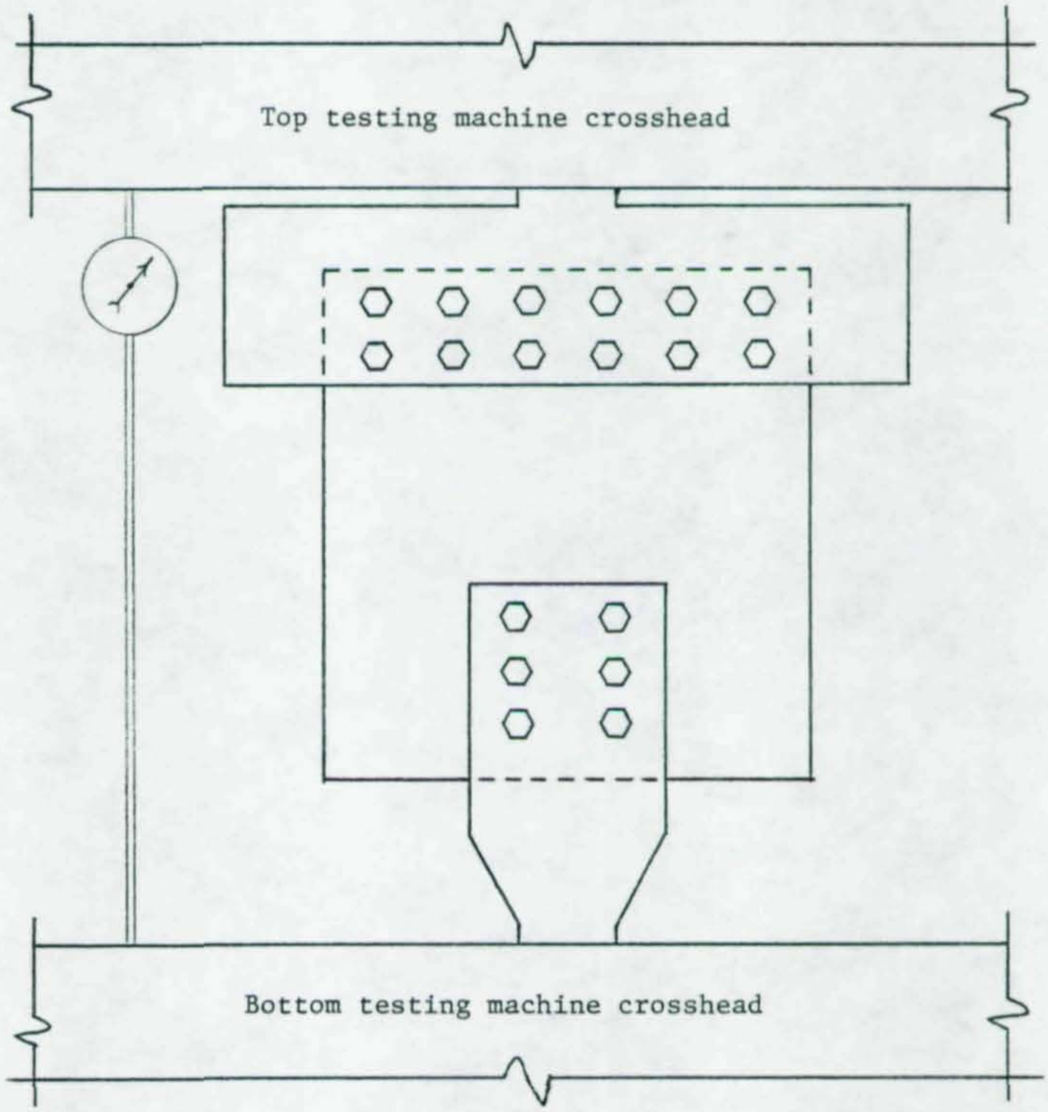

Figure 5.5 Instrumentation for Test Plates Nos. 4 to 28

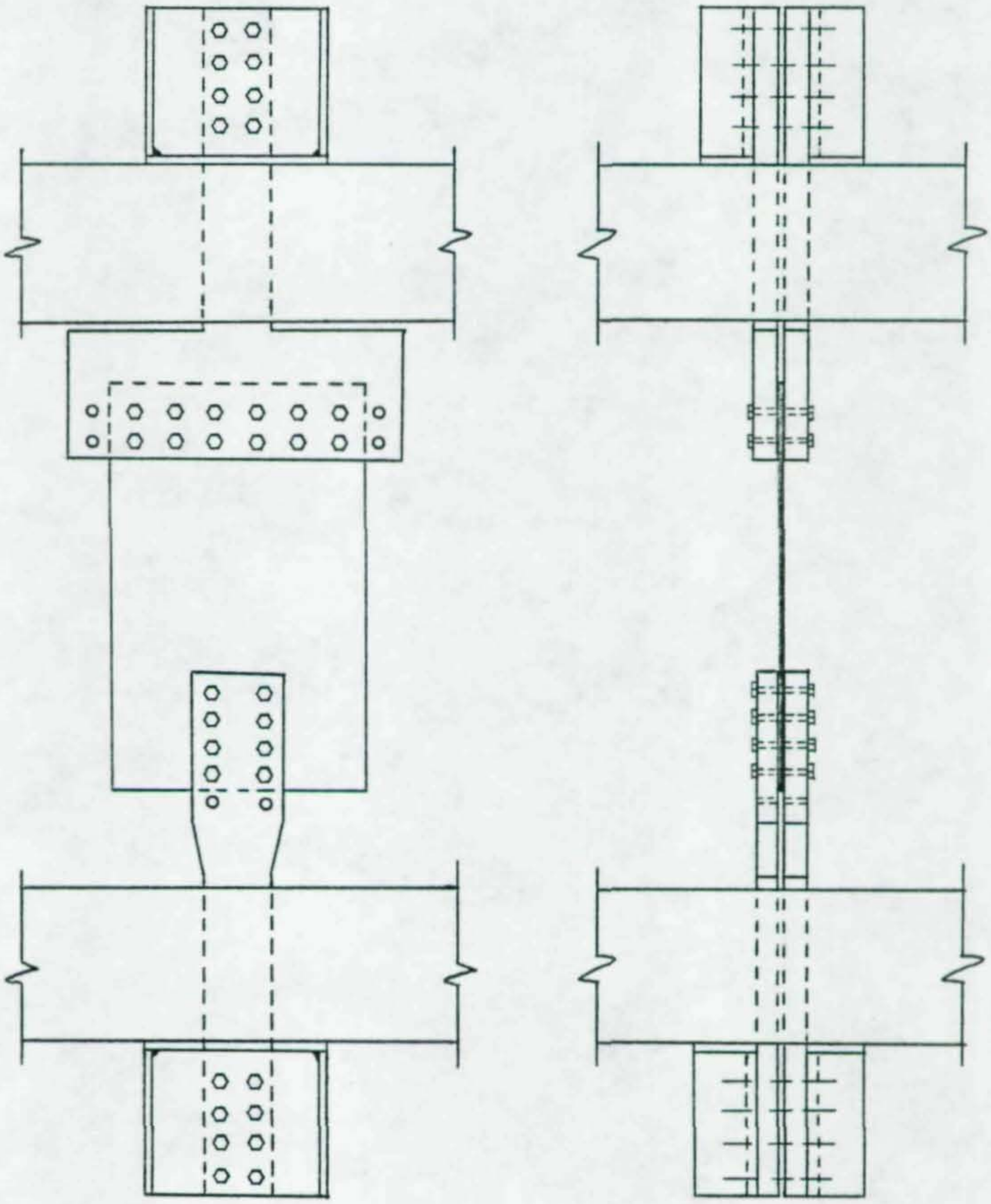

Figure 5.6 Front and Side View of a Typical Test Set-up

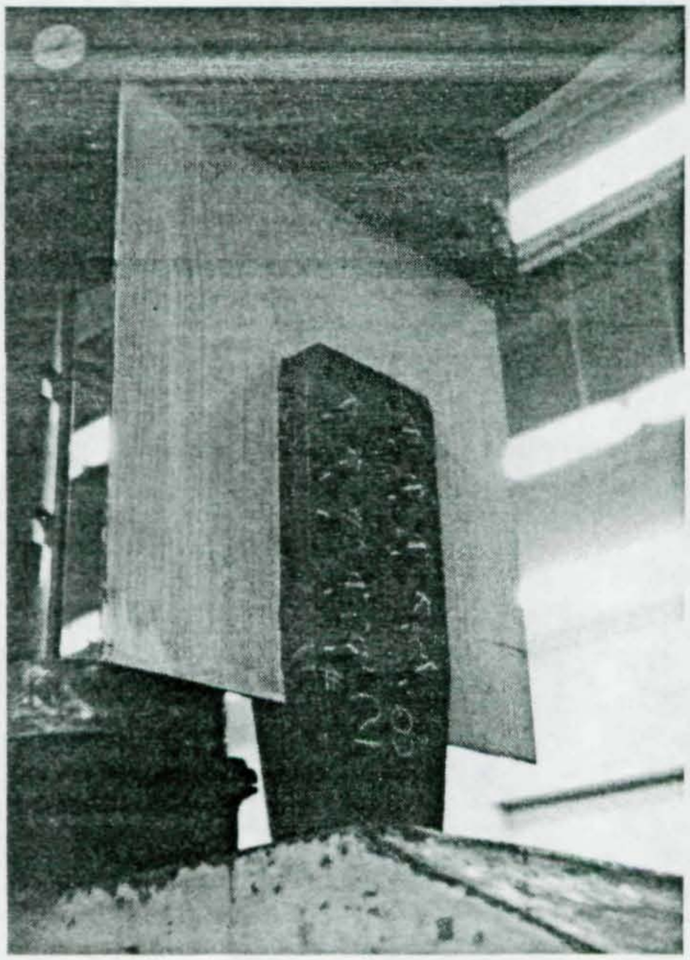

Figure 5.7 Test Set-up for Test Plate No. 28

testing machine did not have an actual machine crosshead separation indicator, but the speed control was kept at the same slow setting for all tests. By recording the time necessary for the machine crossheads to separate 1/10 inch at this speed control setting, it was found that the machine crosshead speed used was approximately 0.06 inch per minute. Loading was continued through the ultimate load; for most plates, loading was continued until a "second strength plateau" was reached, which will be described in more detail in Chapter 6. The gusset test plate was then unloaded completely and carefully removed from the splice plates to prevent scratching of the whitewash.

CHAPTER 6

TEST RESULTS

6.1 Results During Testing

The behavior of all the gusset plates during the testing was very similar. The load-deformation curves thus reflected the following general behavior: 1) slip took place during the elastic loading phase; 2) the plates exhibited a long yield plateau to ultimate load; and 3) the load subsequently dropped to a second strength plateau. As an example, the load-deformation curve that was constructed from the data recorded during the testing of plate no. 28 is shown in Figure 6.1. This curve is typical of the results for the gusset plate tests, as can be seen from the load-deformation data for all of the plates presented in Appendix A.

Out of the 28 gusset plates tested, 12 exhibited some slipping during the elastic loading portion of the load-deformation curve. As the load was steadily increased, a loud metallic click would signal that the tested connection was undergoing a slipping of the bolts into bearing. The load would drop momentarily, because of the elastic strain release occurring in the test set-up. For the test plates experiencing slips, anywhere from one to several occurrences would take place. Test plates nos. 20 and 26, which had oversize holes,

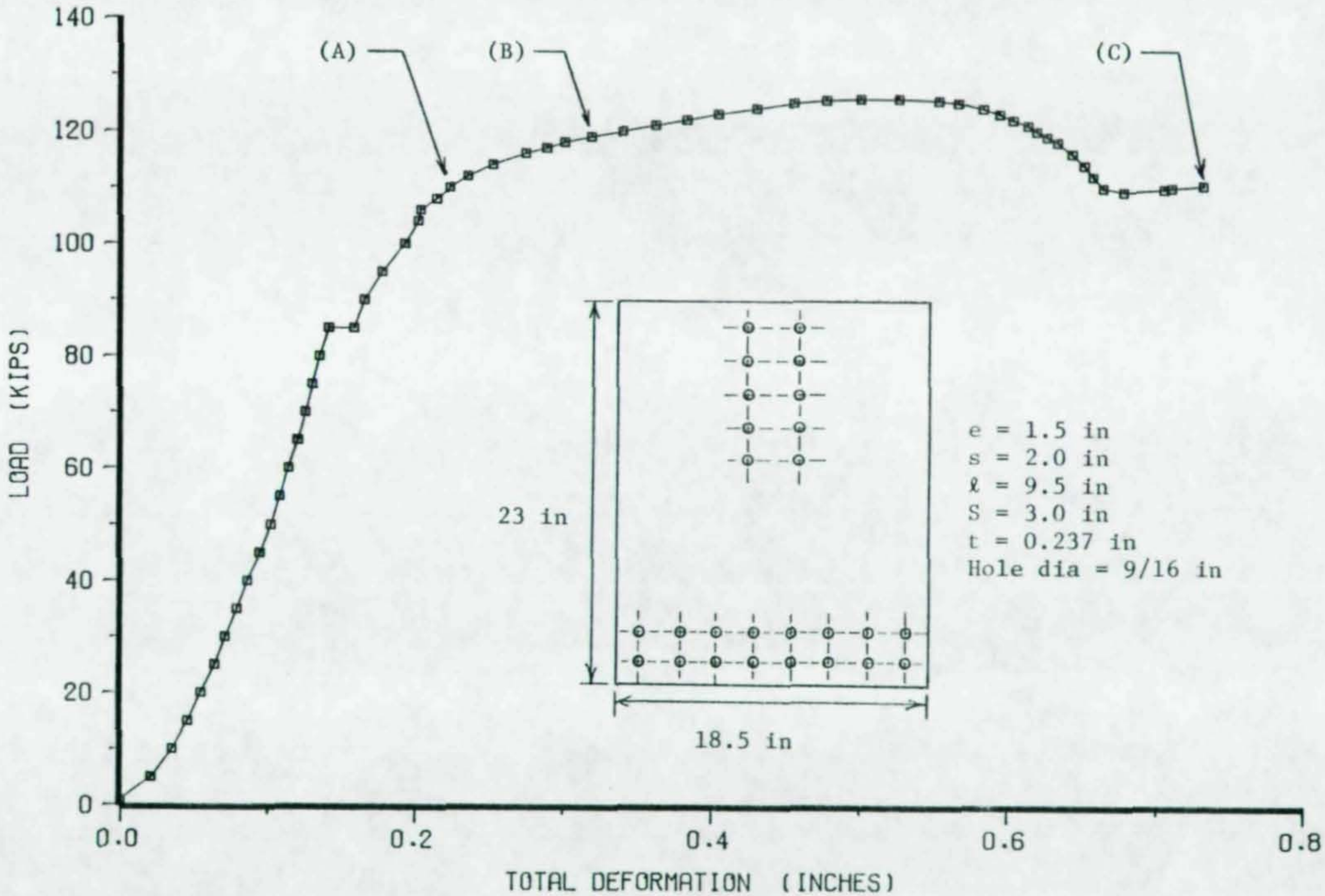

Figure 6.1 Load-Deformation Curve for Test Plate No. 28

experienced the most slip, with the total slip for plate no. 20 amounting to almost 0.2 inch.

As the loading progressed, the load-deformation curve would exhibit increasingly non-linear behavior as the plate material yielded in larger and larger areas. It was found that the occurrence of the first yield lines on the whitewashed plate accurately signaled the point where the change in slope appeared on the load-deformation curve. From Appendix A, it can be seen that test plates with longer tested connections had longer yield plateaus, with gradually increasing capacity through this plateau, reflected on these curves. Figure 6.2 illustrates the progression of the yield lines, which signals the locations of slip planes in the plate. Note that the whitewash shows the presence of yielding in the tension zone at the last row of bolts, and also around the immediate area of the tested connection. For some of the larger plates, compression yield lines at the sides of the plate became visible in the whitewash, as loading continued through the yield plateau. This was caused by shear lag effects, and points out that the material in the corners was not effectively used.

As the ultimate load was approached, the curve would flatten out, and then suddenly drop after the attainment of the ultimate (= peak of curve) strength. From an examination of the plate both during and after the testing, this sudden drop in the load was caused by a progressing tearing failure between the bolts in the last row. Ultimate failure loads for each of the test plates are presented in Table 7.2 of the next chapter.

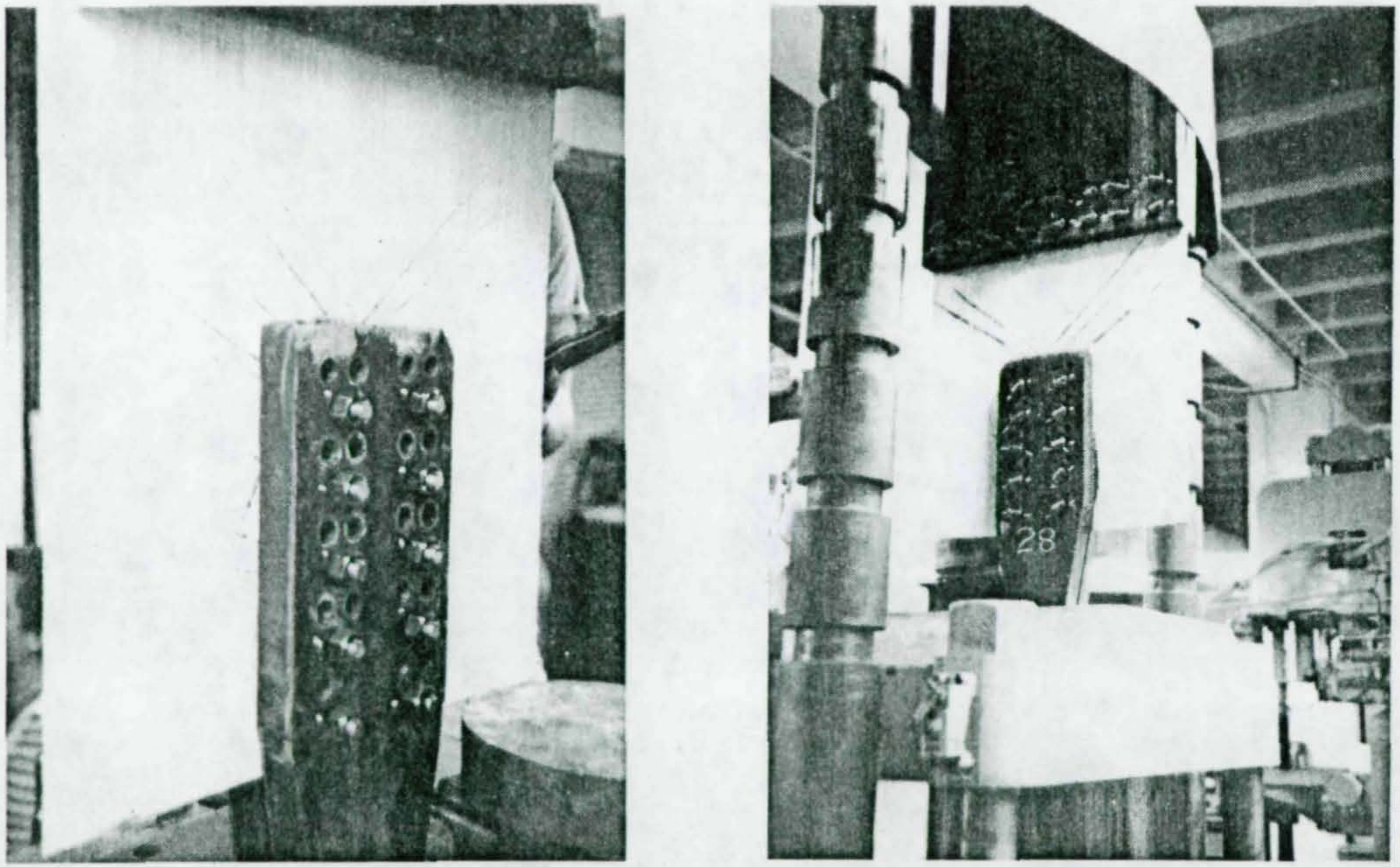

(a) Load = 110 kips (point A on curve of Fig. 6.1)

(b) Load = 119 kips (point B on curve of Fig. 6.1)

Figure 6.2 Growth of Yield Lines During Testing of Plate No. 28

For most plates, recording of the load-deformation data was continued until the load would stabilize at a second strength plateau. This plateau would be reached when the tension failure at the last row of bolts was complete. Once the ultimate strength of the test plate had been reached, its true maximum capacity had been attained, but the connection was still able to undergo deformation at a high percentage of ultimate capacity. Figure 6.3 shows test specimen no. 28 at the end of the loading cycle, illustrating the characteristics of the yield and tear failure zones.

6.2 Failure Modes for Test Specimens

As will be demonstrated, the gusset plate failure modes can be classified according to the type of steel (hot- or cold-rolled) the test plate was fabricated from. Appendix B shows the photographs that were taken of all plates at the end of the loading cycle, which for the majority of the plates was at the onset of the second strength plateau.

For the test specimens fabricated from A283, Grade A, mild (hot-rolled) structural steel (specimens nos. 1 to 17 and 19 to 28), the basic failure mode consisted of a tension failure across the last row of bolts along with an elongation of the bolt holes, as typically shown in Figures 6.3(b) and 6.4(a). None of the test specimens showed significant tearing along the lines of bolts in the direction of the applied load. Oversizing the connection holes (test plates nos. 16, 20, and 26) did not influence the failure mode for this type of steel.

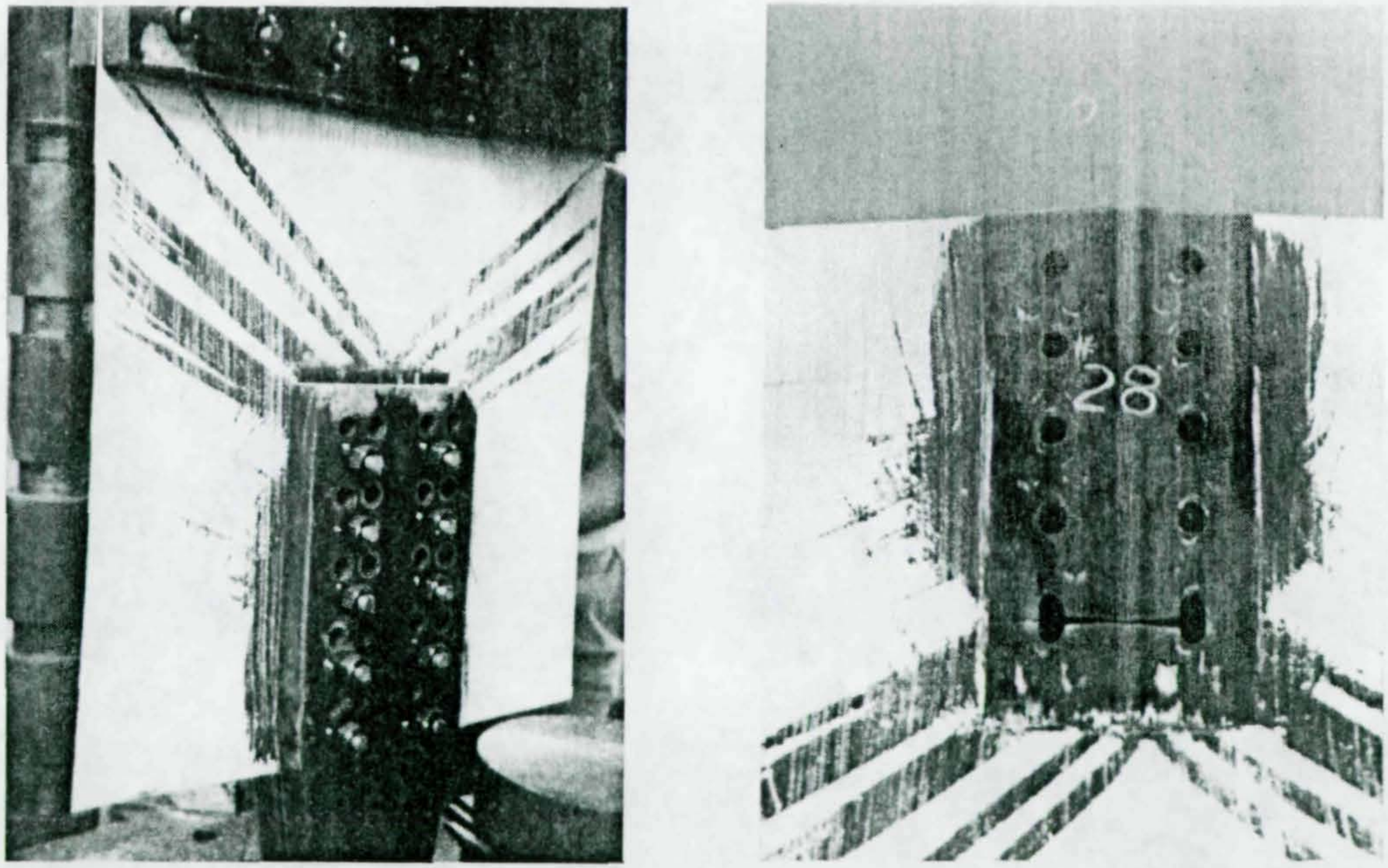

(a) Load = 110 kips (point C on curve of Fig. 6.1)

(b) Specimen removed from the test machine

Figure 6.3 Test Plate No. 28 at the End of the Loading Cycle

For test specimen no. 18, fabricated from A611, Grade D, cold-rolled sheet structural steel, the failure mode also included the tensile failure along the last row of bolts. However, along with the elongation of the bolt holes, the specimen also exhibited some tearing along the bolt lines, as seen in Figures 6.4(b) and 6.5. It was noticed during testing that after the ultimate strength was reached, a metallic ripping sound was heard and was repeated a couple of times with a significant drop in load. The total deformation for this test plate up to the ultimate load was similar to that of the plates which were fabricated from ductile steel, and since no yield lines developed in the whitewash, the deformation must have occurred exclusively in the connection region. This suggests that at the point of ultimate load, the ultimate tensile stress of the material was reached across the last bolt row. The deformations that occurred after the ultimate load was reached were sufficient to cause shear failure along the bolt lines.

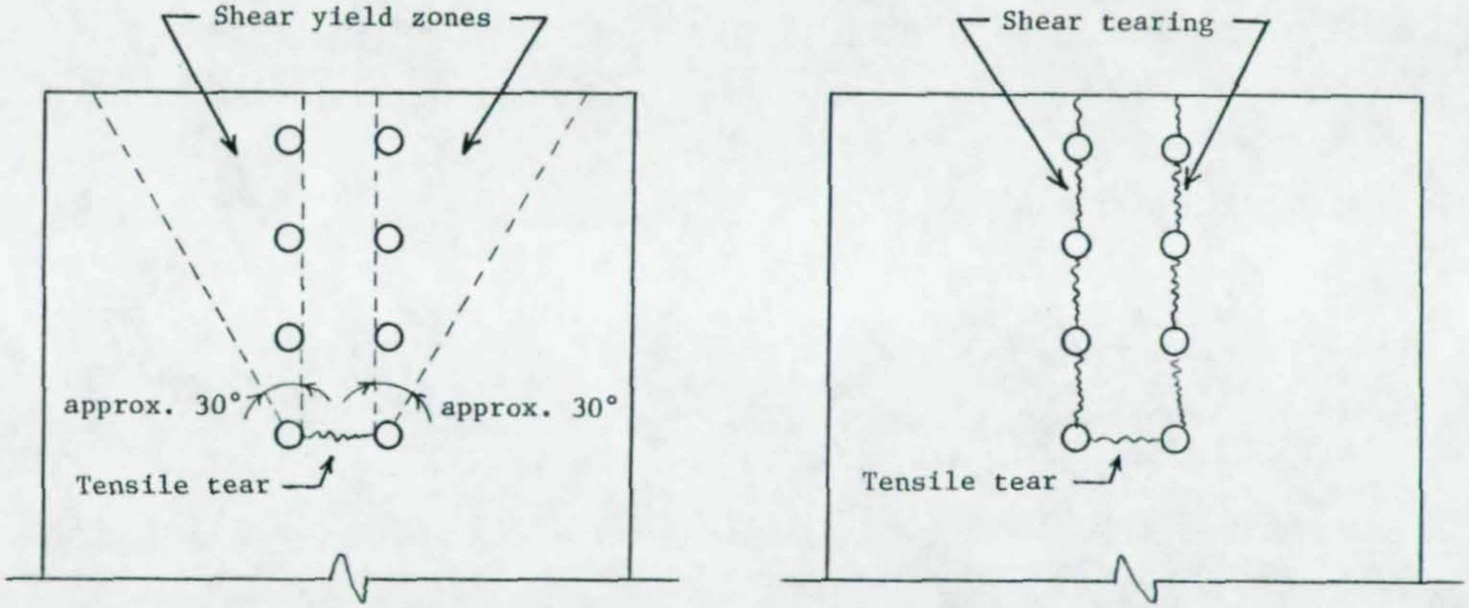

(a) Tensile failure with shear yielding (A283, Grade A steel)

(b) Tensile failure with shear tearing (A611, Grade D steel)

Figure 6.4 Two Basic Failure Modes for the Gusset Test Plates

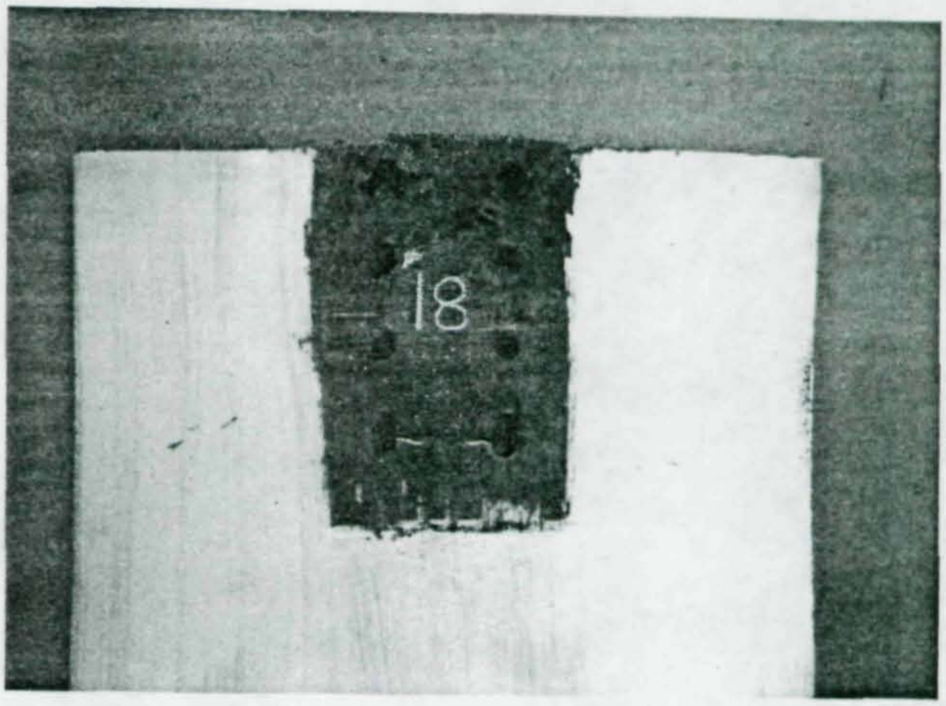

Figure 6.5 Test Plate No. 18 at the End of the Loading Cycle

CHAPTER 7

DEVELOPMENT OF A STRENGTH MODEL

7.1 Previous Test Results

As mentioned earlier, relatively few ultimate strength gusset plate tests have been conducted. In this study, the results of the tests conducted at the University of Illinois in Urbana and the University of Alberta in Edmonton, Alberta, Canada, will be incorporated, along with the results of the present testing program, to develop a suitable strength model for tensile gusset plate connections. This gives a total of 42 gusset plate tests with a fairly wide range of strength parameters that can be used to verify the proposed model.

In the 1958 University of Illinois study [7], only one truss-type connection, AD1, failed at the gusset; Figure 7.1 shows the connection details. During the testing, the rivets in the lower east gusset failed at a total load of 1155 kips. These rivets were replaced with ASTM A325 bolts and then tested to a final failure load of 1235 kips (617.5 kips per gusset). The failure mode for the east gusset is shown in Figure 7.2.

Additional tests were conducted at the University of Illinois in 1963 [8], which resulted in ten additional sets of data that reflected gusset plate failure. These tests incorporated riveted or

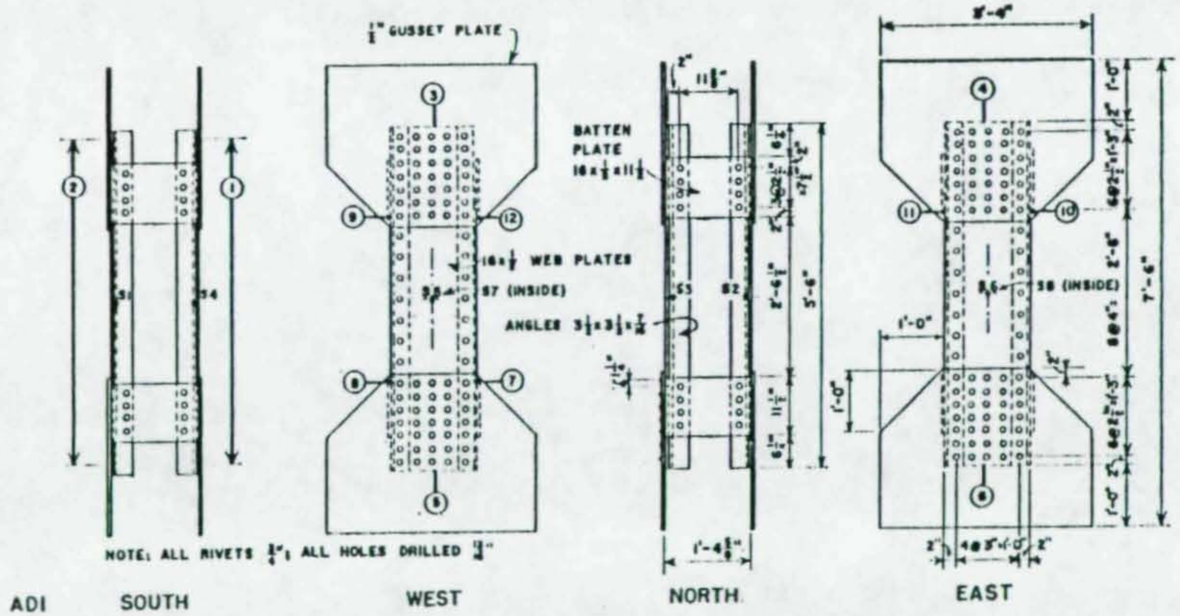

Figure 7.1 Fabrication Details for Test Connection AD1 [7]

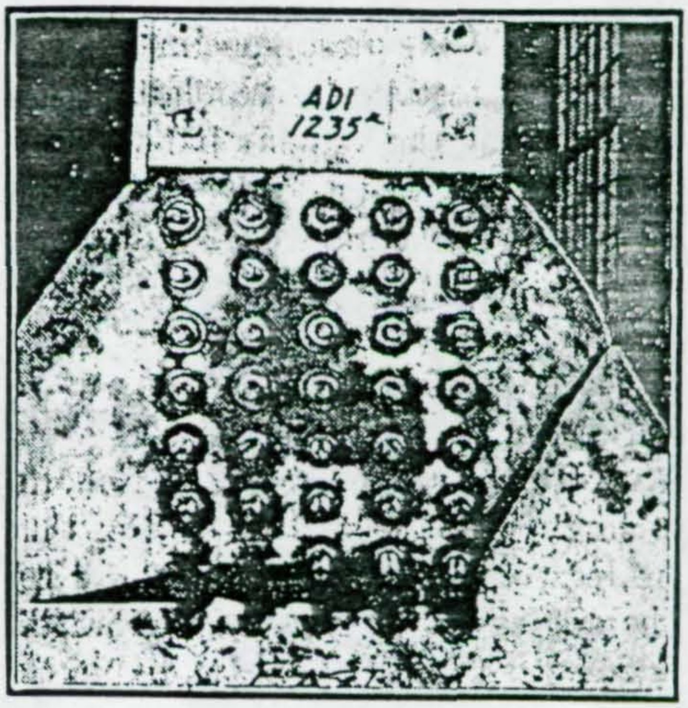

Figure 7.2 Failure Mode for Test Connection AD1 [7]

bolted joints, and the holes were punched or drilled. The influence of these parameters will be examined in the following. Connection details are given in Figure 7.3, and the failure modes for test specimens nos. SA-1-PB and A-1-DB [8] are given in Figure 7.4.

The University of Alberta study [9] yielded three failures of diagonal bracing connections. The general test set-up is shown in Figure 7.5, and gusset plate fabrication details are given in Figures 7.6 and 7.7. The failure mode common to all three gusset plates included tearing of the plate at the last row of bolts in the tension connection, in a direction perpendicular to the applied tensile loads. The 30° gusset (measured from the beam axis) exhibited some additional tearing along the first five bolts in one bolt line. Only the 60° gusset plate tore at the double angle connection that fastened the plate to the column, and at the inner corner of the weld between the plate and the beam.

The connection parameters for the previous tests are summarized in Table 7.1. It should be noted that the test specimens have been renumbered in this study, in order of increasing connection length.

7.2 Strength Model Parameters

The relationship between the ultimate (test) load and the observed failure mode must be considered in order to develop a strength model that accurately reflects the true behavior at ultimate strength. For a tensile gusset plate connection, it appears that the strength model must incorporate two terms: one reflecting the

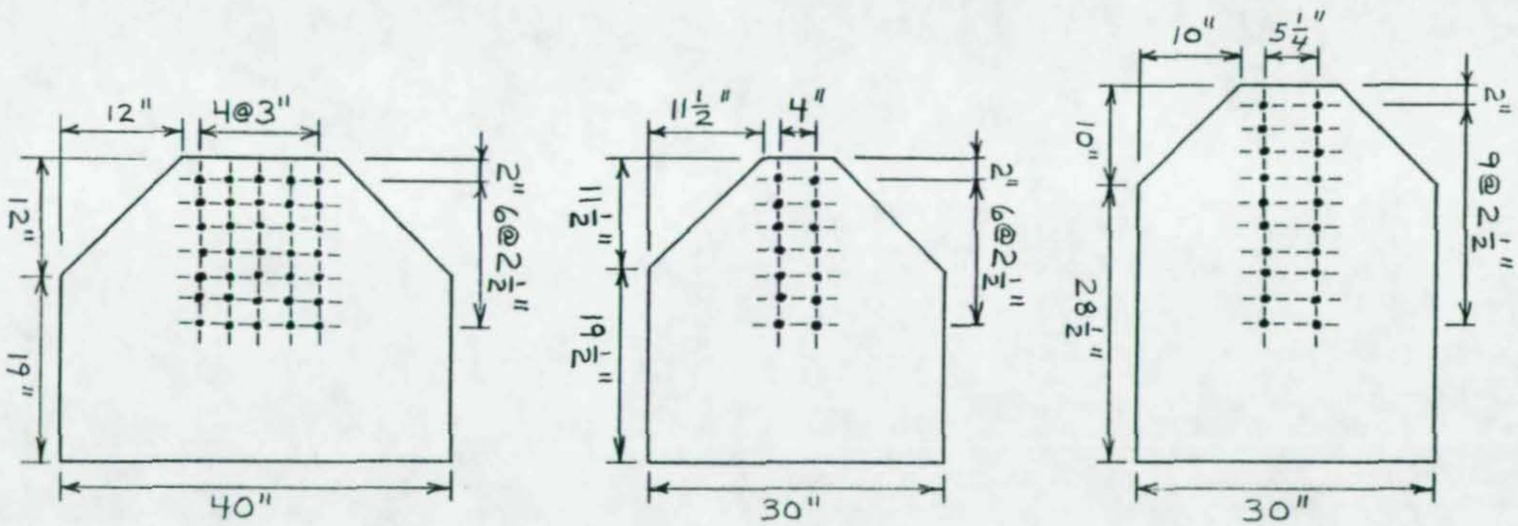

(a) Specimens type A (b) Specimens type SA (c) Specimens type SE

Figure 7.3 Fabrication Details for the Test Connection Gusset Plates Which Failed During the 1963 University of Illinois Study

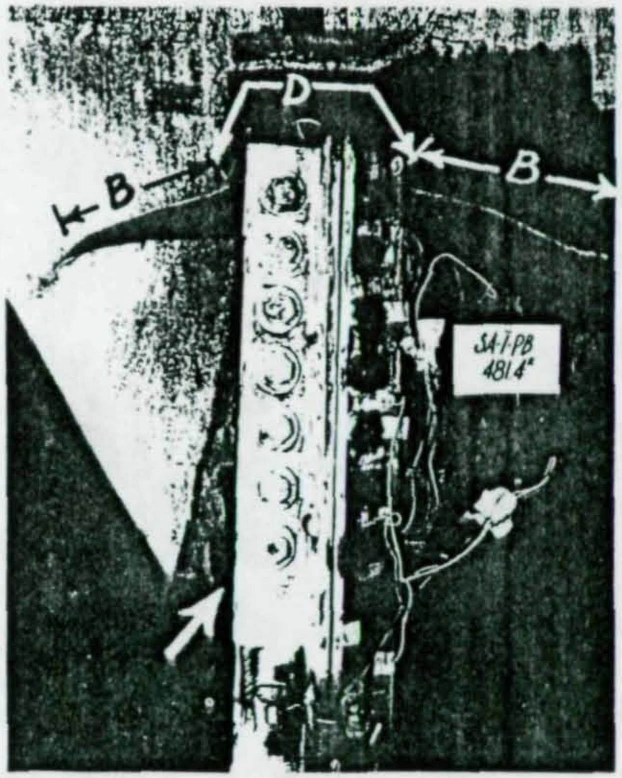

(a) Test connection SA-1-PB

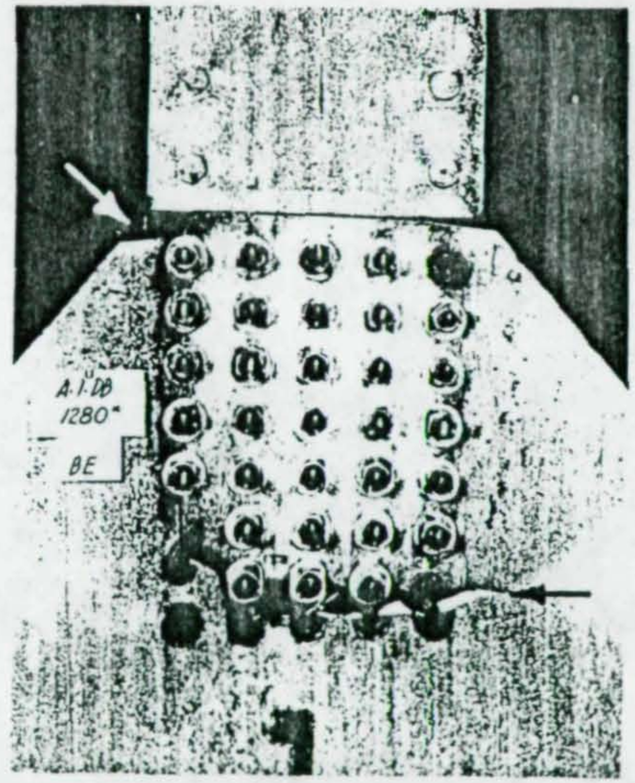

(b) Test connection A-1-DB

Figure 7.4 Failure Modes for Two of the Gusset Plates Tested During the 1963 University of Illinois Study [8]

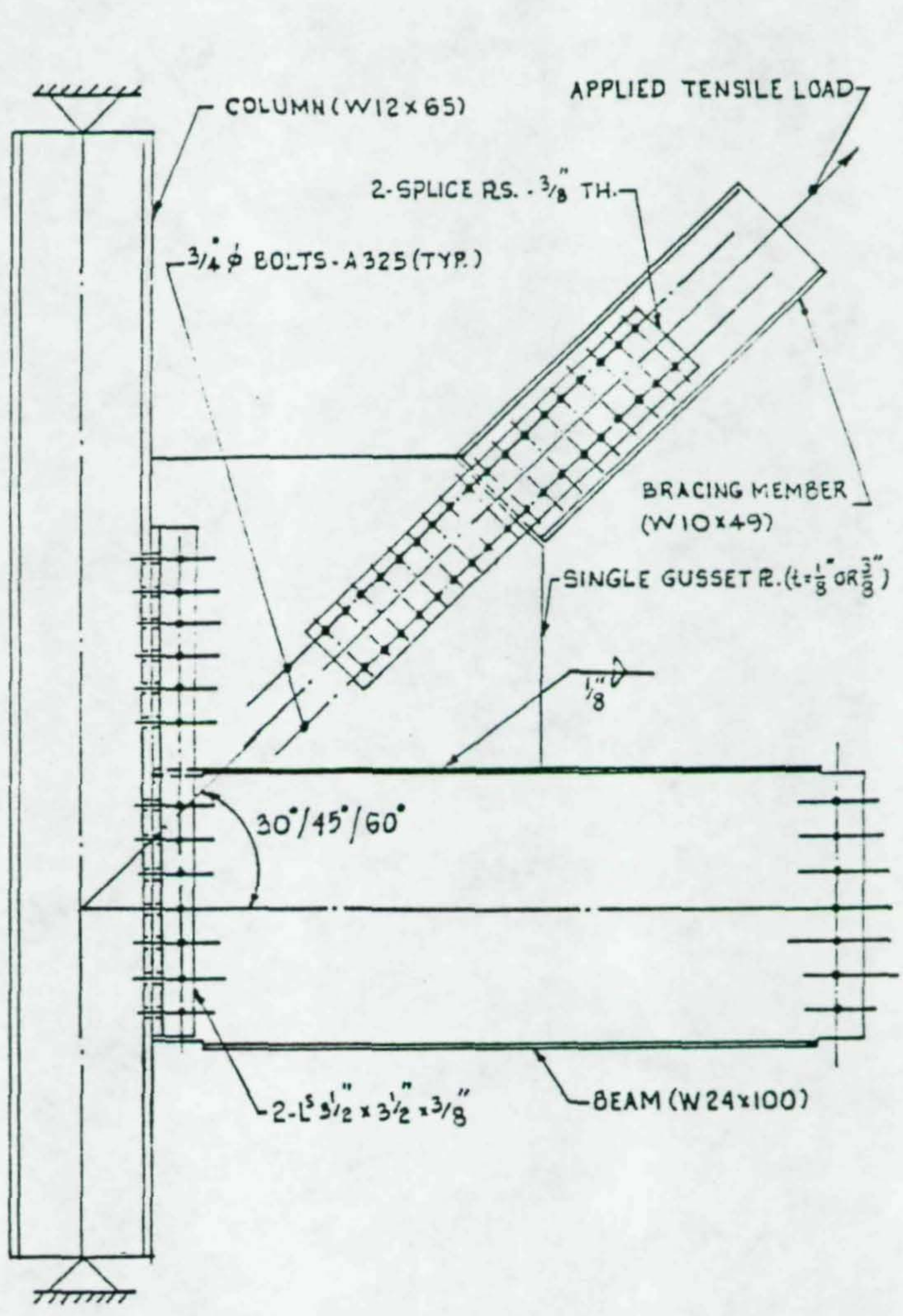

Figure 7.5 General Test Set-up for the University of Alberta Study [9]

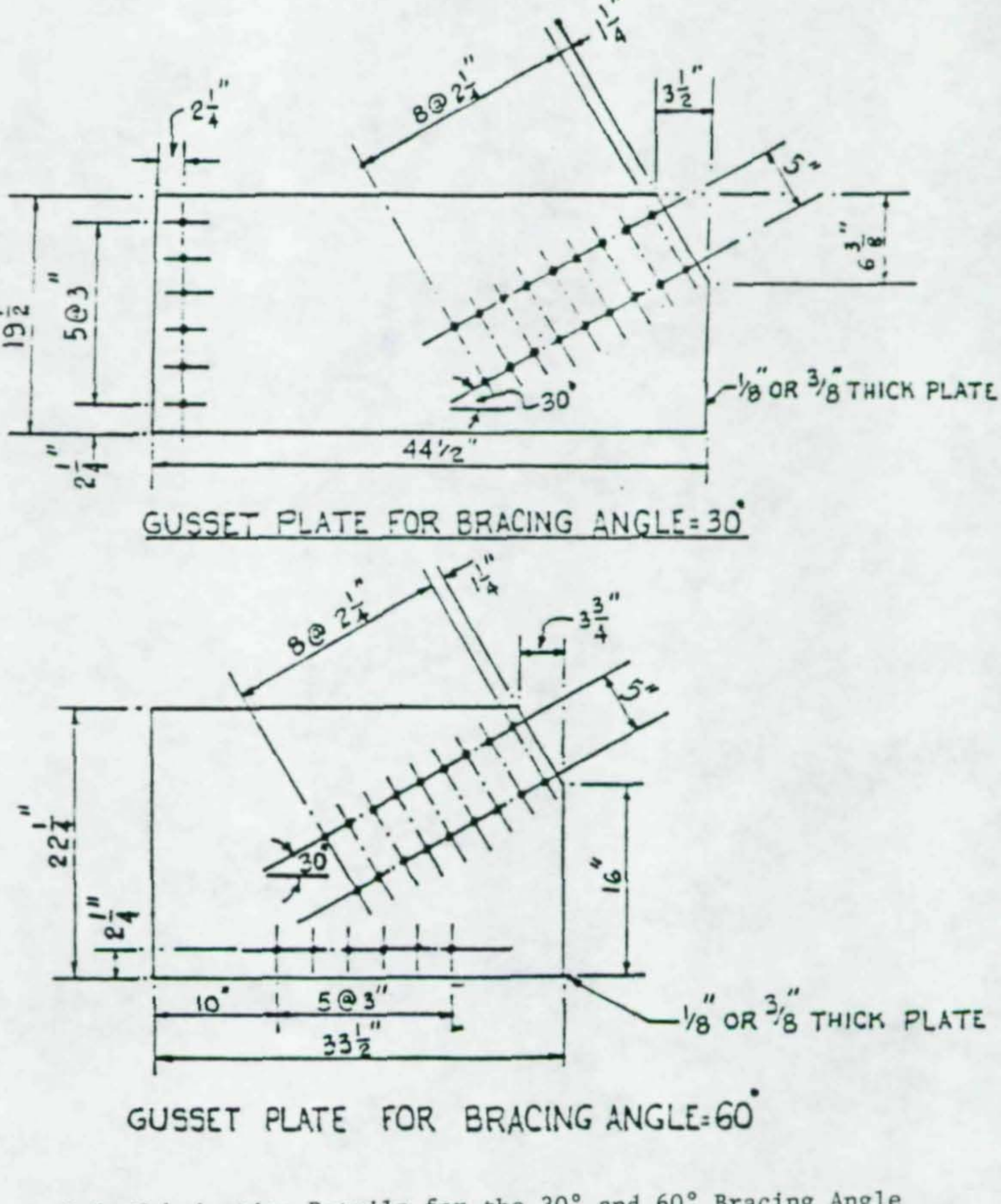

Figure 7.6 Fabrication Details for the 30° and 60° Bracing Angle Gusset Plates [9]

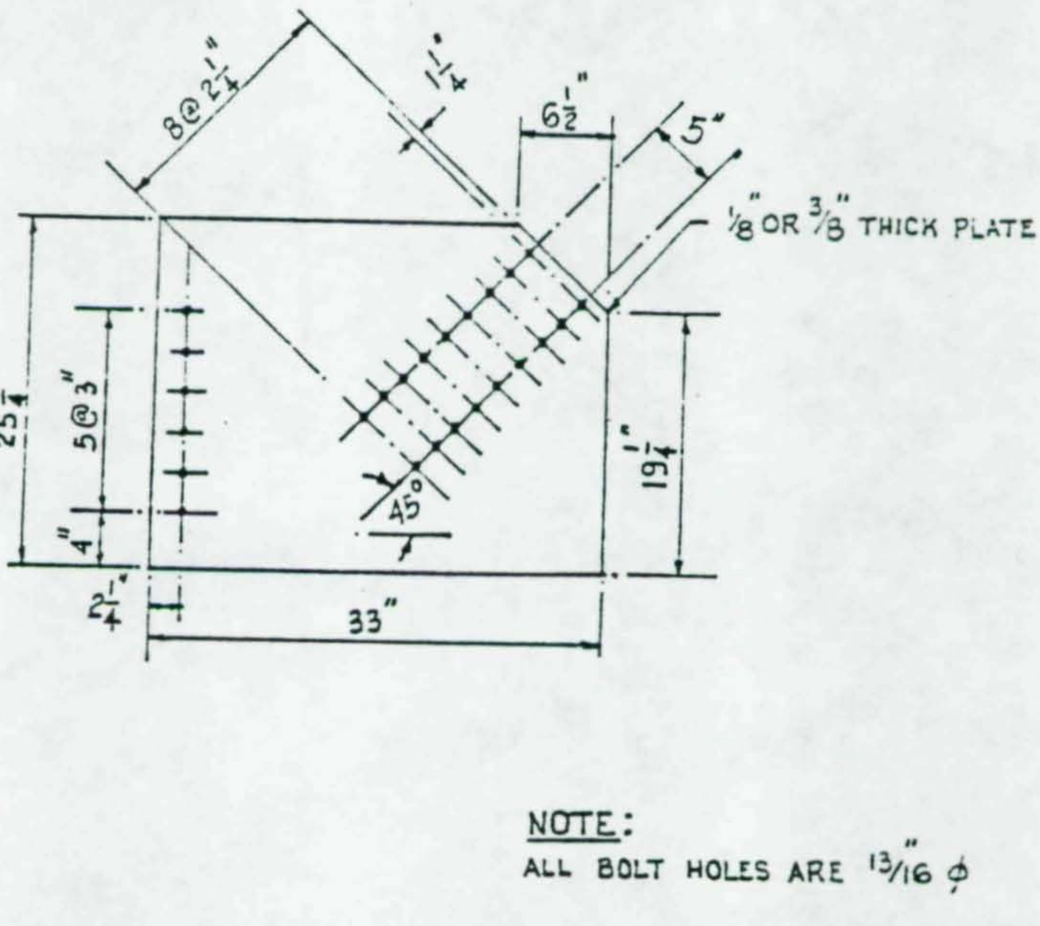

Figure 7.7 Fabrication Details for the 45° Bracing Angle Gusset Plate [9]

Table 7.1 Test Connection Details for Previous Studies

Previous Test No.	New Test No.	Hole Dia (in.)	S (in.)	ℓ (in.)	t (in.)	F_y (ksi)	F_u (ksi)
AD1	29	0.8125	12.0	17.0	0.50	34.2	60.0
A1-DB[a]	30		12.0			36.2	59.0
SA-1-PR	31		4.0			34.9	61.1
SA-2-PR	32						
SA-1-PB	33						
SA-2-PB	34						
SA-2-DB	35						
30°Gusset[b]	36		5.0	19.25	0.125	42.4	55.7
45°Gusset[b]	37						
60°Gusset[b]	38						
SE-2-DR	39		5.25	24.5	0.50	35.9	61.8
SE-2-DB	40						
SE-1-PR	41						
SE-2-PR	42						

[a]For last two letters: D = drilled holes, P = punched holes, R = rivets used in the connection, and B = bolts used in the connection

[b]Measured from the beam axis

tensile resistance developed at the last row of bolts, and one reflecting the shear resistance developed along the outside bolt lines.

For all 42 gusset plate test specimens, a tensile tear across the last row of bolts was observed, regardless of the strength parameters, hole size, or plate material. This would suggest that the theoretical ultimate strength model, in order to accurately model the connection behavior, must incorporate the tensile ultimate stress of the plate material, F_u, over the area between the two outside bolts in the last row. From the data recorded during testing of the 28 plates in the present study, it was found that the drop in strength from the ultimate load to the second strength plateau corresponded approximately to the ultimate tensile strength of the net area at the last row of bolts. That is, as the plate tore, the load was reduced by the magnitude $F_u[t(S-d_{hole})]$.

Ultimate shear resistance is more difficult to define, since the shear behavior varied among the 42 test specimens. For instance, the 28 plates tested during the present study did not display significant tearing along the bolt lines. Only the test plate that was made from the cold-rolled steel (plate no. 18) was observed to tear along the bolt lines, but this occurred after the ultimate strength was reached. This would suggest that the shear stress distribution is not uniform, as has been suggested in early examinations, but rather depends on the particular connection geometry and material.

The contribution of each of these terms (tensile resistance and shear resistance) in the ultimate strength model is shown pictorially in Figure 7.8.

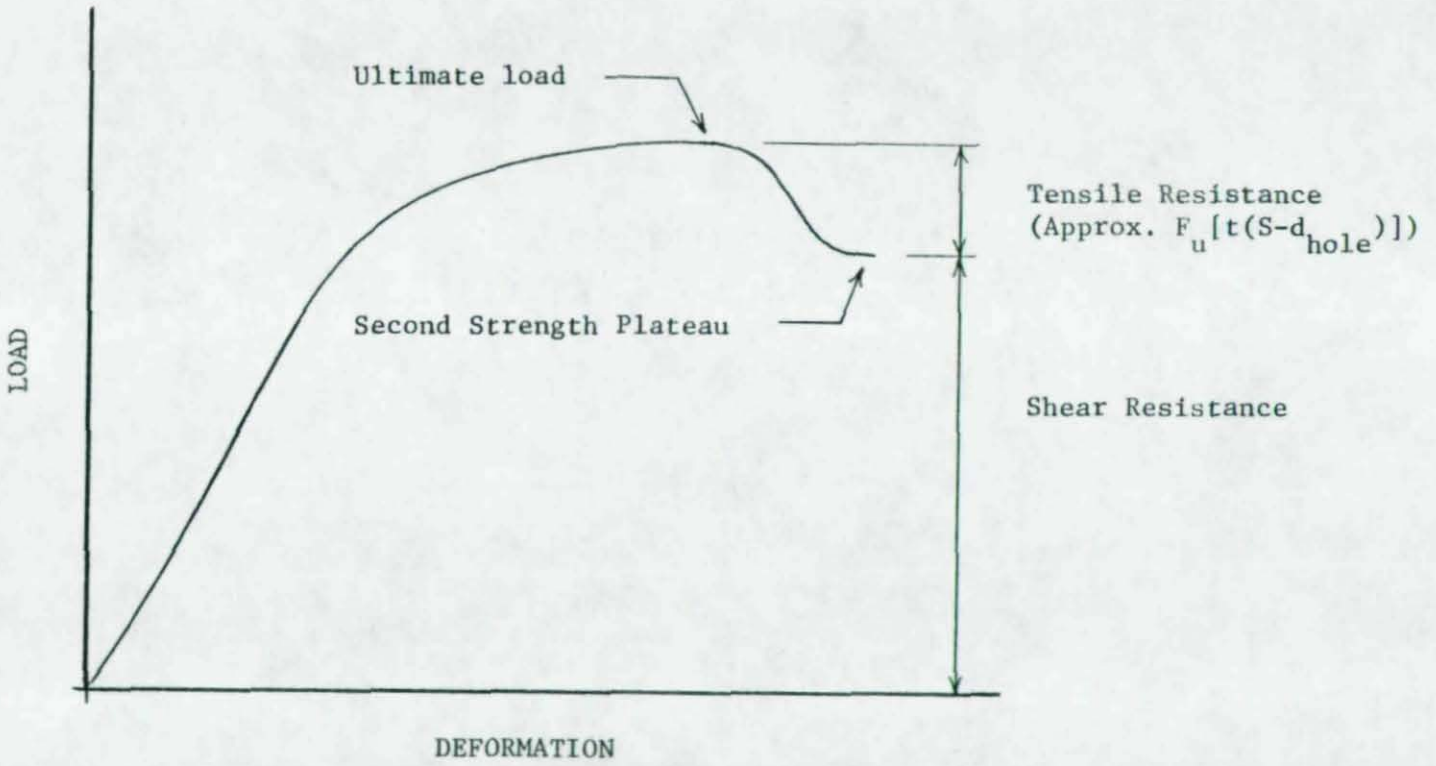

Figure 7.8 General Load-Deformation Diagram Showing Contribution of Tensile Resistance and Shear Resistance in the Ultimate Strength Model

7.3 Investigation of the Four Basic Block-Shear Models

Based on the discussion of the previous section, four basic free body diagrams can be constructed for the connection region; these diagrams are shown in Figure 7.9. The basic difference between the four diagrams is the method of considering the areas (either gross or net) over which the tensile stress and the shear stress act. The ultimate tensile strength, F_u, is the assumed level of stress on the tensile area at ultimate strength. The shear stress, τ, is of unknown magnitude, but is assumed to be distributed uniformly along the shear area. The shear yield stress of steel has been determined to lie within the range of 1/2 to 5/8 of the tensile yield stress. The Von Mises yield criterion for plane stress gives the shear yield stress as $\tau_y = F_y/\sqrt{3}$. This relationship is based on a mechanistic failure model for a ductile material such as steel, and will be used in this study. Therefore, the shear stress magnitude used here is $\tau = F/\sqrt{3}$, where F represents an unknown tensile stress.

From the diagrams shown in Figure 7.9, the following equations describe the ultimate capacity of the four connection models:

1. Gross-gross: $P_{theory} = F_u St + 2(F/\sqrt{3})\ell t$ (7.1-a)
2. Net-gross: $P_{theory} = F_u S_{net} t + 2(F/\sqrt{3})\ell t$ (7.1-b)
3. Gross-net: $P_{theory} = F_u St + 2(F/\sqrt{3})\ell_{net} t$ (7.1-c)
4. Net-net: $P_{theory} = F_u S_{net} t + 2(F/\sqrt{3})\ell_{net} t$ (7.1-d)

The value for the shear stress, $F/\sqrt{3}$, has purposely been left in general terms to allow for variations of this undefined stress term.

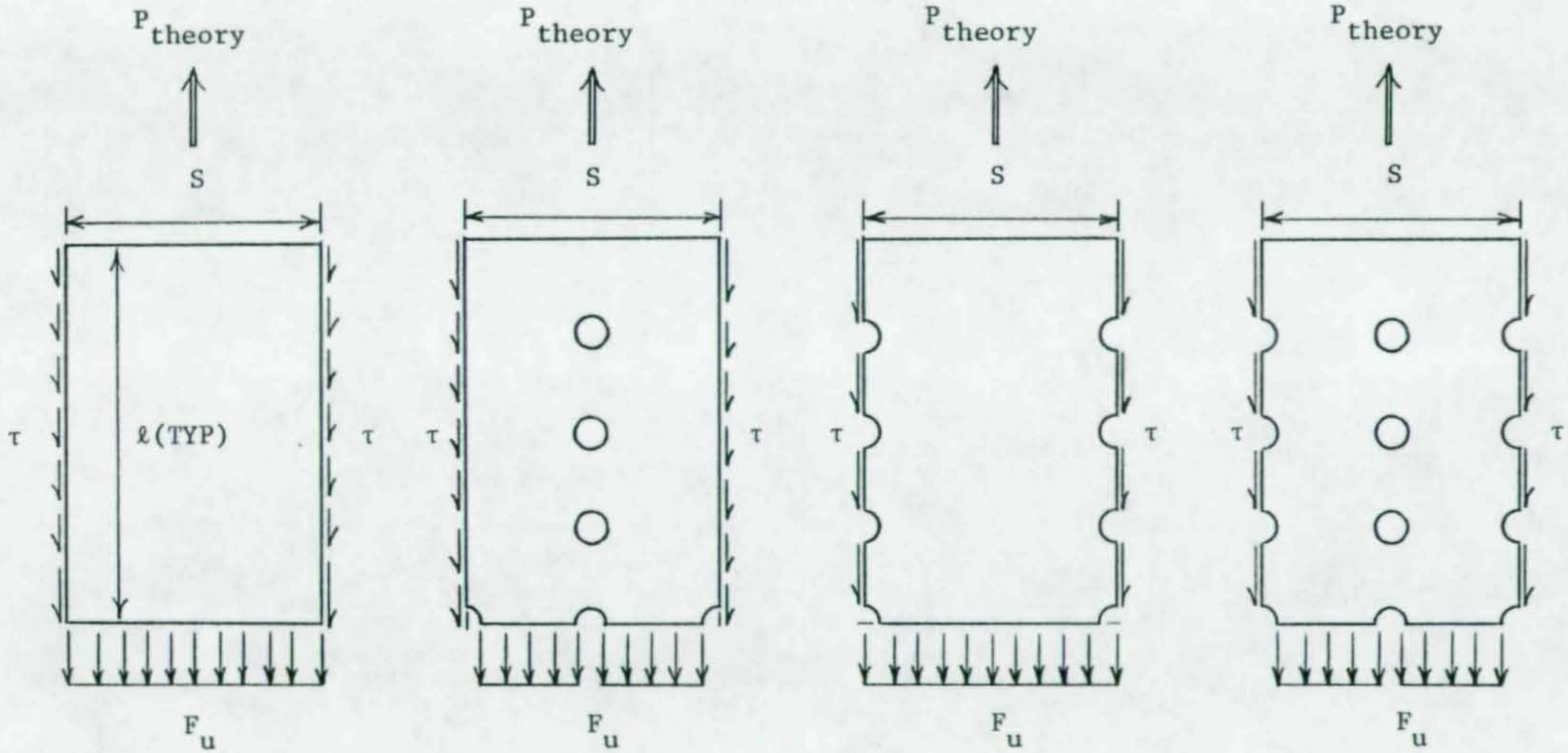

(a) Tensile gross area; shear gross area

(b) Tensile net area; shear gross area

(c) Tensile gross area; shear net area

(d) Tensile net area; shear net area

Figure 7.9 Four Basic Free Body Sections

Table 7.2 summarizes the observed failure loads for each of the 42 tested gusset plates. To compare the actual failure loads to those obtained by computing, using the models of Figure 7.9 and Equations 7.1, it is convenient to use the non-dimensional term, P, which is known as the professional factor in Load and Resistance Factor Design terminology [19, 20]. The professional factor is an indicator of the accuracy of the model, and it is given by the expression:

$$P = \frac{\text{Test Ultimate Strength}}{\text{Theoretical Ultimate Strength}}$$

A value of P = 1.0 would indicate perfect agreement between the strength model and the observed strength. The results of these comparisons for the different connection models are shown in Figures 7.10(a), 7.10(b), 7.10(c), and 7.10(d), which correspond to the results using Equations 7.1-a, 7.1-b, 7.1-c, and 7.1-d, respectively, for the theoretical strength models. In each figure, two extremes of shear stress are used: $\tau = \tau_y$ and $\tau = \tau_u$.

Figure 7.10(a) shows that using the ultimate shear stress value along the bolt lines gives a much larger theoretical failure load (small professional factor), while using the shear yield stress gives a smaller theoretical failure load for the majority of the tests. In Figure 7.10(b), using the ultimate shear stress appears to work well for the shorter connections (smaller gusset plate test number), while the shear yield stress gives good results for the longer connections. Both Figures 7.10(c) and 7.10(d) show that using the net area for the shear effect underestimates the failure load by a large margin for a majority of the test specimens.

Table 7.2 Observed Ultimate Load for Each Test Specimen

Test No.	P_{test} (kips)	Test No.	P_{test} (kips)
1	54.6	22	114.9
2	55.2	23	109.6
3	67.6	24	118.0
4	73.6	25	105.1
5	71.5	26	131.2
6	81.1	27	112.0
7	76.2	28	125.7
8	83.4	29	617.5
9	80.6	30	640.0
10	89.9	31	483.8
11	84.2	32	476.5
12	91.6	33	481.4
13	79.5	34	482.0
14	95.0	35	504.1
15	85.2	36	142.7
16	99.8	37	148.1
17	88.1	38	158.4
18	154.5	39	772.0
19	92.9	40	778.0
20	119.7	41	576.0
21	105.0	42	582.0

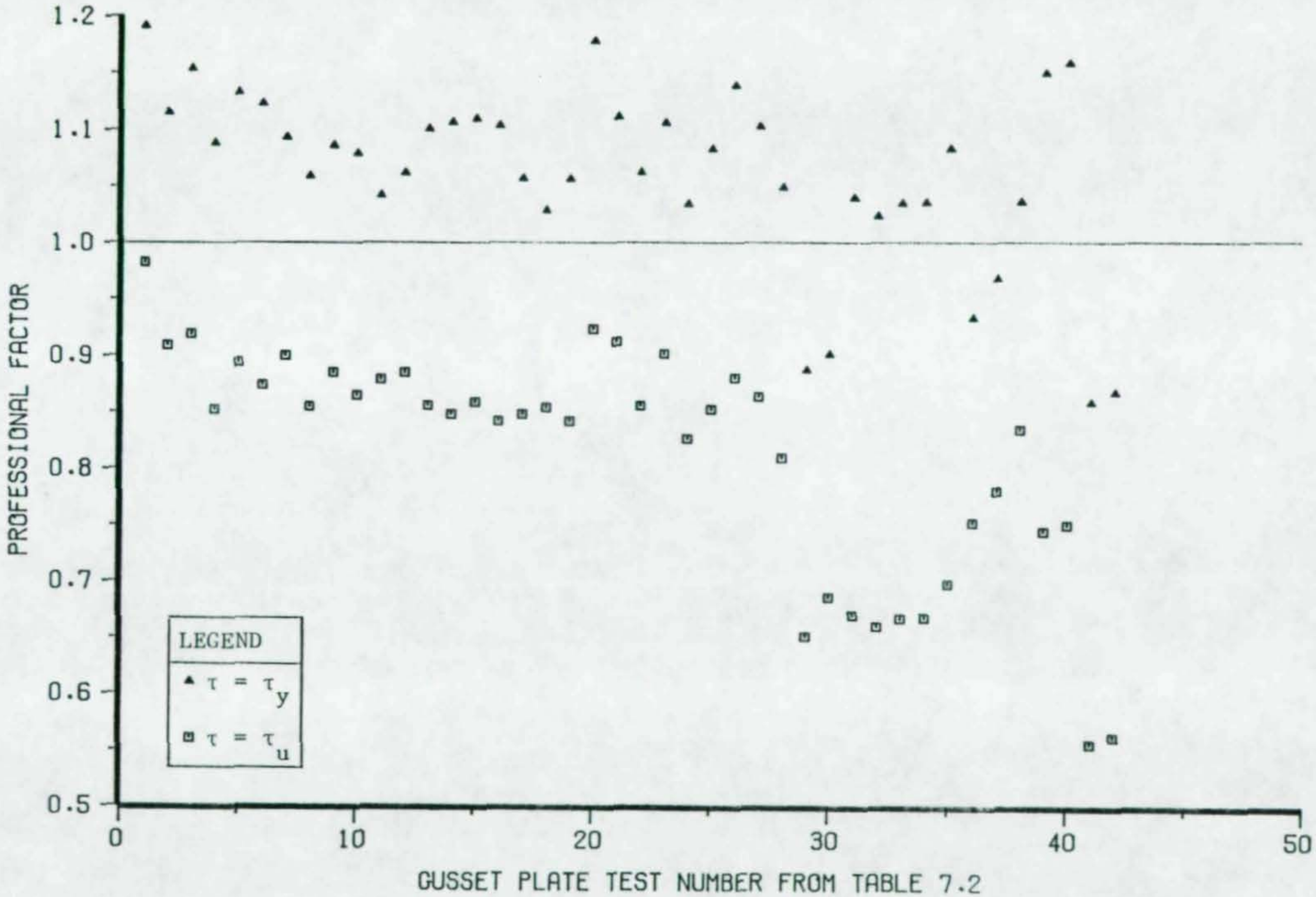

Figure 7.10(a) Professional Factor Using Tensile Gross Area and Shear Gross Area

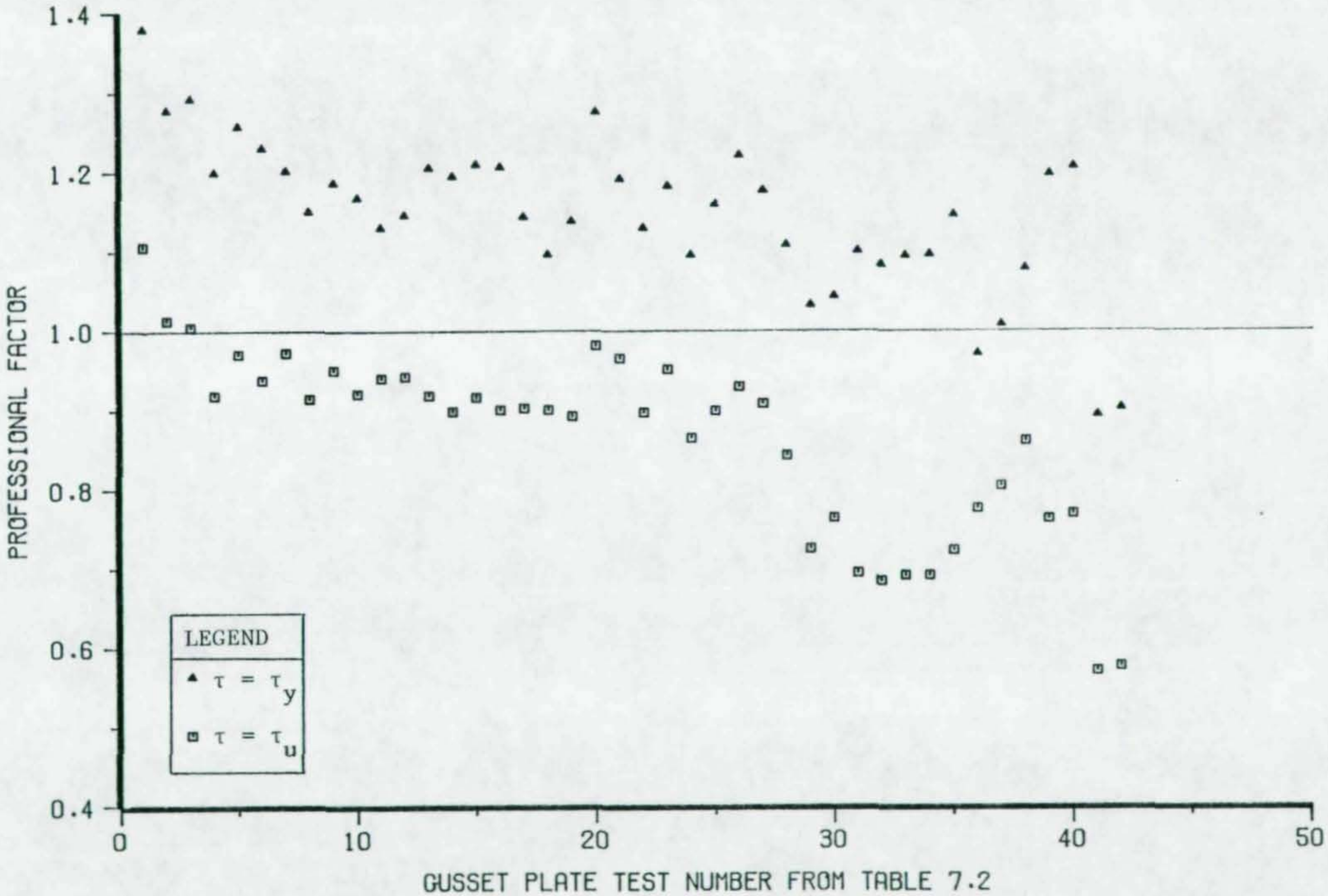

Figure 7.10(b) Professional Factor Using Tensile Net Area and Shear Gross Area

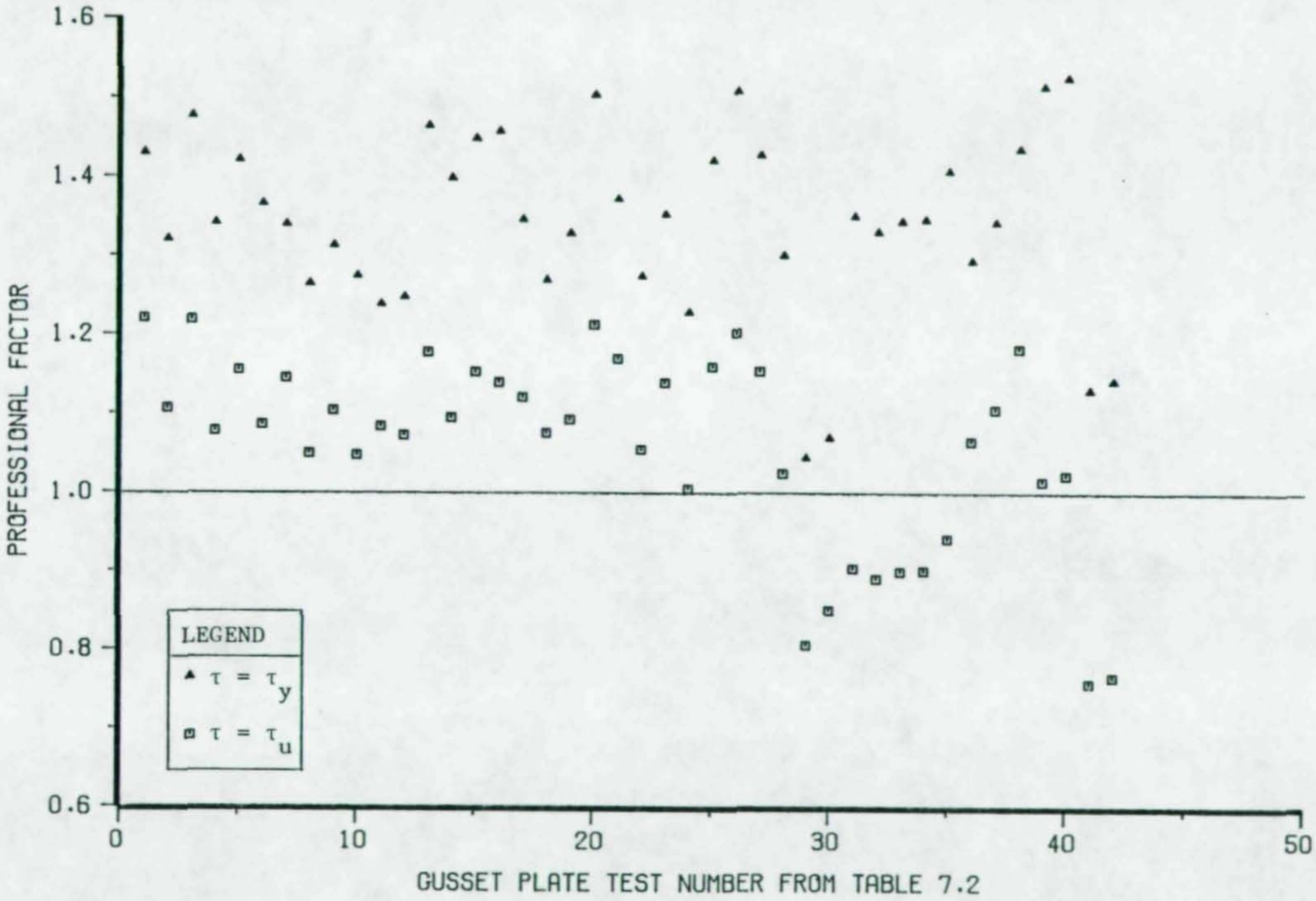

Figure 7.10(c) Professional Factor Using Tensile Gross Area and Shear Net Area

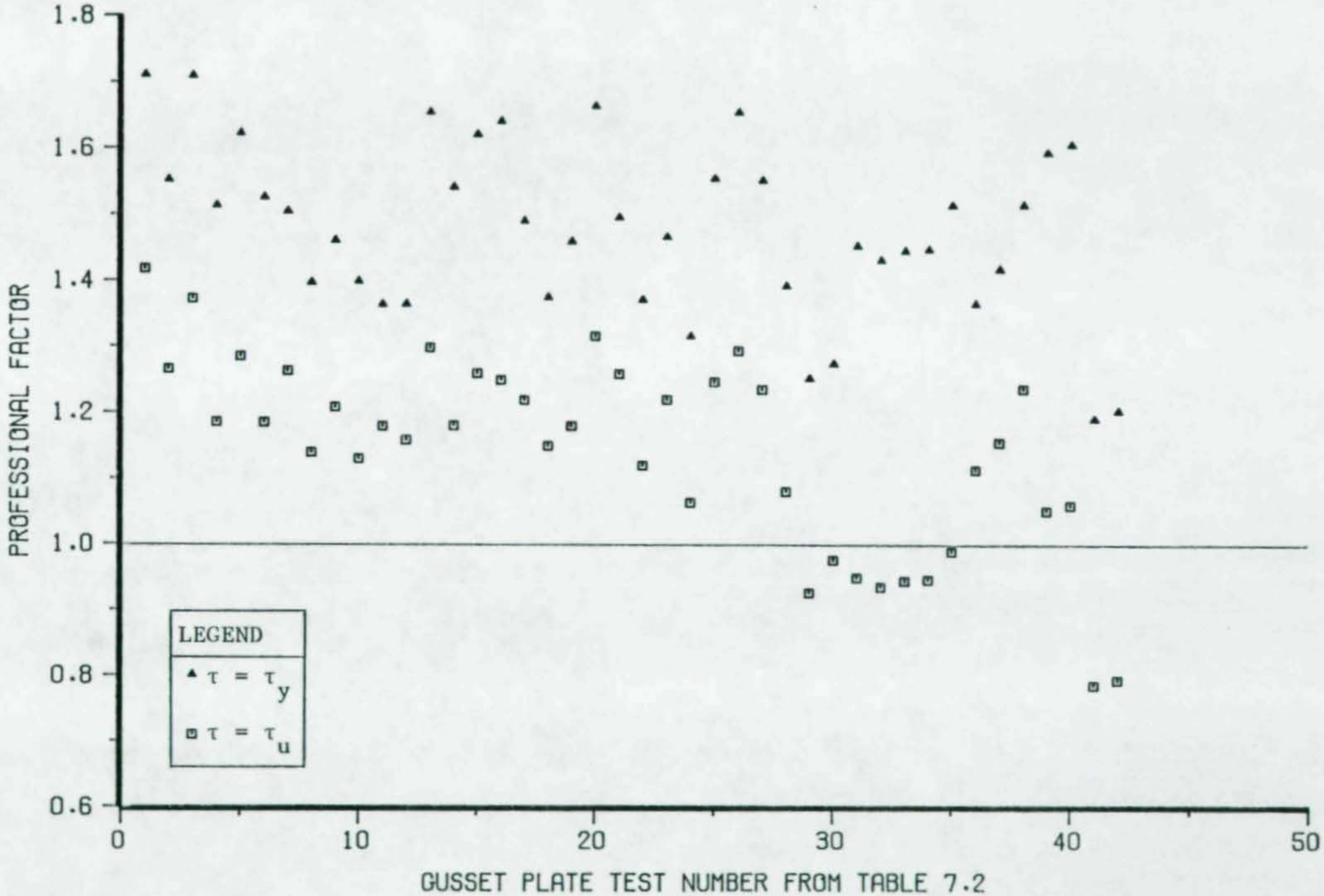

Figure 7.10(d) Professional Factor Using Tensile Net Area and Shear Net Area

The conclusion is that the block-shear model utilizing the net tensile area and the gross shear area, as illustrated in Figure 7.9(b), is the most acceptable of the four basic models. It can also be concluded that as the gusset plate connection length increases (corresponds to an increasing test specimen number, as they have been arranged), the professional factor decreases. This indicates that the effect of varying the connection length is important, and that it must be incorporated in a rational and complete gusset plate model.

7.4 Modification of the Net Tensile -- Gross Shear Strength Model

Figure 7.10(b) shows that for short connections, the ultimate shear stress acting on the gross connection length area would be appropriate, while for longer connections, the tendency is to approach the shear yield stress. This would indicate the need to adjust the assumed uniformly distributed shear stress as a function of the connection length. This can be accomplished by considering an interpolation between the yield and ultimate shear stress, expressed in terms of the tensile stress ($\tau_{eff} = F_{eff}/\sqrt{3}$), as the following:

$$F_{eff} = (1 - C_{\ell})F_y + C_{\ell}F_u \tag{7.2}$$

where:

F_{eff} = Effective tensile stress, ksi

C_{ℓ} = Connection length factor

The variable, C_ℓ, is the linear interpolation factor; if C_ℓ equals zero, the F_{eff} equals the tensile yield stress, and if C_ℓ equals one, then F_{eff} equals the tensile ultimate stress.

Using the net tensile area -- gross shear area block-shear model, it is possible to determine the required value for C_ℓ to give exact agreement with the observed ultimate strength for each test. Figure 7.11 illustrates this results as a function of the connection length, ℓ.

Many possible curves could be fit through the points, but a least squares straight line has been used for this study. The equation of this line in Figure 7.11 is:

$$C_\ell = 0.9383 - 0.04163\ell \qquad (7.3)$$

where:

C_ℓ = Connection length factor to be used in Equation 7.2

ℓ = Total connection length, in.

It is interesting to note that for very short connections, a value of F_{eff} approaching F_u is obtained, and for connections longer than 22.5 inches, the value for F_{eff} is less than F_y. This result appears intuitively correct, since longer connections would tend not to slip into bearing at mid-length of the connection.

Using Equation 7.3 to determine the connection length factor, the effective uniform shear stress, expressed in terms of the effective tensile stress, can be obtained from Equation 7.2. Using this effective stress in Equation 7.1-b, the theoretical ultimate strength can be obtained. Figure 7.12 shows the resulting professional factor

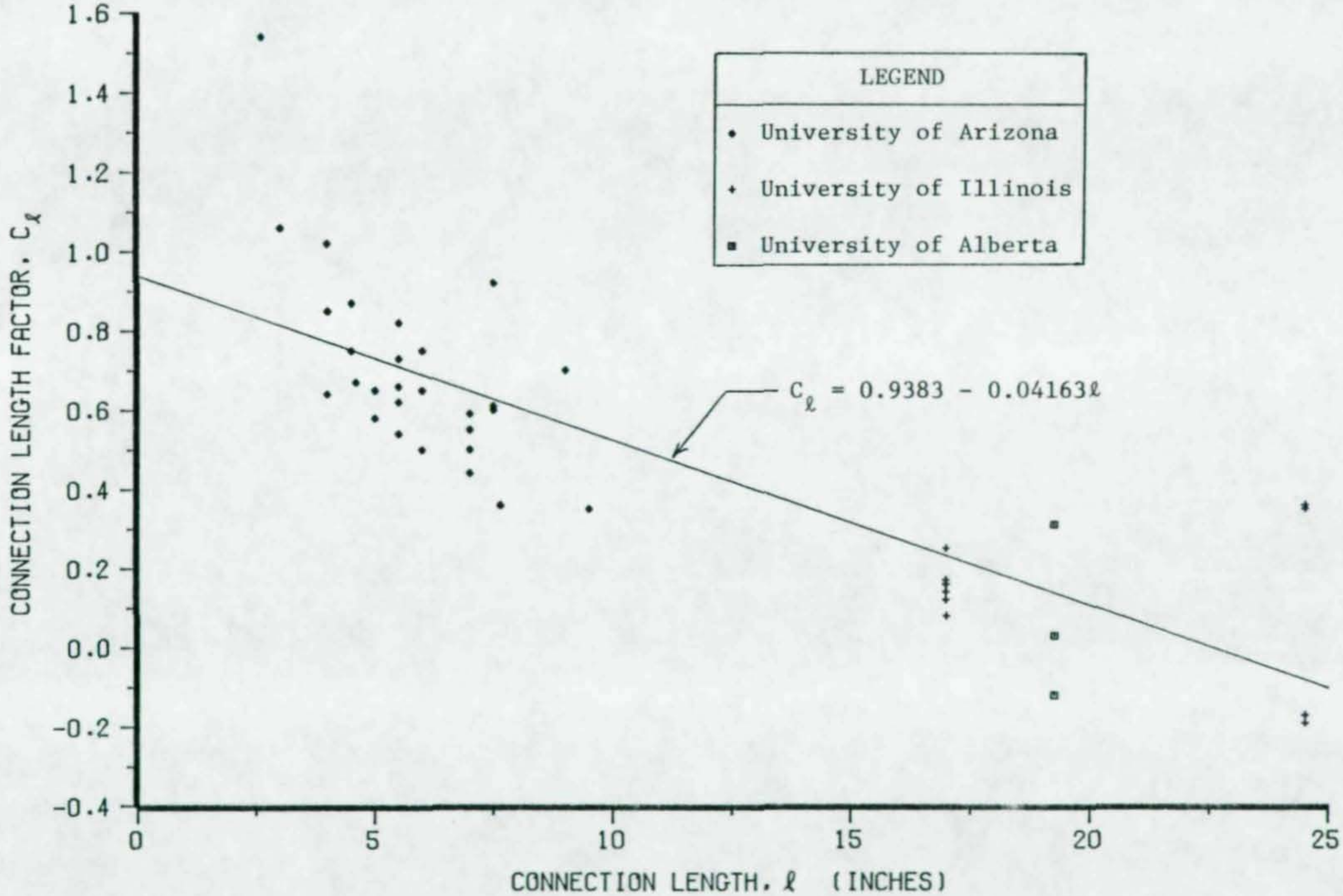

Figure 7.11 Values of the Connection Length Factor to Give P = 1.0, Expressed as a Function of the Connection Length

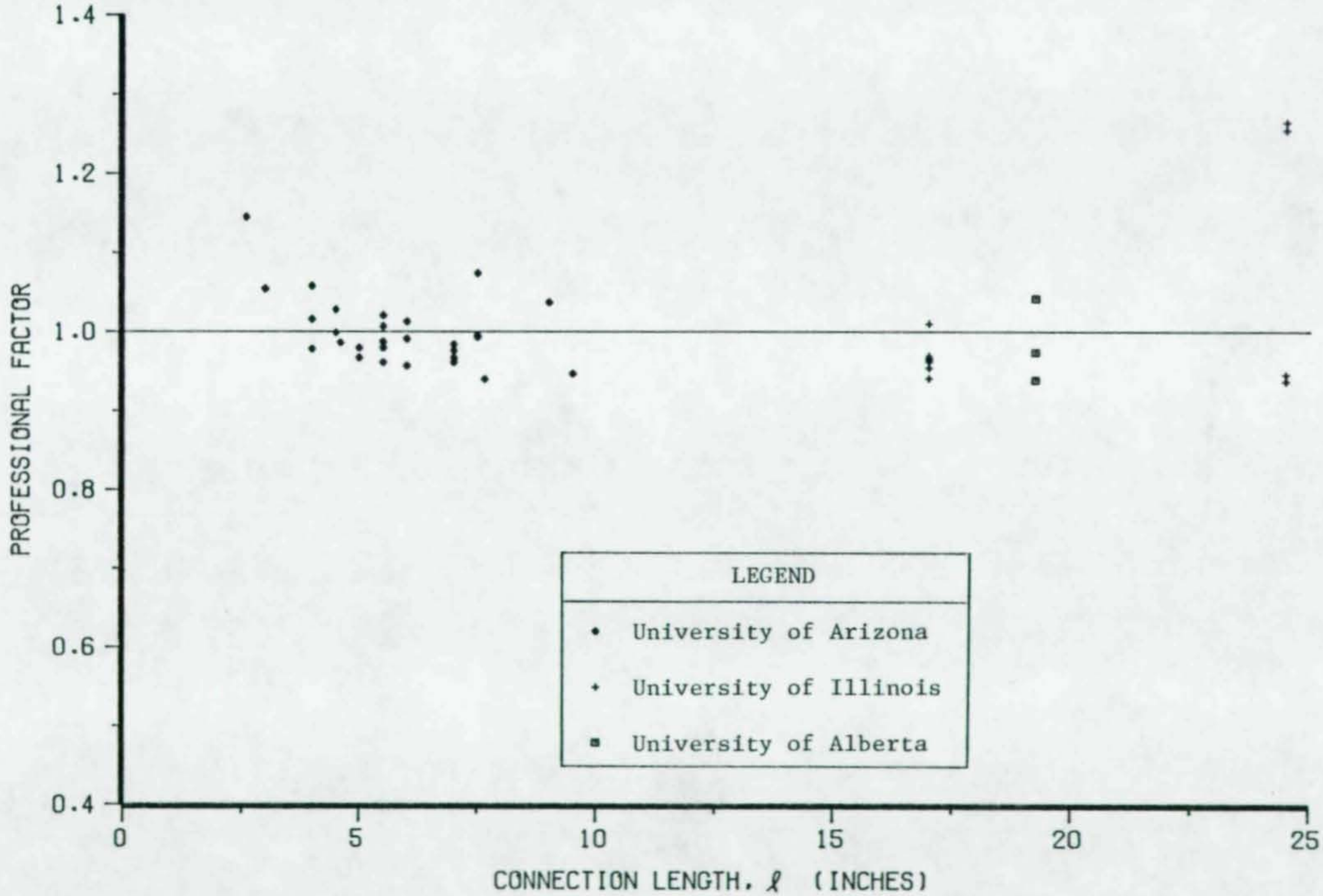

Figure 7.12 Professional Factor vs. Connection Length Using 42 Data Points

vs. connection length; the results of this figure can be compared to the data in Figure 7.10(b). For the 28 gusset plates tested during the present study, the mean value for the professional factor, P, is 1.000, with a coefficient of variation, V_P, of 0.0439. For all 42 tests, P_m is 1.003 with a coefficient of variation of 0.0716.

7.5 Refinement of Strength Model

Figure 7.12 shows that three of the 42 test plates exhibited much larger observed strength than would be expected. Test plate no. 1 had almost the same observed strength as plate no. 2. Both plates had two bolts in a line with a pitch of 1.5 inches, and the only difference was that plate no. 1 had an end distance of 1.1 inches, or 0.40 inch less than plate no. 2. It is conceivable that the edge distance is more critical for short connections, and plate no. 1, therefore, should have exhibited less strength. It is not clear why this did not take place, but it is believed that since plate no. 1 was the first to be tested, some testing error might have evolved.

Test plates nos. 39 to 42 are plates with similar geometry and material, but the fabrication of plates no. 39 and 40 involved drilling the bolt holes, while the holes were punches for plates 41 and 42. The drilled test plates showed an increase in ultimate strength of approximately 34 percent over the otherwise identical punched hole plates. This increase in the strength of the drilled specimens can be attributed to the added ductility of the plate material in the immediate vicinity of the holes. However, comparing test plates nos. 31 to 34 (all with punched holes) to test plate no. 35 (drilled holes) showed an increase in ultimate strength of only 5 percent (test plates nos. 31 to 35 have similar geometry and material). It is therefore not conclusive that drilling holes dramatically increases connection strength; also, most plates less than 3/4 inch thick would probably be fabricated by punching holes.

Based on the above evaluations, it is justifiable to discard the results from test plates nos. 1, 39, and 40, since they introduce test parameters that are not quantifiable and comparable to the other plates. Figure 7.13 shows the least square line that has been developed on the basis of the remaining 39 gusset plate test results, and the expression for the connecion length factor is given as:

$$C_\ell = 0.9467 - 0.04658\ell \qquad (7.4)$$

Using this expression for C_ℓ to determine the effective shear stress, Equation 7.1(b) can be used to obtain the theoretical strength.

The professional factor for each of the remaining 39 tests is plotted in Figure 7.14. The mean value of P for the remaining 27 of the University of Arizona test results is 1.000, with a coefficient of variation of 0.0338. For all 39 tests, P_m is 1.001, with a coefficient of variation of 0.0322. This can be compared to the values of $P_m = 1.003$ and $V_p = 0.0716$ for all 42 tests. It can be concluded that the proposed strength model, allowing for a uniform shear stress that is a function of the connection length, very closely predicts the observed ultimate strength.

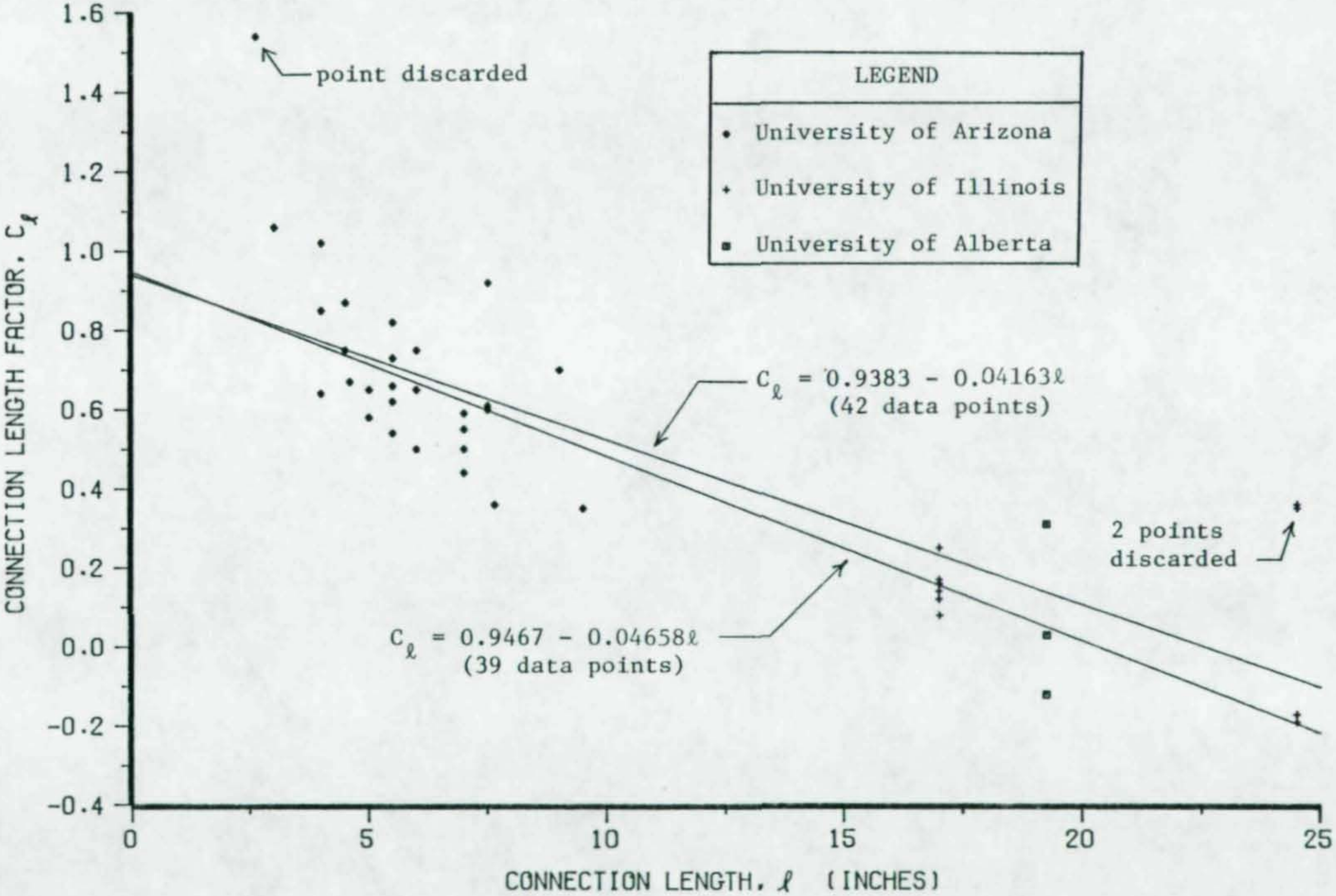

Figure 7.13 Least Squares Lines for 39 and 42 Data Points

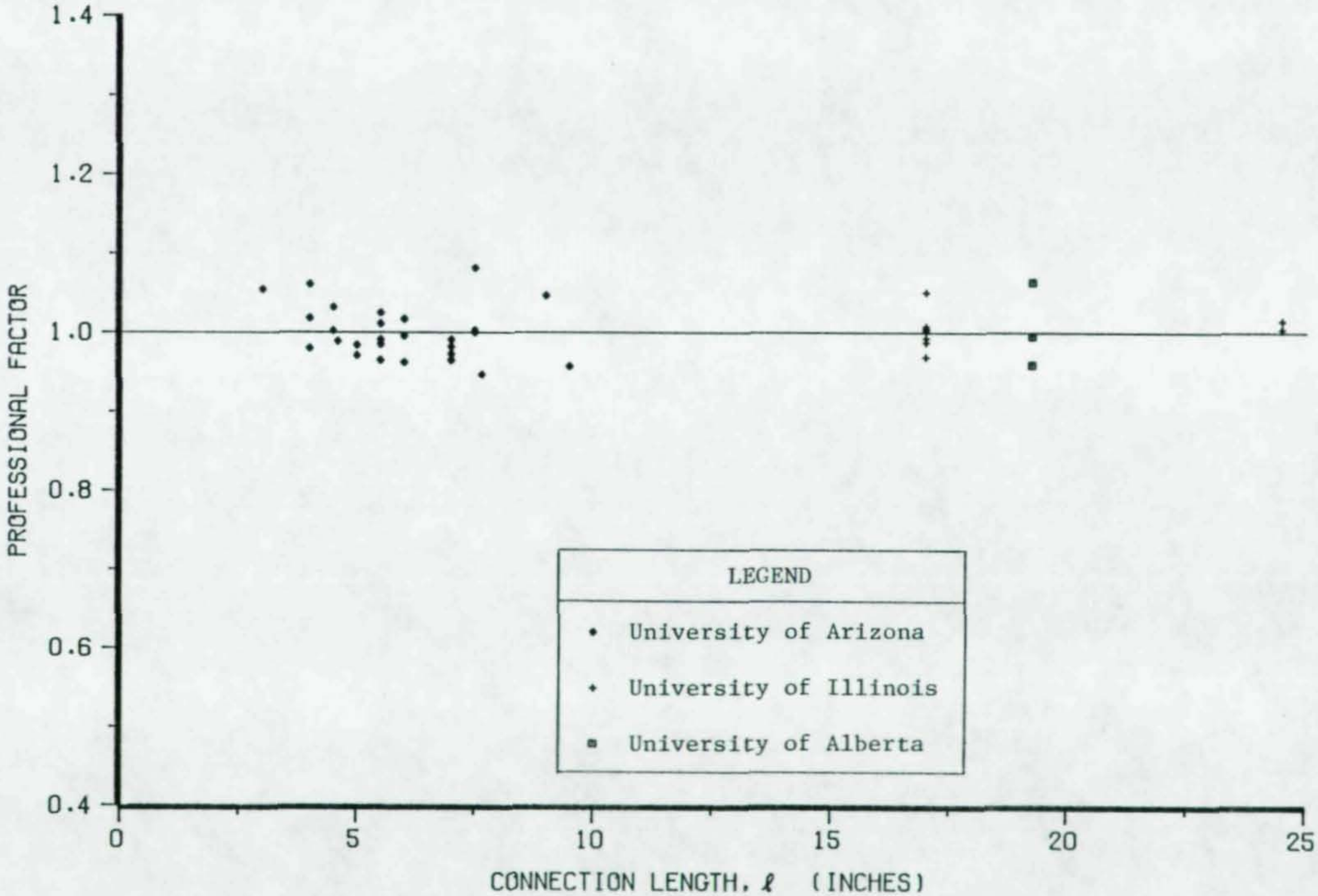

Figure 7.14 Professional Factor vs. Connection Length Using 39 Data Points

7.6 Investigation of Effects of Other Strength Parameters

It has been determined that connection length plays an important role in the proposed block-shear strength model, both for determining the effective average shear stress (by C_ℓ) and the shear area (ℓt). In order to analyze the effects of the other variables, both those directly used in the equations and those not included, it is convenient to plot the professional factor vs. each individual variable to observe its isolated effect. This has been done in Figures 7.15 to 7.23, in which the variables considered are the edge distance, the bolt pitch, the outside bolt gage, the plate thickness, the fastener size, the general plate geometry, the yield stress and ultimate tensile stress of the plate material, and the ratio of yield stress to ultimate tensile stress. It is emphasized that the ratio of yield to ultimate tensile stress in part expresses the level of ductility of the plate material.

It can be concluded that the effect of each strength parameter contained in the proposed block-shear equations is properly considered, and no additional strength parameters need to be included. The points on each figure lie approximately at the same level above and below the 1.0 line, with no well-defined additional relationships existing between the observed variable and the professional factor. The relatively small scatter of the data points can be attributed in part to random influences of the testing process, such as differences in the

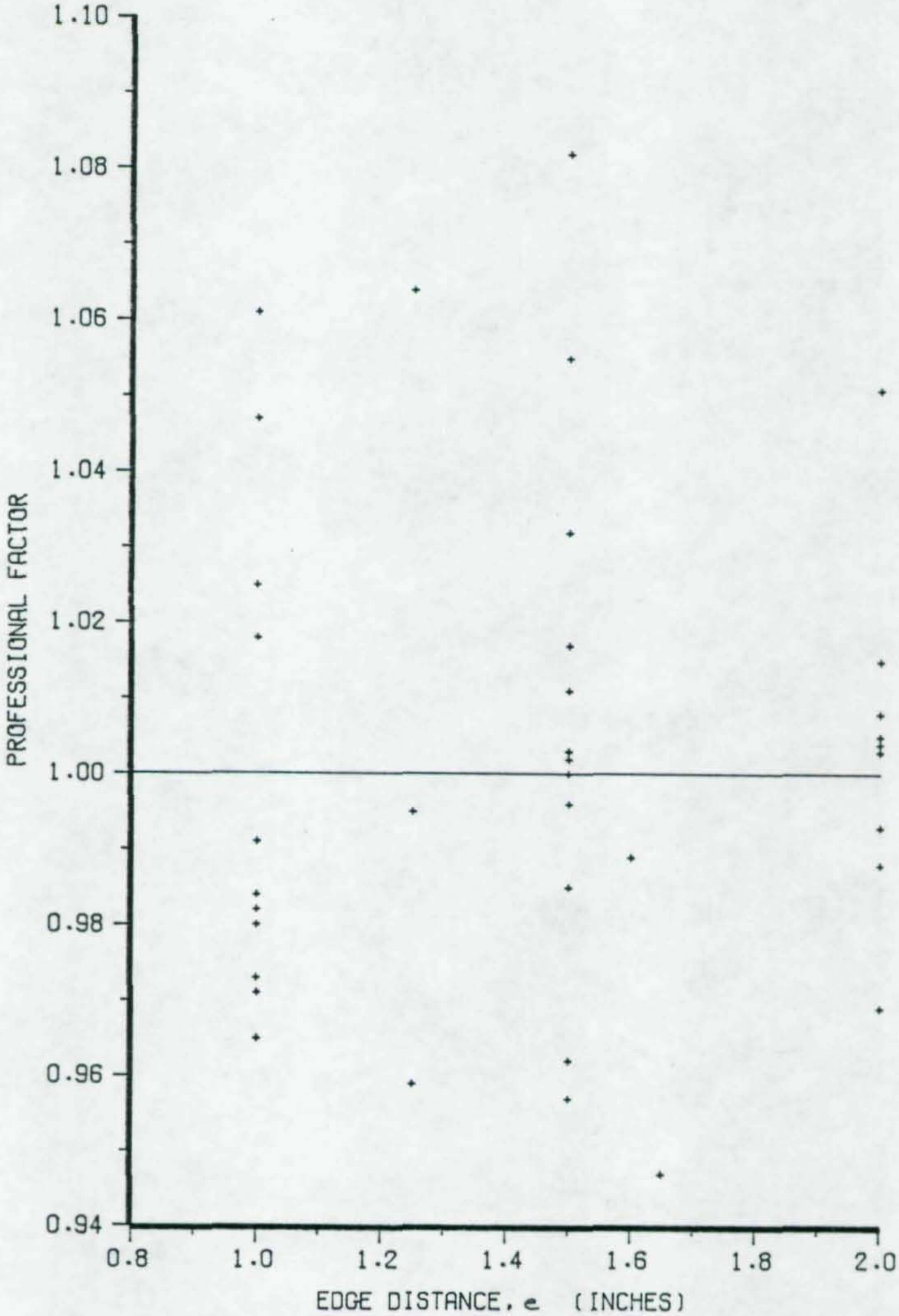

Figure 7.15 Professional Factor vs. Edge Distance

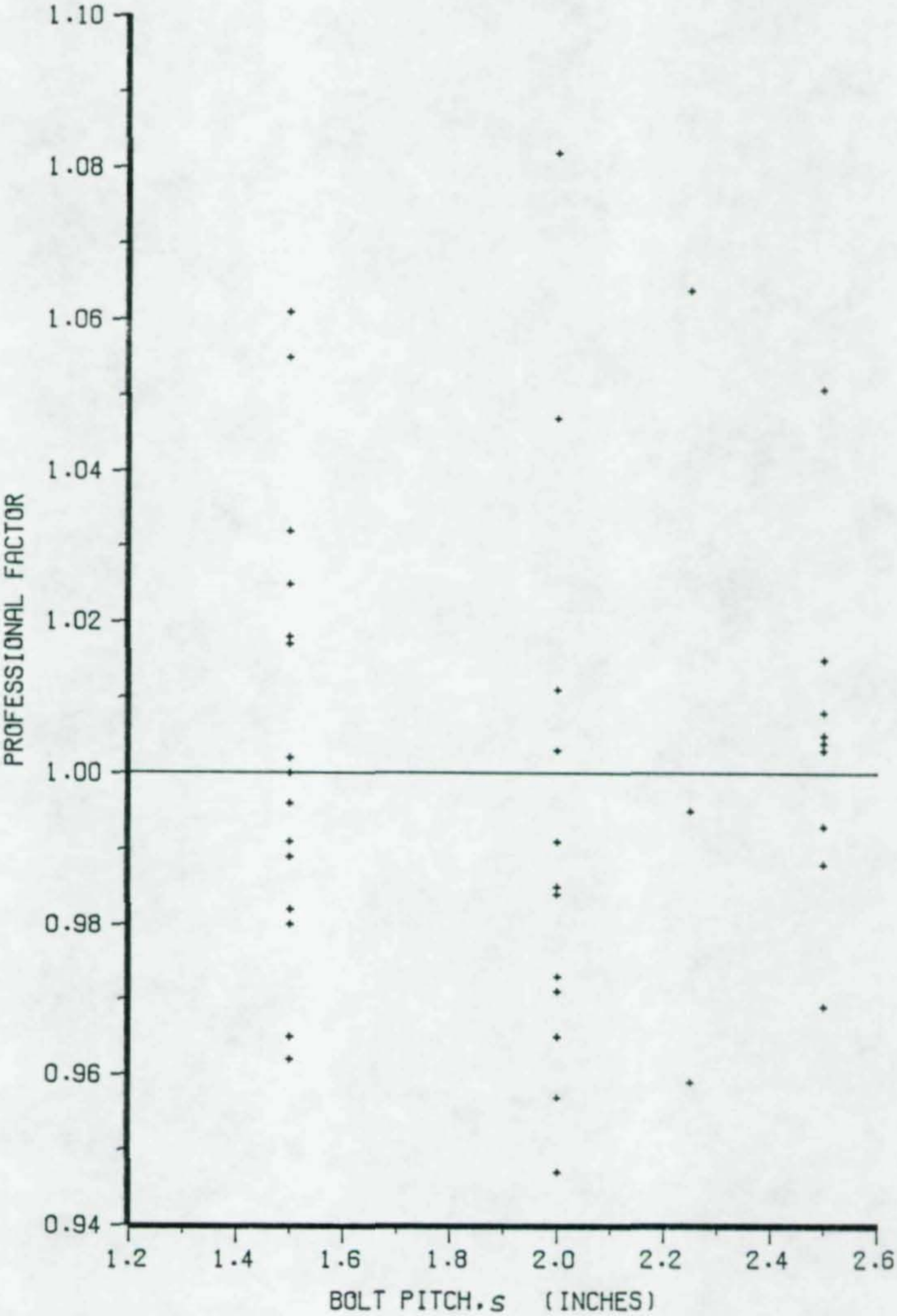

Figure 7.16 Professional Factor vs. Bolt Pitch

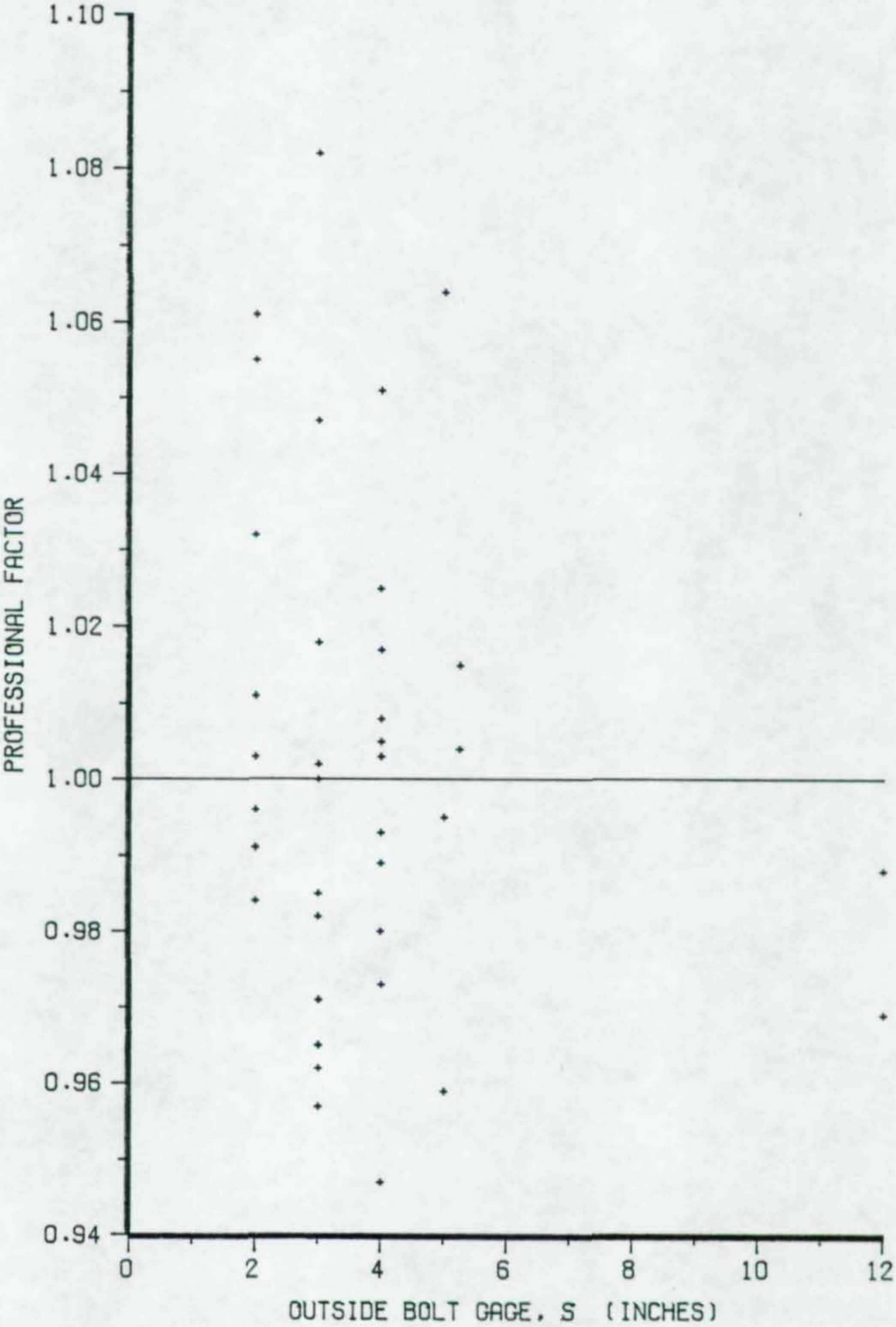

Figure 7.17 Professional Factor vs. Outside Bolt Gage

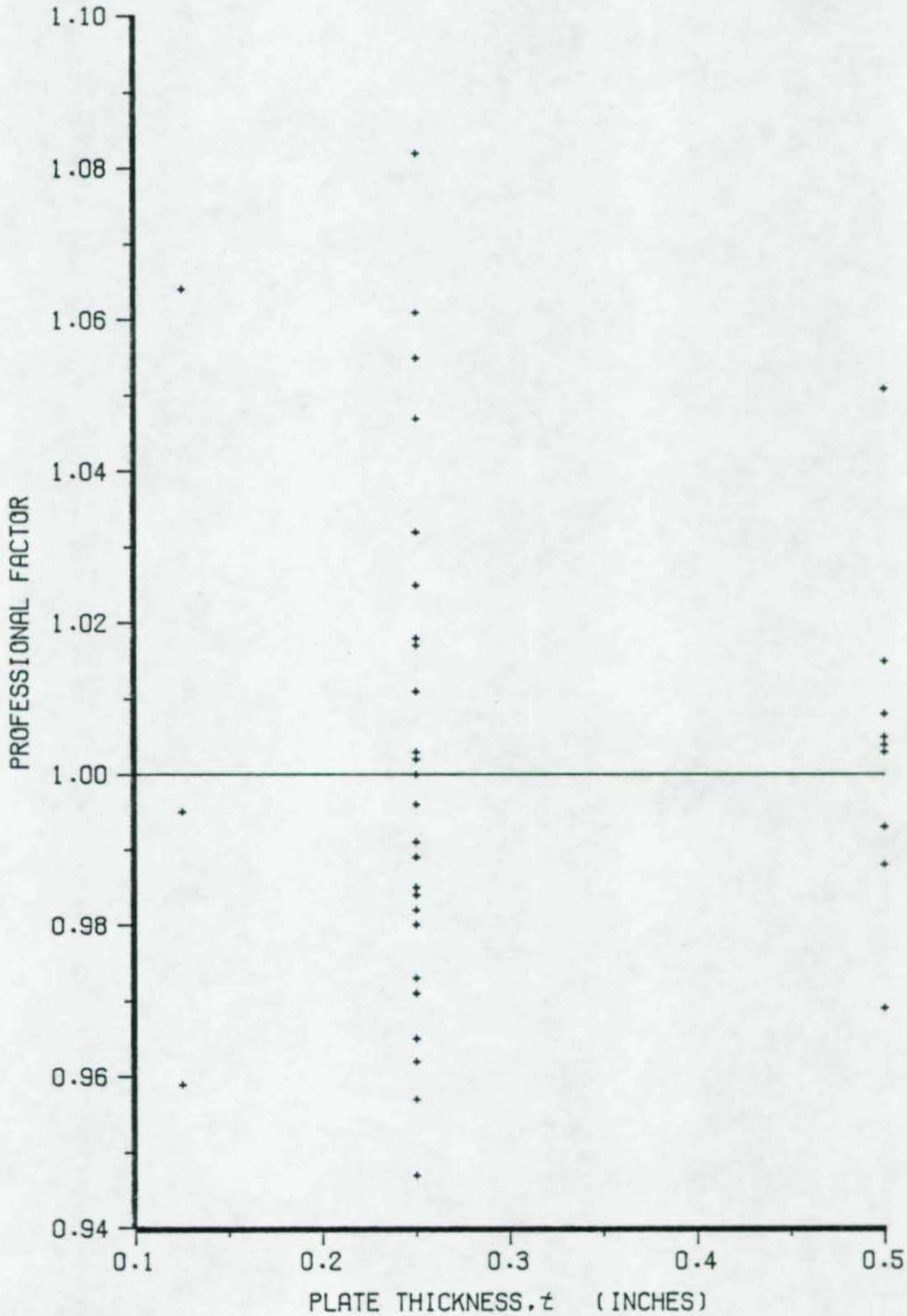

Figure 7.18 Professional Factor vs. Plate Thickness

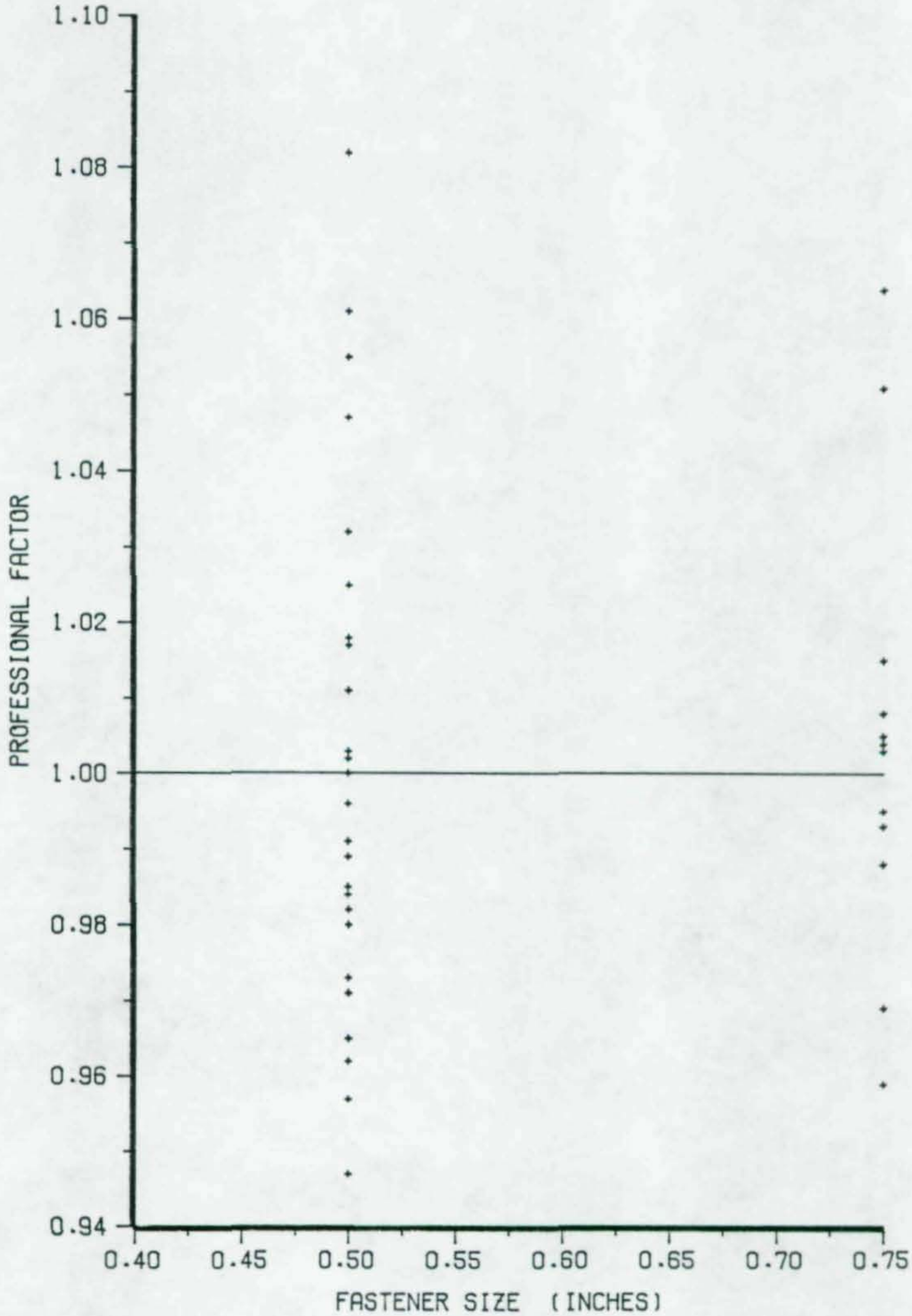

Figure 7.19 Professional Factor vs. Fastener Size

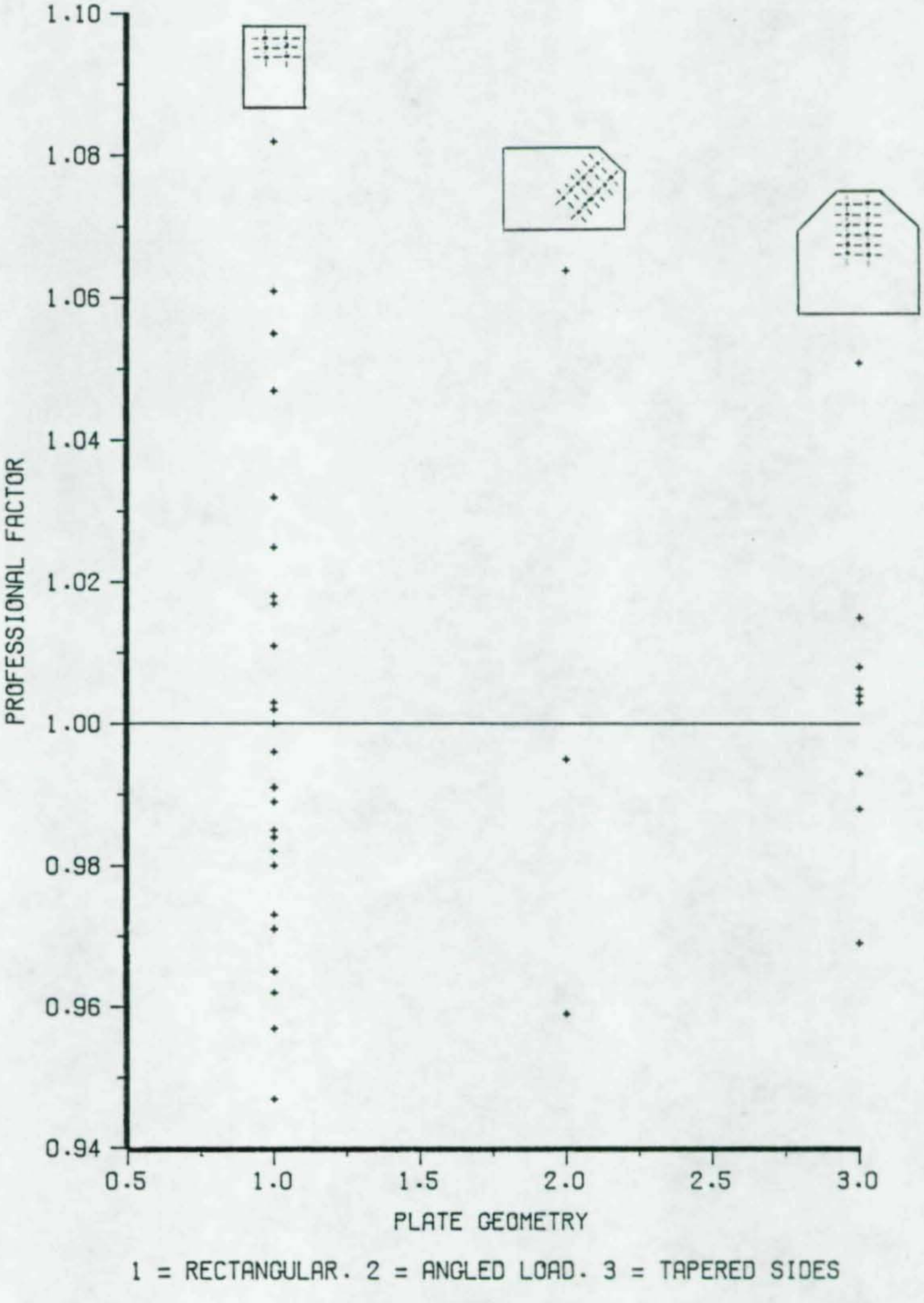

Figure 7.20 Professional Factor vs. Plate Geometry

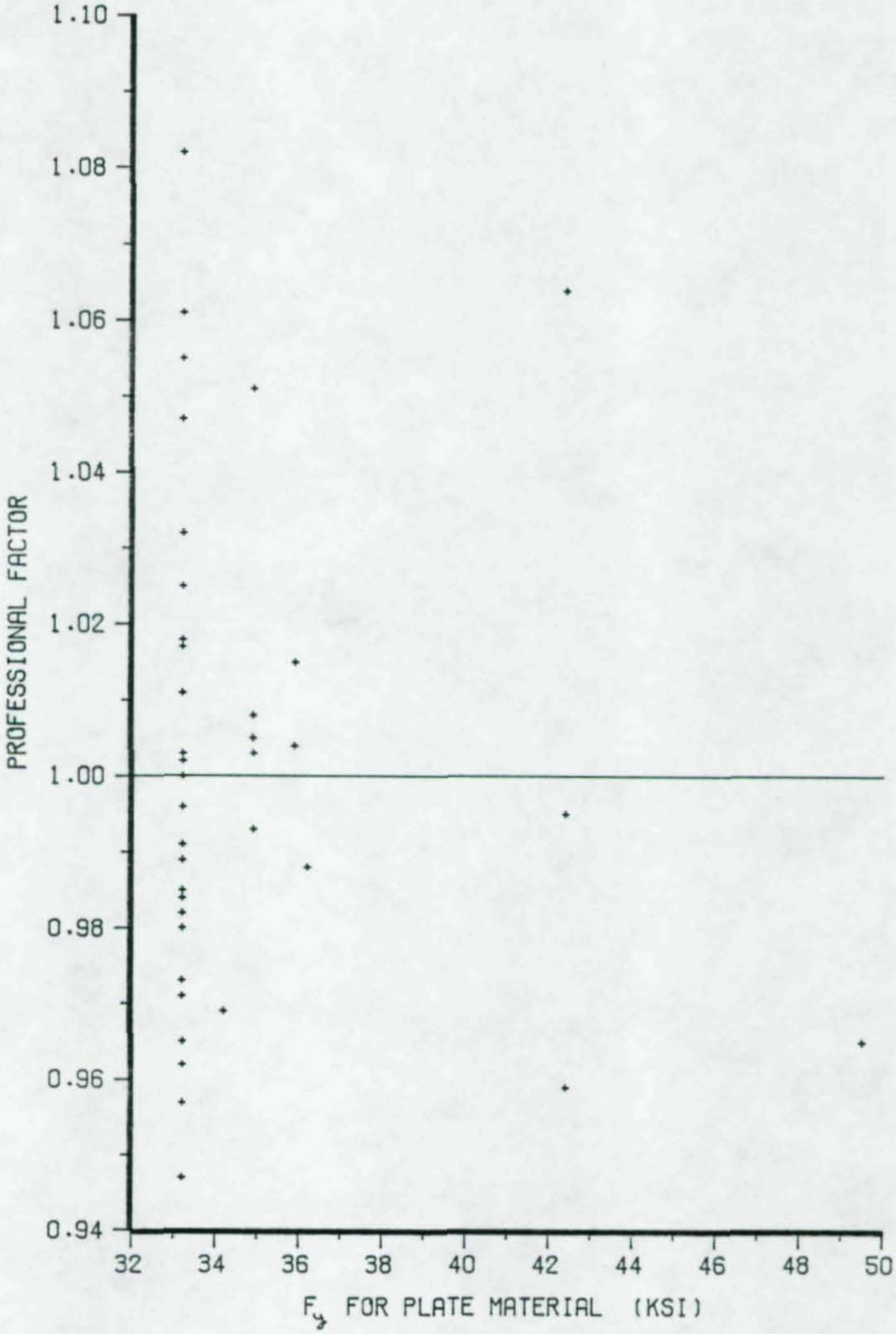

Figure 7.21 Professional Factor vs. Plate Material Yield Stress

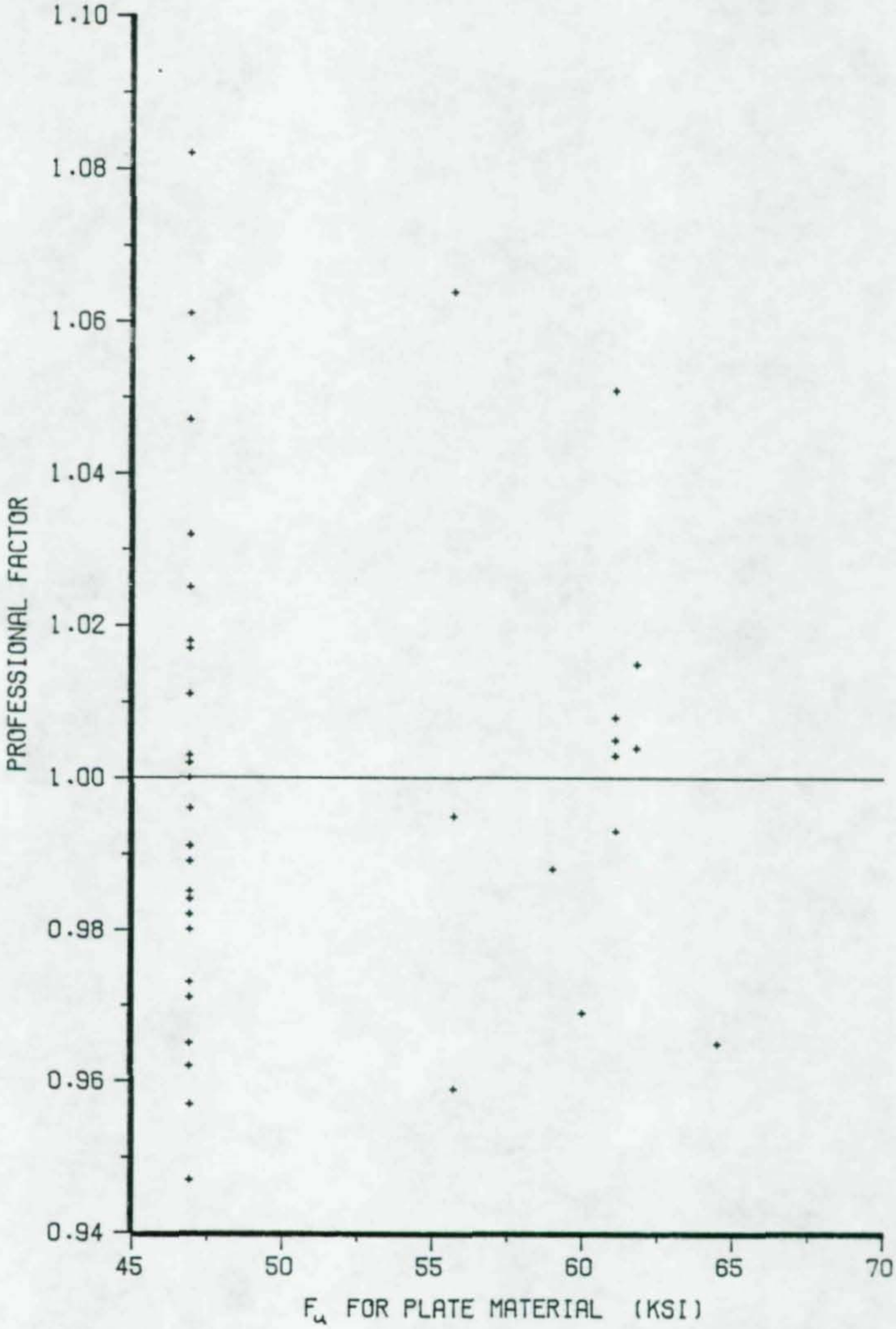

Figure 7.22 Professional Factor vs. Plate Material Ultimate Tensile Stress

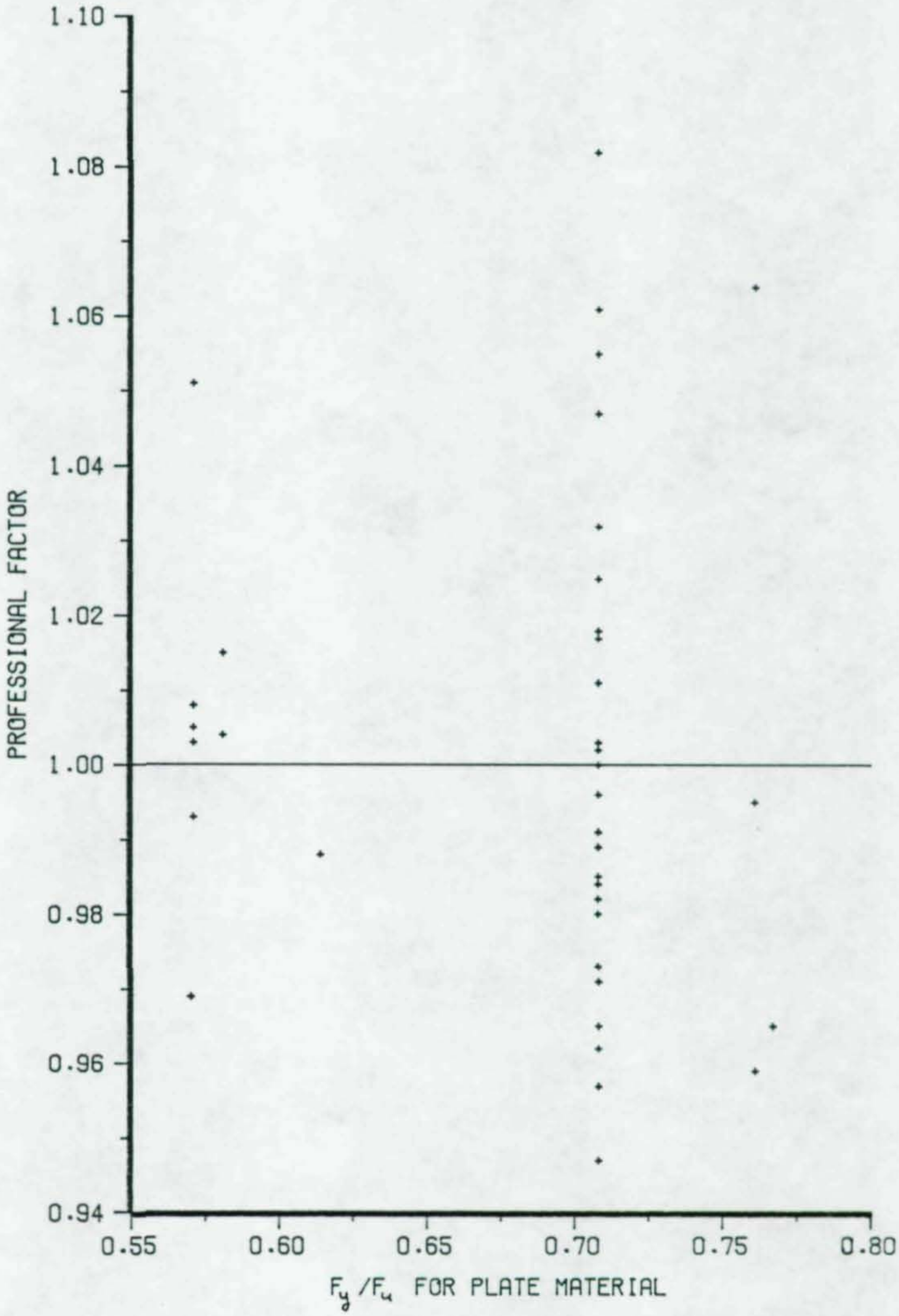

Figure 7.23 Professional Factor vs. Plate Material Yield Stress to Ultimate Tensile Stress Ratio

testing speed, non-symmentrical loading, and so on. In other words, the variability of the results cannot be explained through rational mechanistic models.

7.7 Summary and Final Proposed Strength Model

This chapter has presented the detailed development of a valid strength model, based on test results obtained in this study and through earlier, related work. The strength model that is proposed has been shown to be a reliable measure of gusset plate ultimate strength over a wide range of structural (geometric and material) variables.

In order to simplify the proposed equations, all constants should be rounded off to two decimal places. This results in the following set of equations, which gives the nominal ultimate resistance of a gusset plate loaded in tension:

$$R_n = F_u S_{net} t + 1.15 F_{eff} \ell t \tag{7.5}$$

$$F_{eff} = (1 - C_\ell) F_y + C_\ell F_u \tag{7.6}$$

$$C_\ell = 0.95 - 0.047\ell \tag{7.7}$$

where:

R_n = Nominal ultimate resistance of connection, kips

S_{net} = Net gage between outside bolts,

= S - (no. holes - 1) *hole diameter, in.

ℓ = Total connection length, in.

t = Plate thickness, in.

F_y = Plate material yield stress, ksi

F_u = Plate material ultimate tensile stress, ksi

F_{eff} = Effective tensile stress, ksi

C_ℓ = Connection length factor (non-dimensional).

This simplification of the original equation gives the following values for the arithmetic mean of the professional factor and its coefficient of variation, using the results for the 39 tests that have been incorporated:

$$P_m = 1.00$$

$$V_P = 0.033$$

It is therefore seen that the performance of the model is excellent also in statistical terms, giving a low coefficient of variation, and a mean equal to 1.0 for results of a wide range of strength parameters.

CHAPTER 8

RESISTANCE FACTOR FOR BOLTED TENSILE GUSSET PLATE CONNECTIONS

The motivation behind developing an ultimate strength model for gusset plates is its eventual incorporation into a limit states design procedure. Having a reliable model, it remains to develop the corresponding resistance factor, based on the Load and Resistance Factor Design (LRFD) format. This development will be presented in the following. For a more detailed treatment of the subject of LRFD design, References 19 to 23 give adequate documentation.

The mean strength, R_m, and its coefficient of variation, V_R, are given by the expression [19, 20]:

$$R_m = R_n P_m M_m F_m \tag{8.1}$$

$$V_r = \sqrt{V_P^2 + V_M^2 + V_F^2} \tag{8.2}$$

The coefficient P_m is the mean value of the professional factor, and the statistics of this term have been determined in Chapter 7 as $P_m = 1.00$ and $V_p = 0.0033$. The coefficient M_m represents the mean value of the ratio of the actual static yield stress to the specified minimum yield stress. The data for the statistics of this coefficient have been determined as $M_m = 1.10$ and $V_M = 0.11$ [21]. The coefficient F_m represents the mean value of the fabrication factor, and its statistics have been determined as $F_m = 1.00$ and $V_F = 0.05$ [20]. The fabrication factor is representative of the geometric accuracy of the component in question.

Incorporating the above data for M, F, and P and their coefficients of variation gives the following values for R_m and V_R using Equations 8.1 and 8.2, respectively:

$$R_m = 1.10R_n$$

$$V_R = 0.125$$

The resistance factor, ϕ, is given by the expression [19, 20]:

$$\phi = \exp(-0.55\beta V_R)\frac{R_m}{R_n} \qquad (8.3)$$

All terms in this expression have been determined in the preceding, except β, which represents the reliability index; an increasing value of β represents a decreasing probability of failure. It has been considered good practice to make connections stronger than the parts being joined in order to give ample warning of impending failure. On this basis, connections in general have been assigned a value of $\beta = 4.5$, while the members they connect (beams, columns, etc.) have been assigned a value of $\beta = 3.0$ [22]. Both of these values of β will be used to calculate the resistance factor, to obtain a range of values for this factor. From Equation 8.3, the values for ϕ are:

For $\beta = 4.5$: $\phi = 0.81$

For $\beta = 3.0$: $\phi = 0.89$

From these results, an average value for the resistance factor of $\phi = 0.85$ would be acceptable, considering the low variability in the strength model.

CHAPTER 9

APPLICATION OF BLOCK-SHEAR TO DESIGN OF GUSSET PLATES

9.1 Development of Design Curves

The strength model proposed in Chapter 7 lends itself well to the preliminary design of gusset plates. For instance, Equations 7.5, 7.6, and 7.7 can be combined into one expression relating plate thickness to the variables R_n, S_{net}, ℓ, F_y, and F_u. For a given type of steel, F_y and F_u are known, so the expression relates the gusset plate thickness directly to nominal strength (R_n) and connection size (S_{net} and ℓ).

The above concepts have been applied for gusset plates of A36 steel (F_y = 36 ksi and F_u = 58 ksi) and is shown in Figure 9.1, in which R_n/t has been plotted as a function of ℓ and S_{net}. The result is a family of parabolas, since the strength model is a function of ℓ^2. Interpolation between parabolas (fixed values for S_{net}) is linear, since the strength model is a linear function of S_{net}. These design curves can be constructed for any type of steel, but A36 is probably the most common steel grade used for detail material.

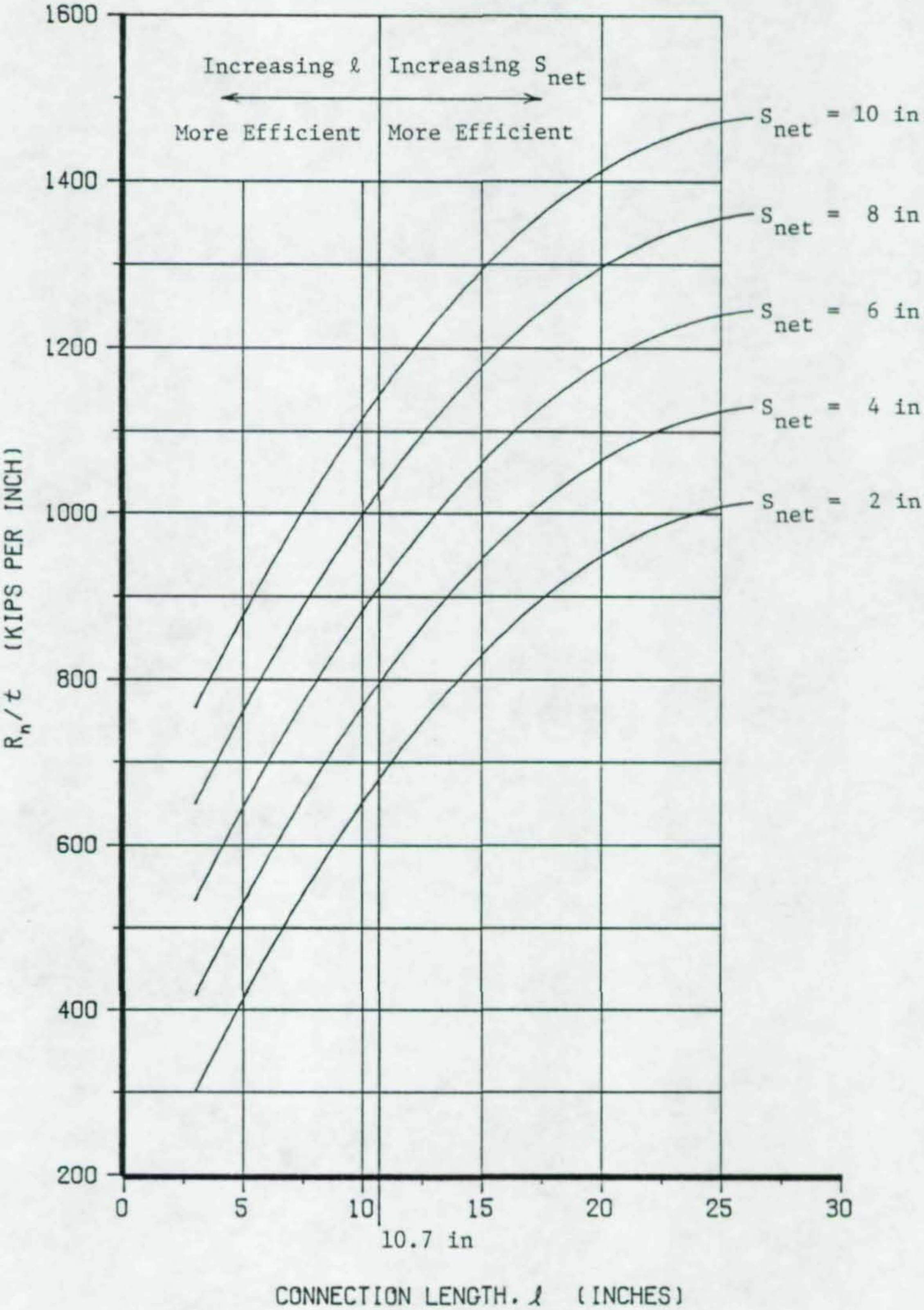

Figure 9.1 Design Curves for A36 Steel Plate Material

Figure 9.1 shows that as the length of a connection increases, the rate of increasing gusset plate capacity decreases. This suggests that it is more efficient to increase the outside bolt gage (S_{net}) for connections longer than 10.7 inches, if possible. Since data is only available for connections up to 25 inches in length, it is not recommended that interpolation be extended beyond this limit.

9.2 Illustrative Analysis and Design Problem

Figure 9.1 can be used in either of two ways: 1) if t has previously been chosen, then the connection size (ℓ and S_{net}) can be determined; or 2) if the connection size has been determined, then the necessary gusset plate thickness can be obtained. Either way, many combinations of gusset plate thickness and connection size can be checked quickly to determine the best design for the gusset plate connection.

For the purpose of illustration, consider the design of the gusset plate connection shown in Figure 9.2. It has been determined that two angles 8x6x1/2 with 12 A325 bolts in two lines (six bolts per line) will be adequate, using the proposed LRFD specification [23]. To aid in the gusset plate design, it has also been determined that the minimum connection length for spacing requirements is 14.5 inches, and the possible range of S_{net} is 1.4375 inches $\leq S_{net} \leq$ 4.6875 inches, due to spacing requirements [23]. Many combinations are possible, but since the minimum connection length (14.5 inches) is greater than 10.7 inches, the maximum value for S_{net}, 4.6875 inches, would be most efficient. With ℓ = 14.5 inches and S_{net} = 4.6875 inches, Figure 9.1 gives a value of R_n/t = 970 kips/inch. Therefore:

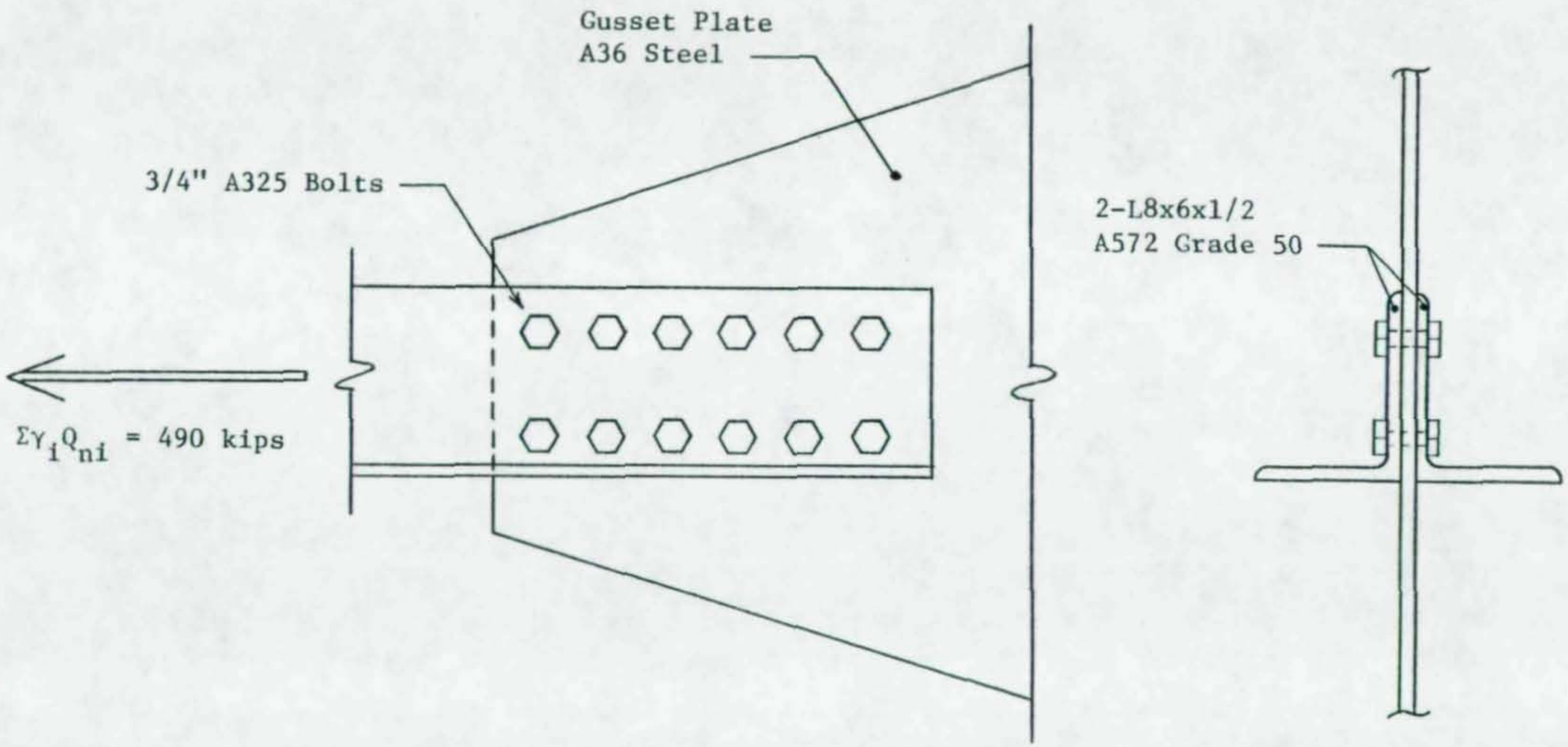

Figure 9.2 Details of the Gusset Plate Connection to be Designed

$$\frac{\Sigma\gamma_i Qni = 490 \text{ kips}}{t} \leq \frac{\phi R_n}{t} = 970 \text{ kips/in.}$$

A value of $\phi = 0.85$ as determined from Chapter 8 is used to obtain the necessary plate thickness:

$$t \geq \frac{490 \text{ kips}}{\phi 970 \text{ kips/in.}} = \frac{490 \text{ kips}}{(0.85)(970 \text{ kips/in.})} = 0.594 \text{ in.}$$

Therefore, a gusset plate thickness of 5/8 inches (0.625 in.) is adequate, and a total connection length, $\ell = 14.5$ inches and outside bolt gage, $S = 5.5$ inches could be used.

If a thinner gusset plate must be used, say 9/16 inches, the required value of R_n/t is:

$$\frac{\Sigma\gamma_i Qni}{\phi t} = \frac{490 \text{ kips}}{(0.85)(9/16 \text{ in.})} = 1025 \text{ kips/in.} \leq \frac{R_n}{t}$$

With this value for R_n/t and $S_{net} = 4.6875$ inches, Figure 9.1 gives the required total gusset connection length as $\ell = 16.5$ inches.

For the analysis problem, the design with the 9/16 inch thick gusset plate will be checked. From Equation 7.7,

$$C_\ell = 0.95 - 0.047(16.5) = 0.175$$

The effective stress becomes, from Equation 7.6,

$$F_{eff} = (1 - 0.175(36) + (0.175(58) = 39.9 \text{ ksi.}$$

The nominal strength is then given by Equation 7.5 as:

$$R_n = (58)[5.5 - (13/16)](9/16) + 1.15(39.9)(16.5)(9/16)$$
$$= 578.8 \text{ kips}$$

By the LRFD criterion, $\Sigma\gamma_i Qni \leq \phi R_n$:

$$490 \text{ kips} \leq (0.85)578.8 \text{ kips}) = 492 \text{ kips} \qquad \underline{\text{O.K.}}$$

Therefore, the gusset plate thickness and connection size are adequate.

This sample design and analysis problem demonstrates the ease with which gusset plate connections can be sized using the proposed procedure. Naturally, for the complete connection design, the limit state of yielding on the gross cross-section just below the last row of bolts, and the limit state of tensile failure on the net section at the last row of bolts must also be checked.

CHAPTER 10

SUMMARY AND RECOMMENDATIONS FOR FUTURE RESEARCH

10.1 Summary

This study has been concerned with the analysis of the results of ultimate strength tests performed during the present and previous studies, which leads to a design procedure for gusset plates loaded in tension.

The test results show that all failure modes consist of a tensile tear across the last row of bolts, with various stages of shear yielding along outside lines of bolts. The latter depends on the connection length.

Based on these observations, various block-shear models are developed, and the theoretical results of each model are compared to the observed ultimate strength. The block-shear model incorporating tensile ultimate stress on the net area between the last row of bolts and a uniform effective shear stress acting on the gross area along the outside bolt lines is selected as the most realistic ultimate strength model. The analyses based on this model show that the uniform effective shear stress can be expressed as a linear function of the connection length.

A final ultimate strength model is proposed, which incorporates the following parameters in the equations: plate thickness, connection length, net gage between outside bolt lines, and plate material tensile yield and tensile ultimate stress. This proposed strength model reliably predicts the ultimate strength of the 39 valid gusset plate tests to within a few percent of the actual ultimate strength. The accuracy of the proposed model is not affected by such factors as plate boundaries, fastener size, or edge distance to the first bolt holes.

Based on the equations for the ultimate strength model, typical design curves for A36 steel are presented to demonstrate the ease at which tensile gusset plate connections can be sized and gusset plate thicknesses selected to give maximum connection efficiency.

10.2 Recommendations for Future Research

The 39 gusset plate tests considered in the development of the final strength model have included a wide range of strength parameters. However, it may prove worthwhile to conduct similar additional tests, especially of connection length within the range of 10 to 16 inches.

This study did not address the problems of compressive gusset plate connections, nor the related problem of gusset plate buckling, which are important future considerations. Also, the combined effect on ultimate strength of multiple members framing into one gusset plate and gusseted connections in close proximity to boundary elements are important areas to investigate further.

APPENDIX A

LOAD-DEFORMATION DATA AND TEST
SPECIMEN FABRICATION DETAILS FOR THE
PRESENT STUDY

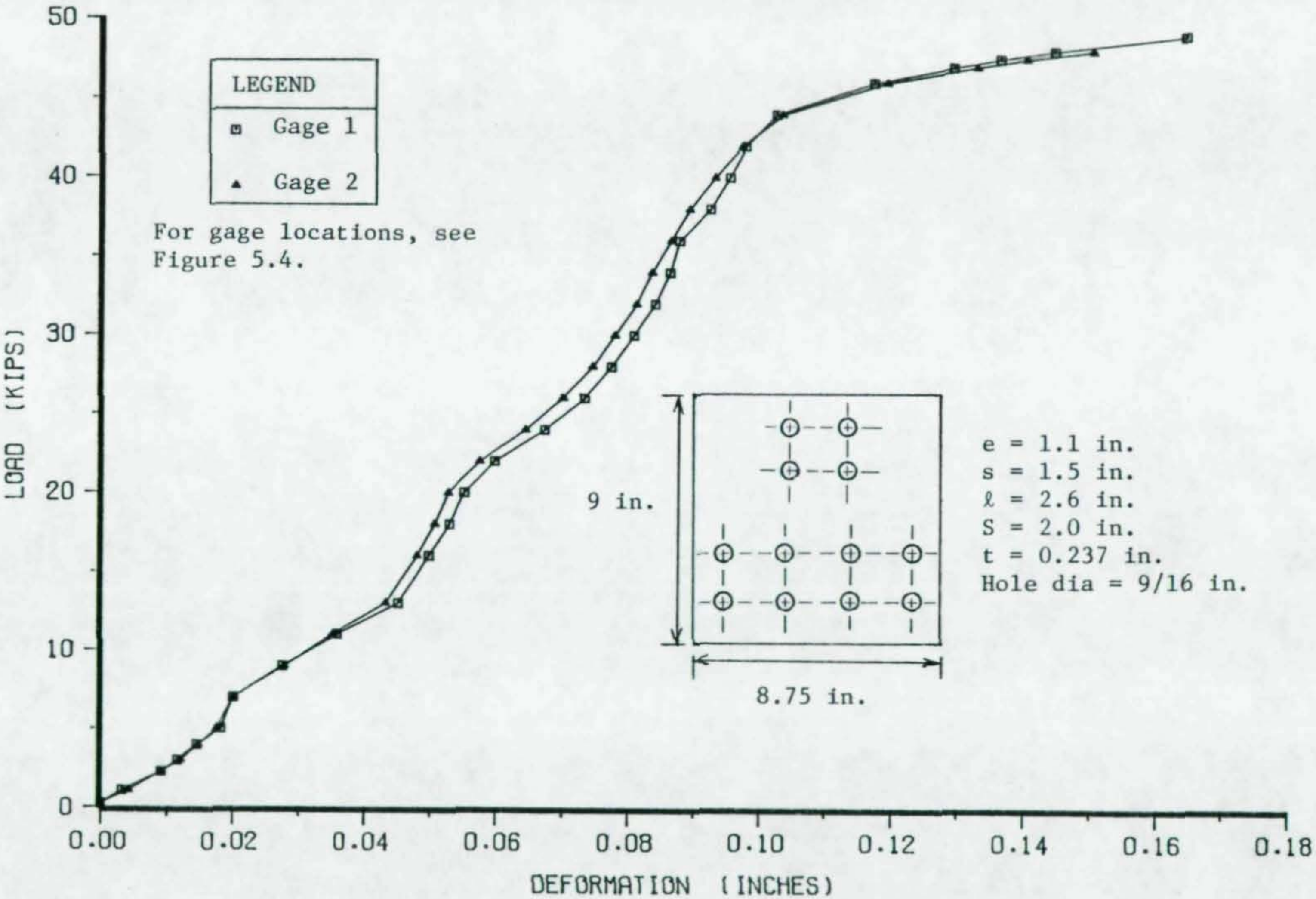

TEST PLATE 1. ULTIMATE STRENGTH = 54.6 KIPS.

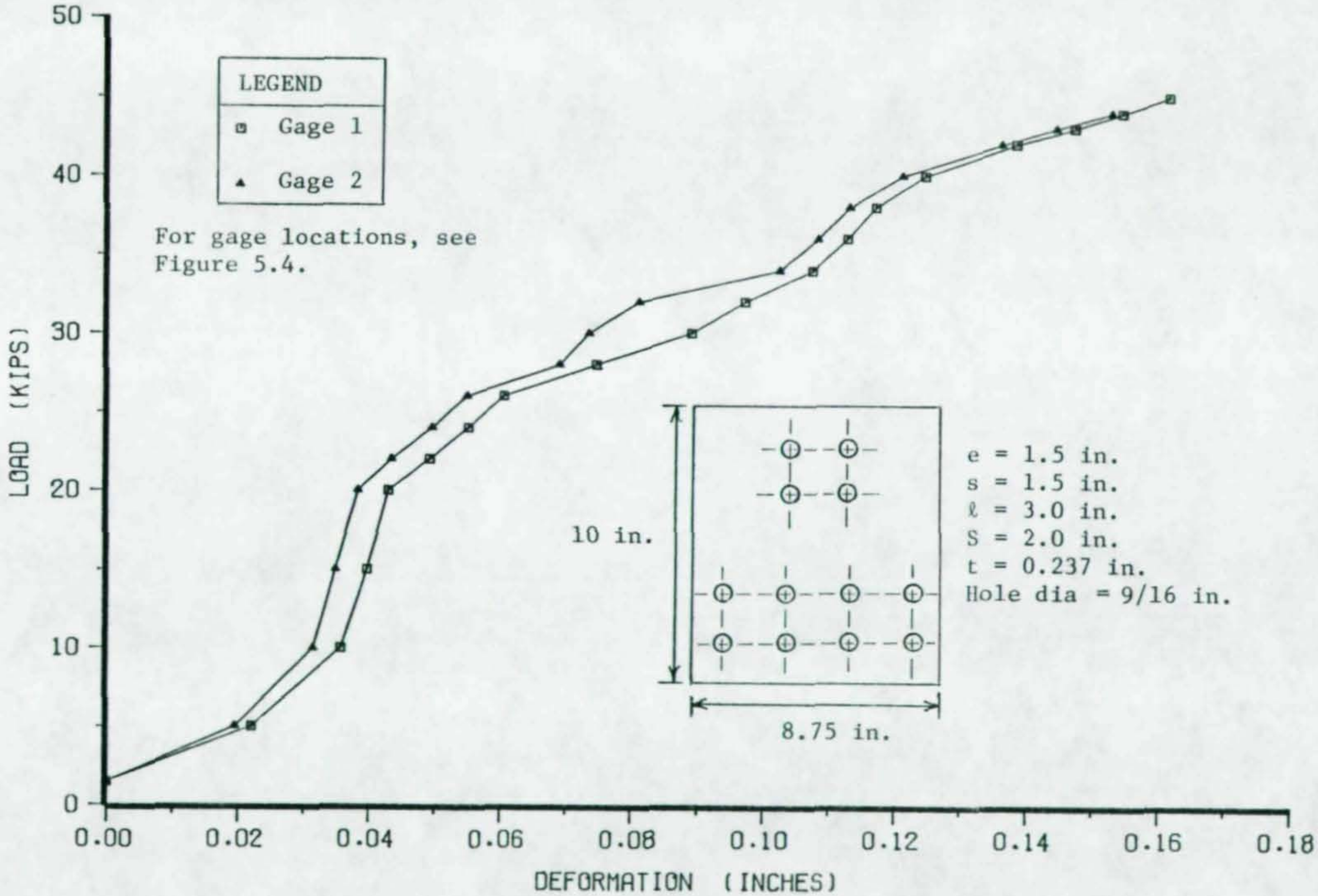

TEST PLATE 2. ULTIMATE STRENGTH = 55.2 KIPS.

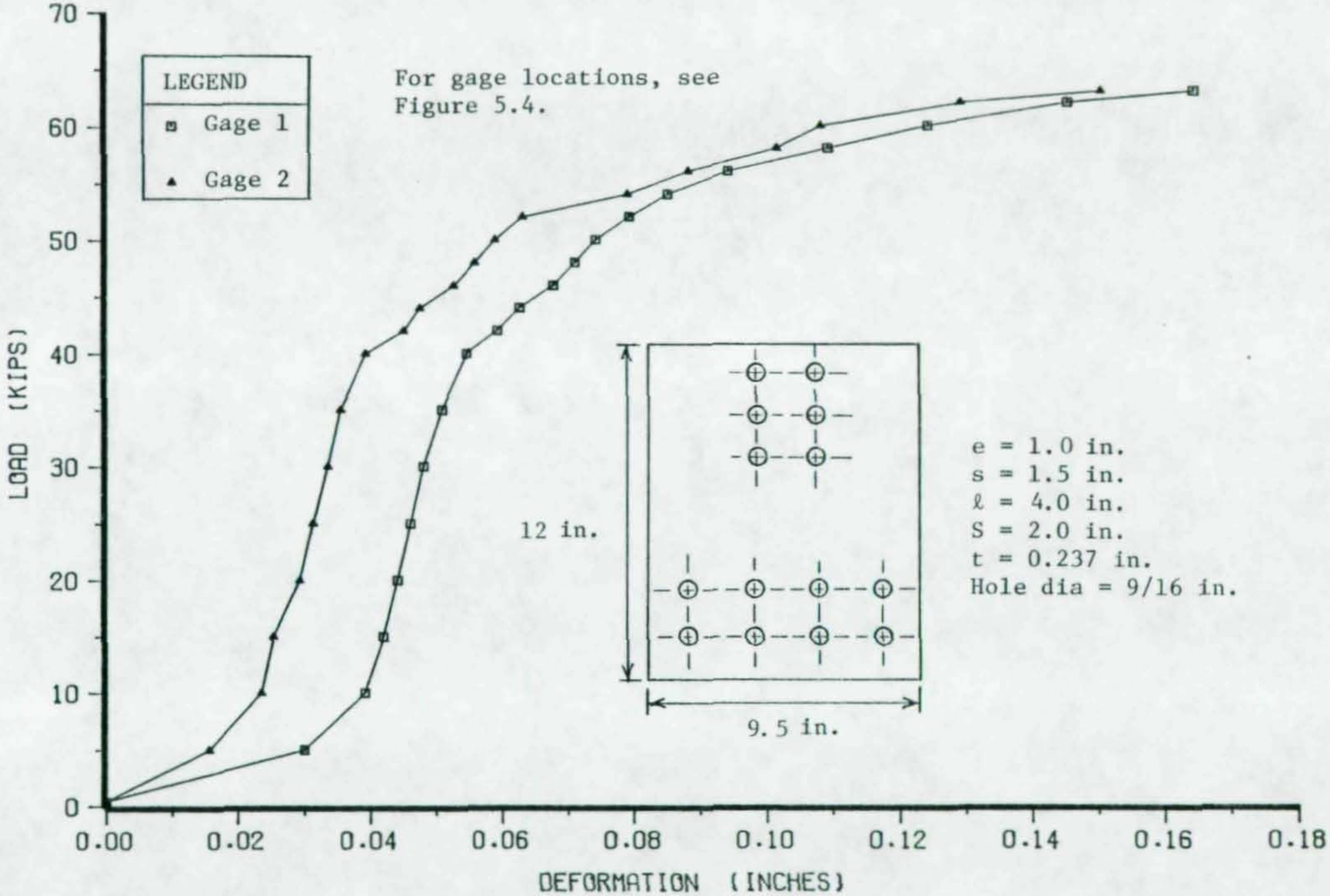

TEST PLATE 3. ULTIMATE STRENGTH = 67.6 KIPS.

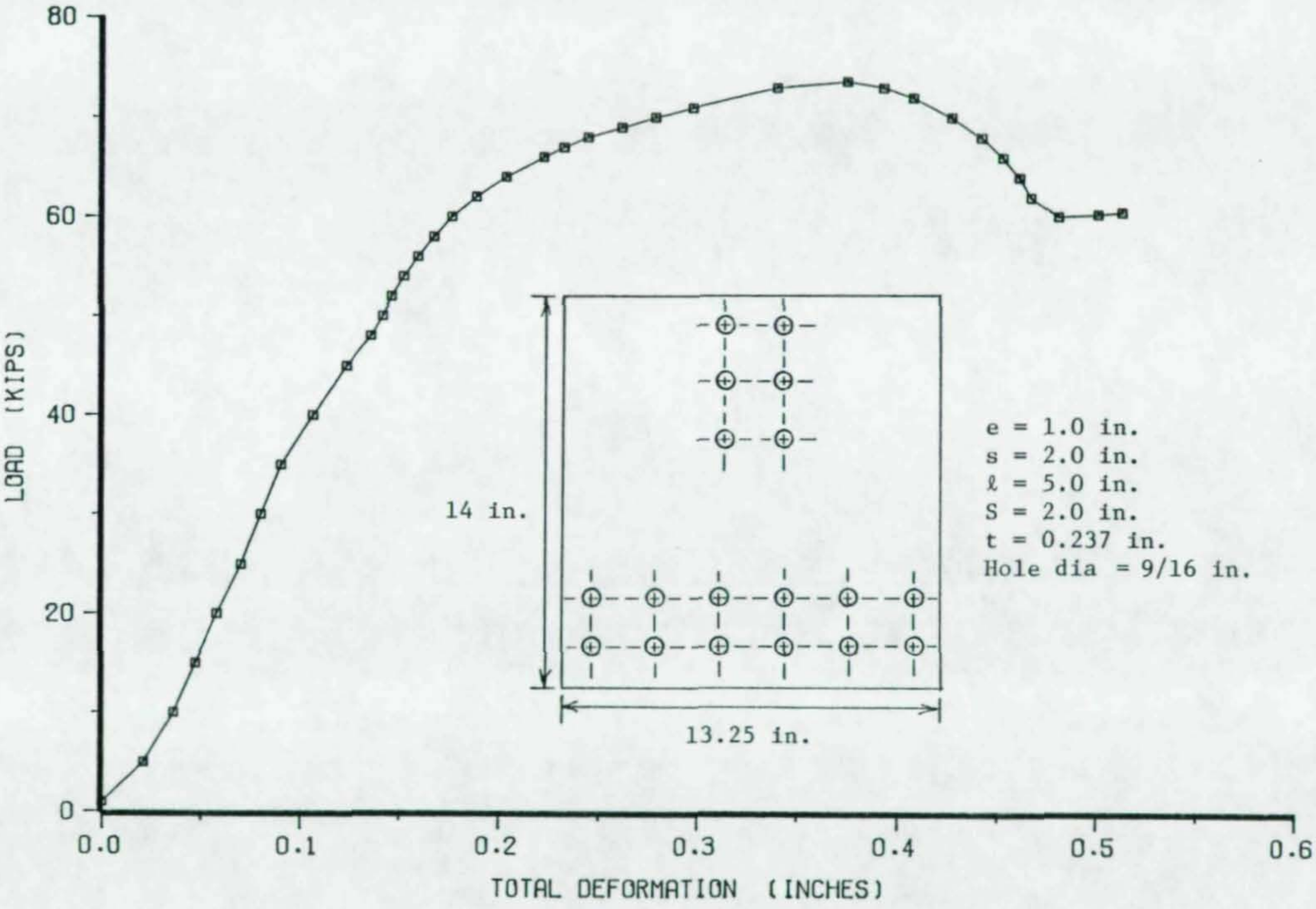

TEST PLATE 4. ULTIMATE STRENGTH = 73.6 KIPS.

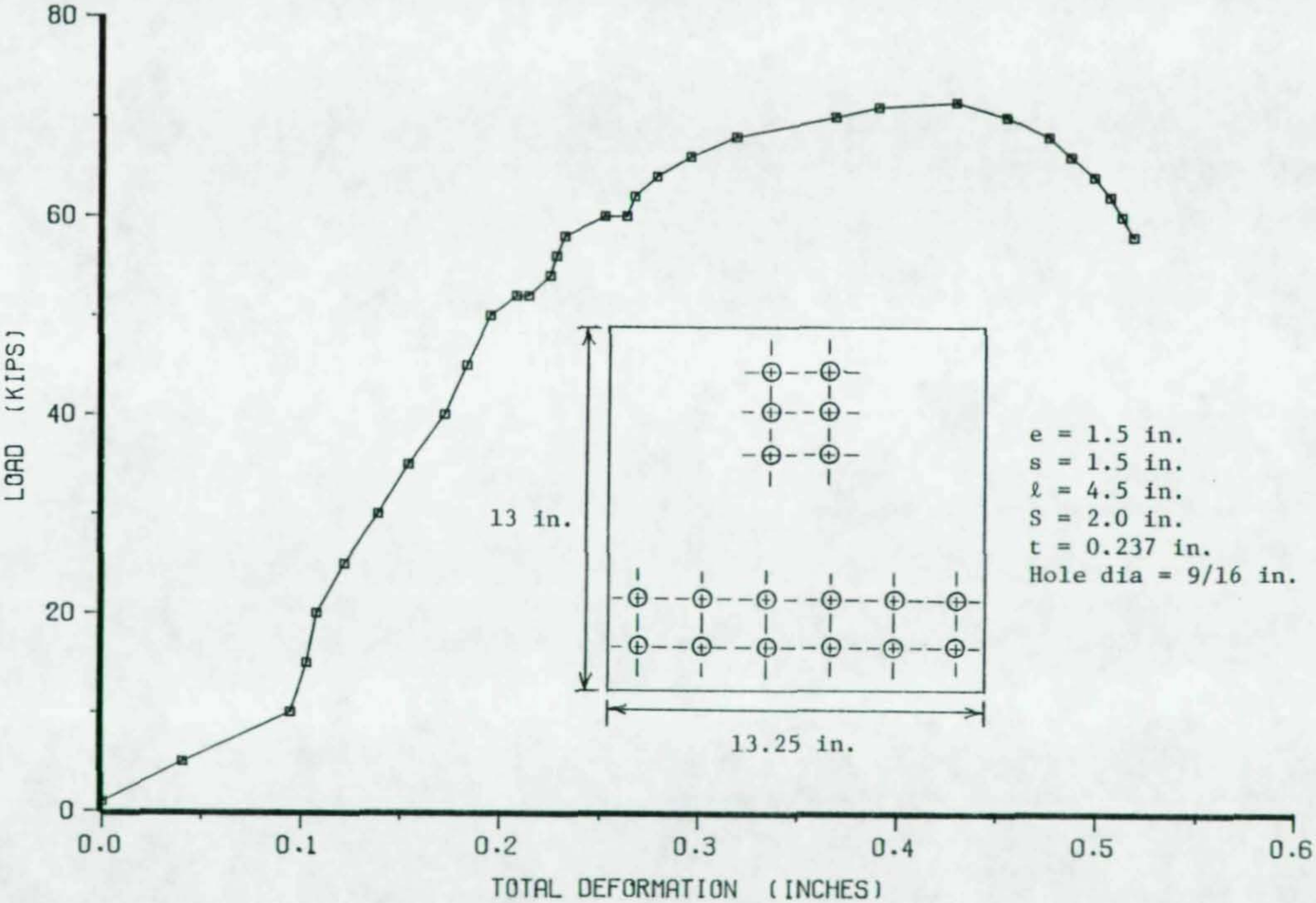

TEST PLATE 5. ULTIMATE STRENGTH = 71.5 KIPS.

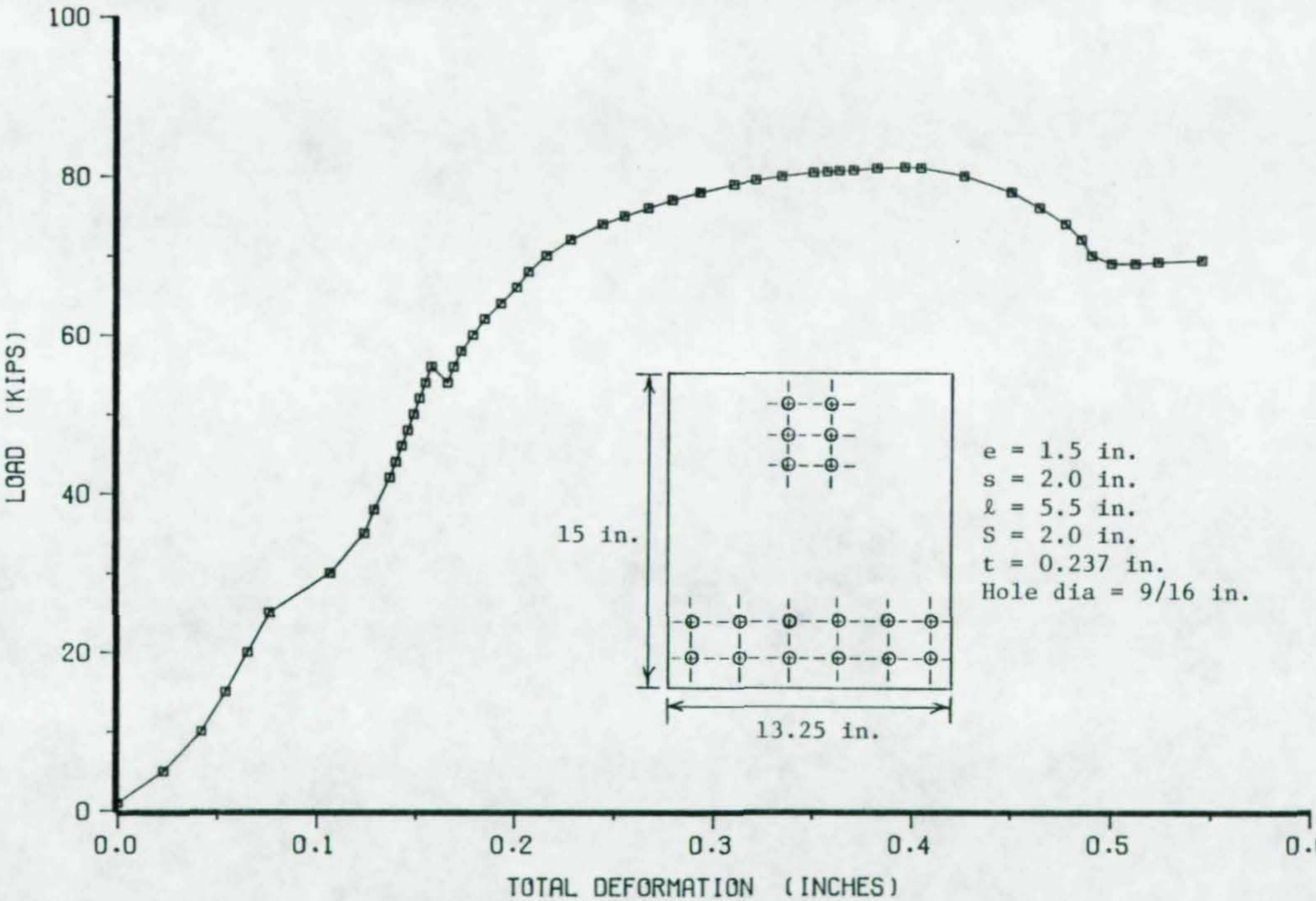

TEST PLATE 6. ULTIMATE STRENGTH = 81.1 KIPS.

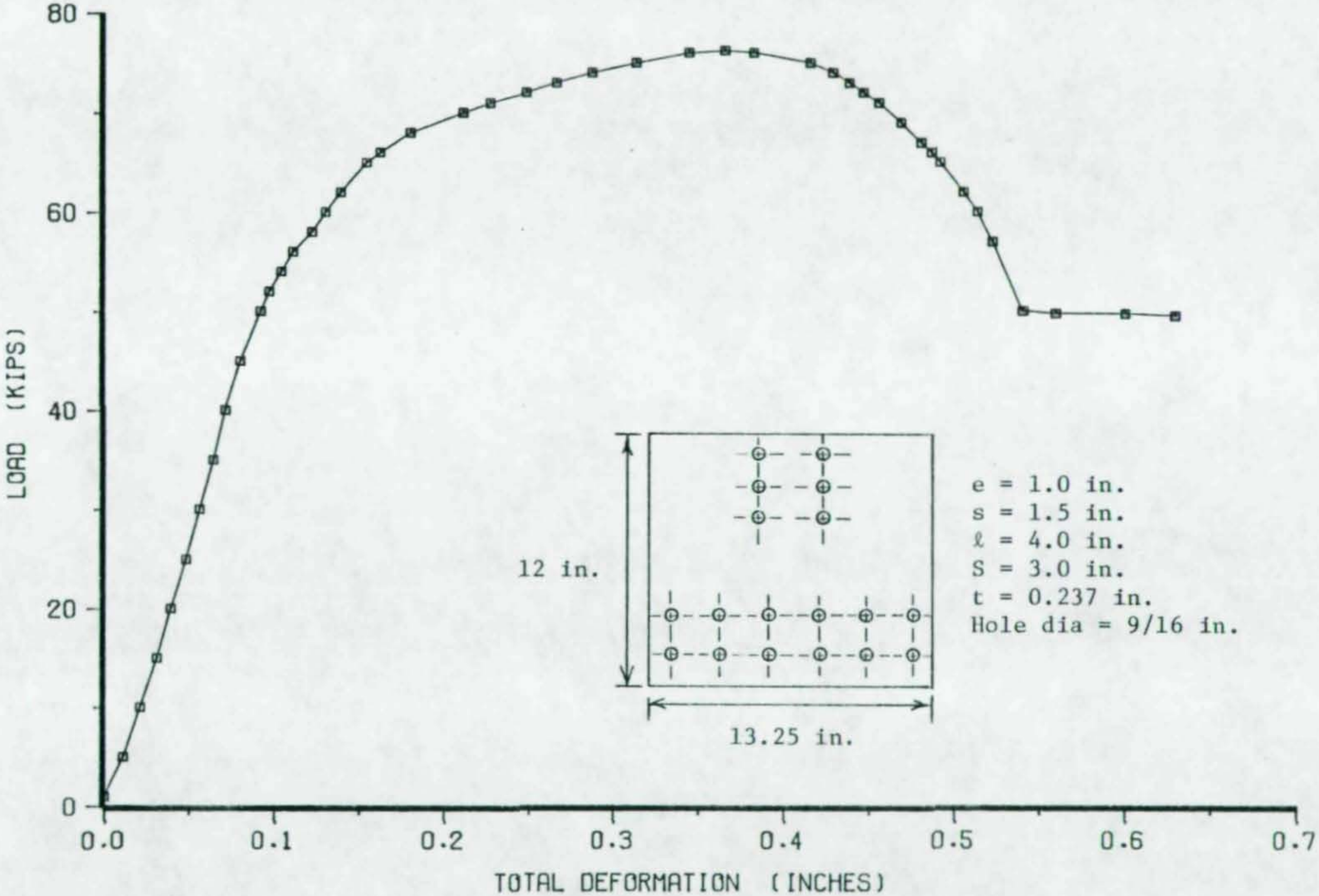

TEST PLATE 7. ULTIMATE STRENGTH = 76.2 KIPS.

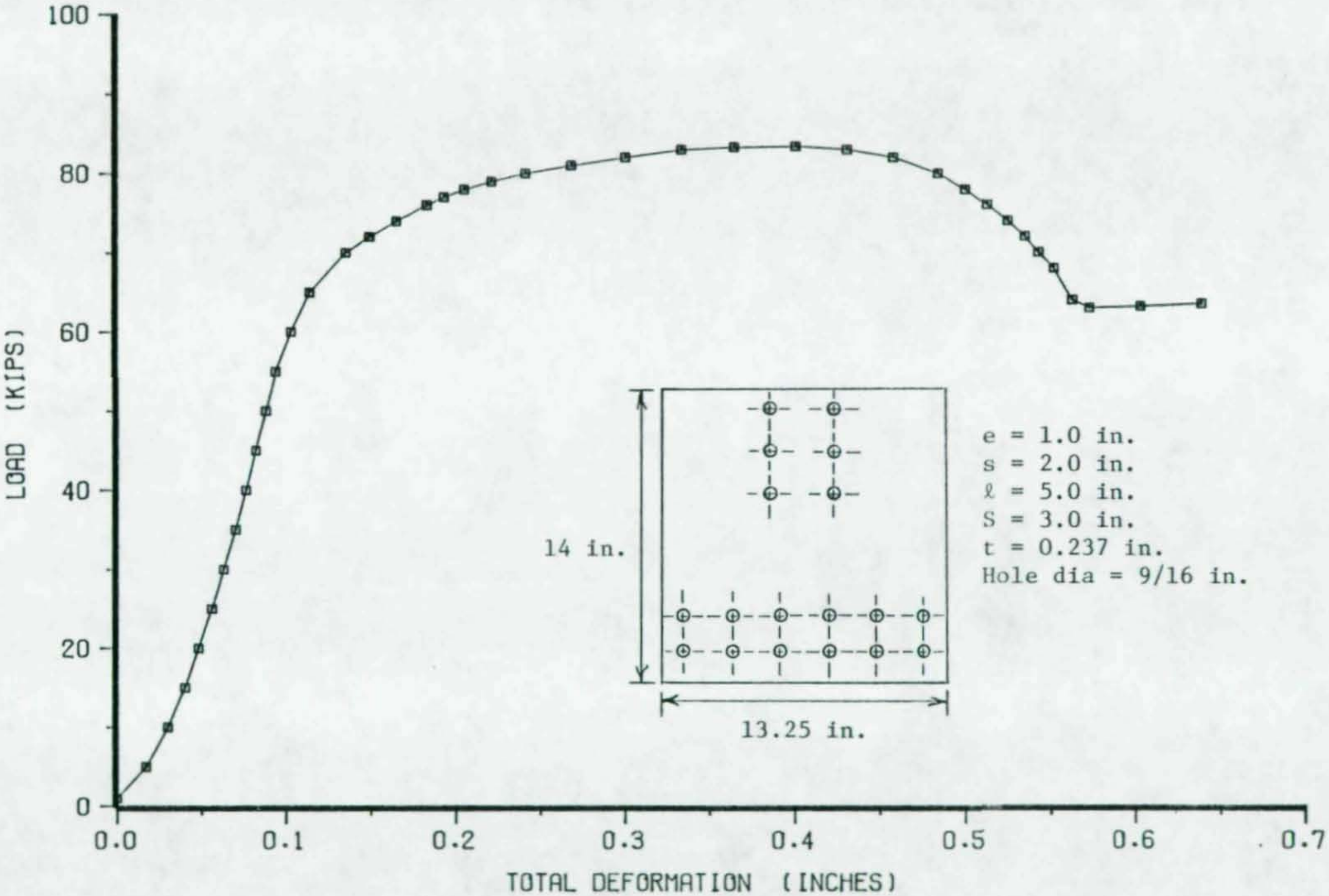

TEST PLATE 8. ULTIMATE STRENGTH = 83.4 KIPS.

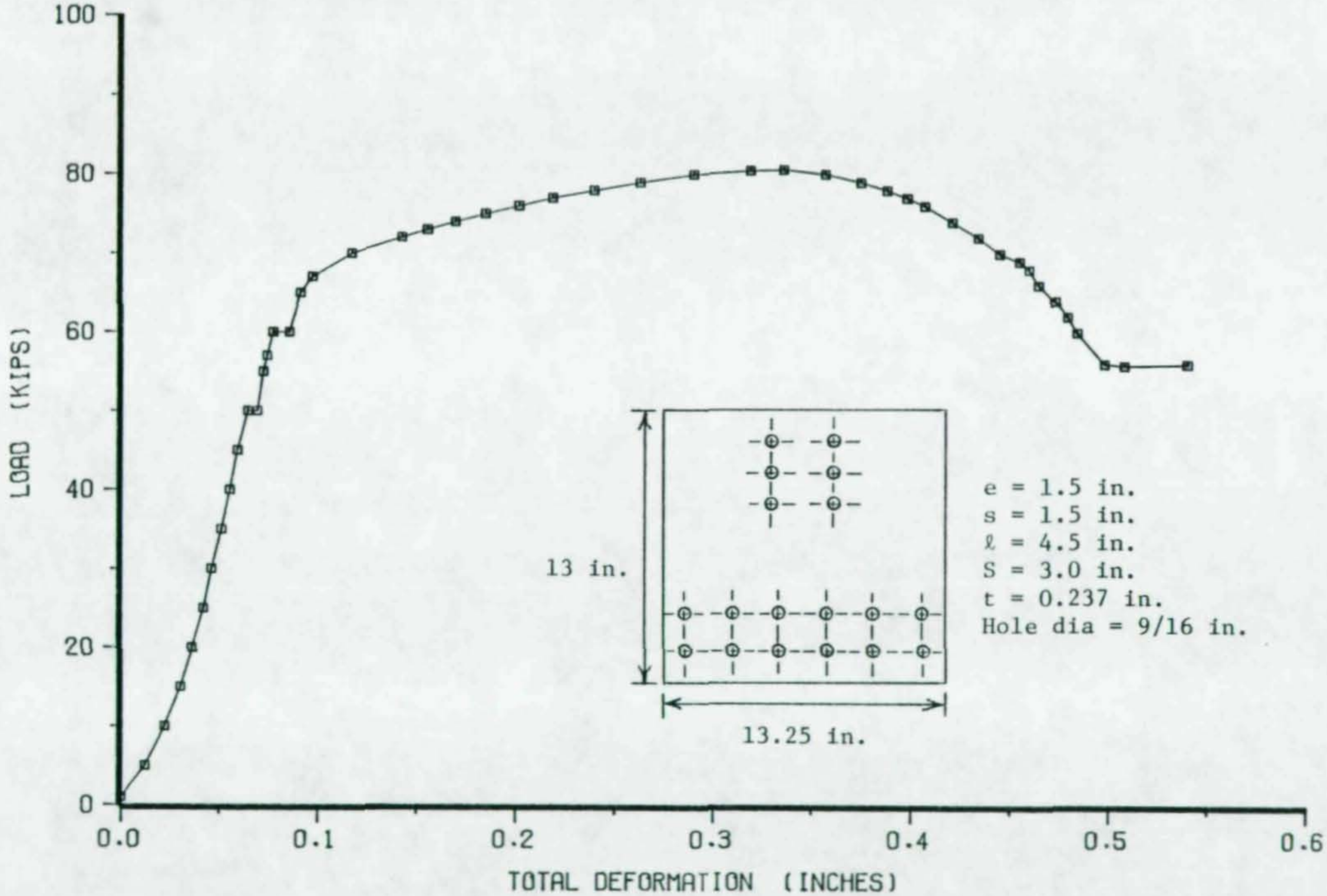

TEST PLATE 9. ULTIMATE STRENGTH = 80.6 KIPS.

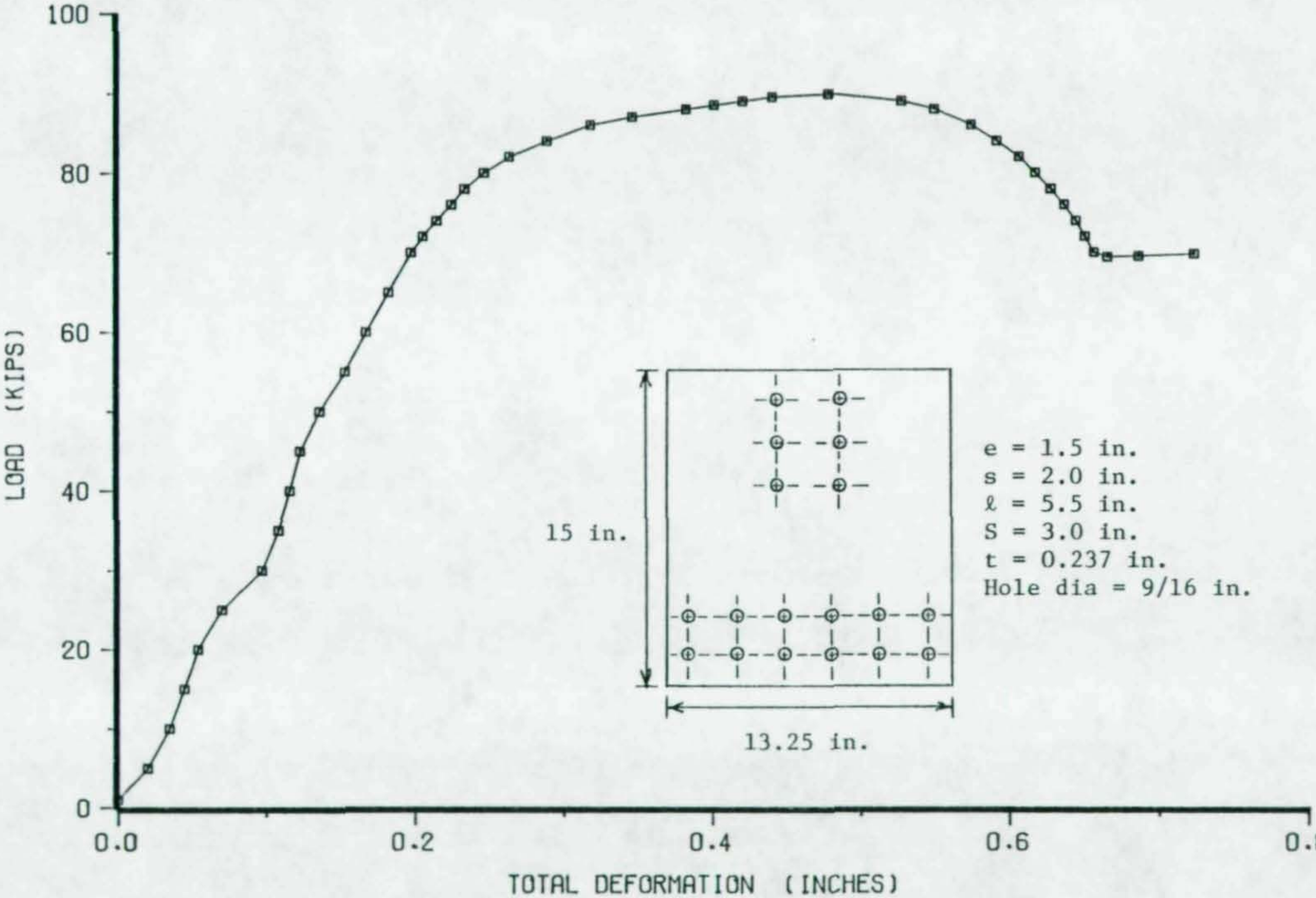

TEST PLATE 10. ULTIMATE STRENGTH = 89.9 KIPS.

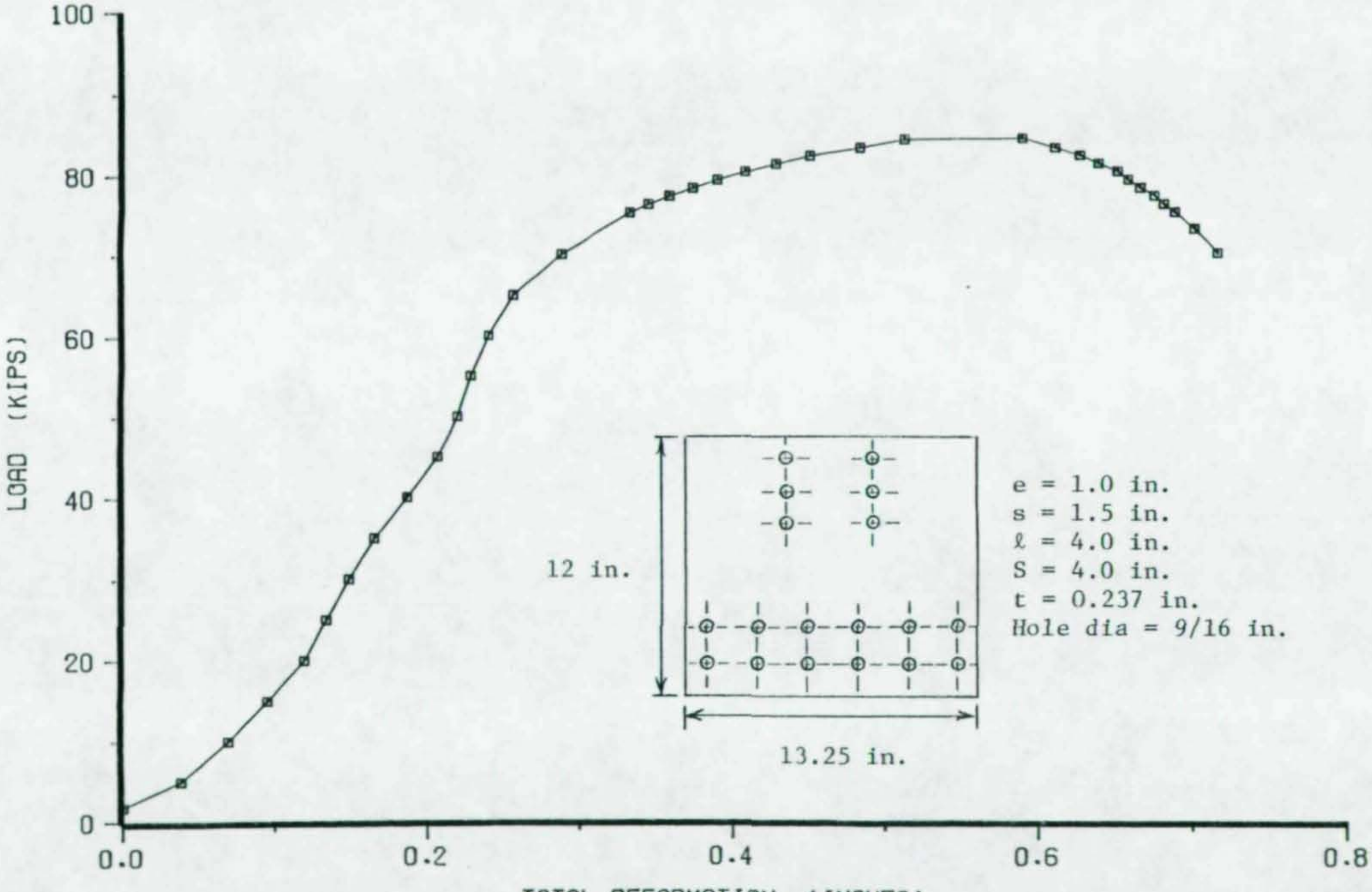

TEST PLATE 11. ULTIMATE STRENGTH = 84.2 KIPS.

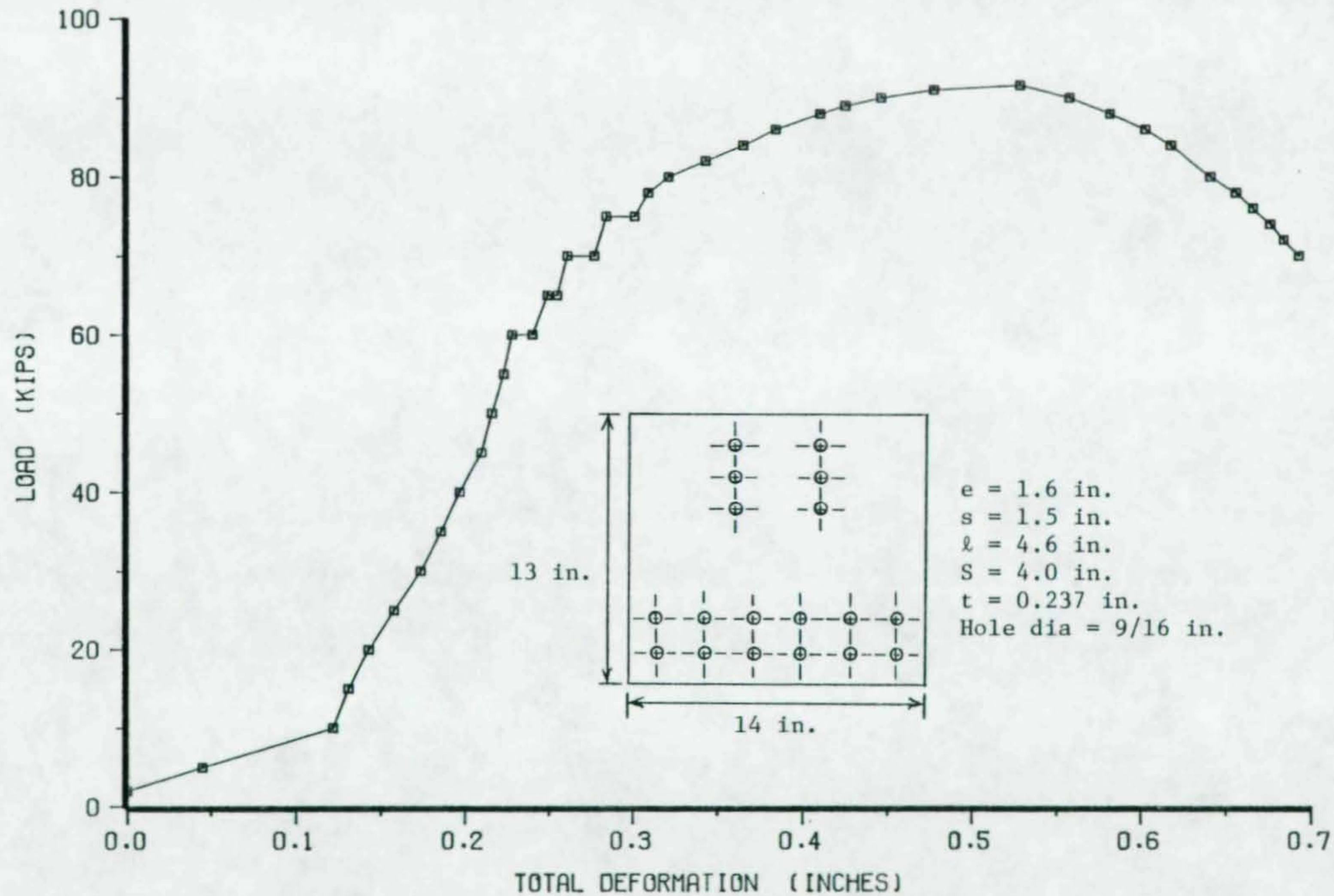

TEST PLATE 12. ULTIMATE STRENGTH = 91.6 KIPS.

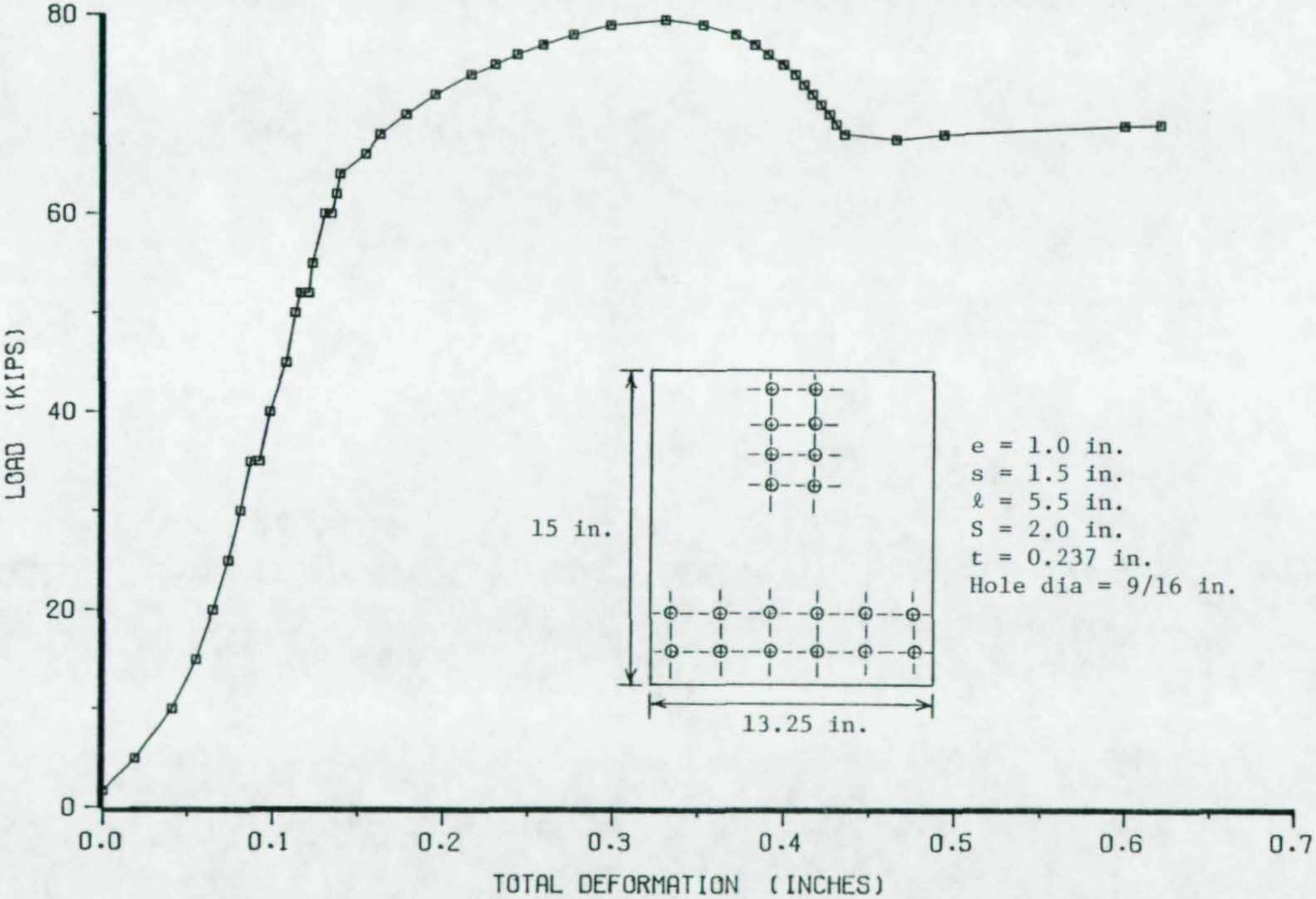

TEST PLATE 13. ULTIMATE STRENGTH = 79.5 KIPS.

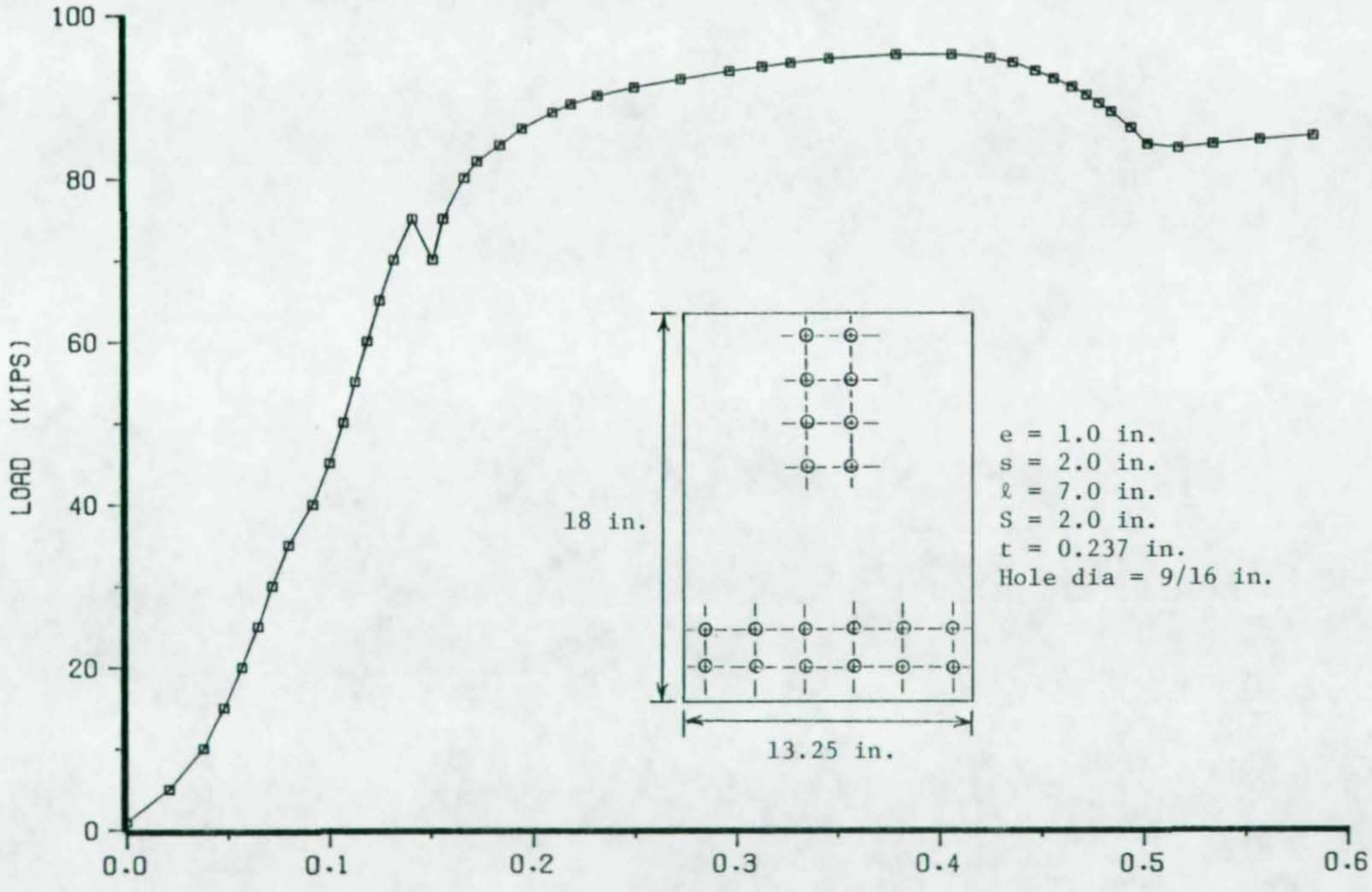

TEST PLATE 14. ULTIMATE STRENGTH = 95.0 KIPS.

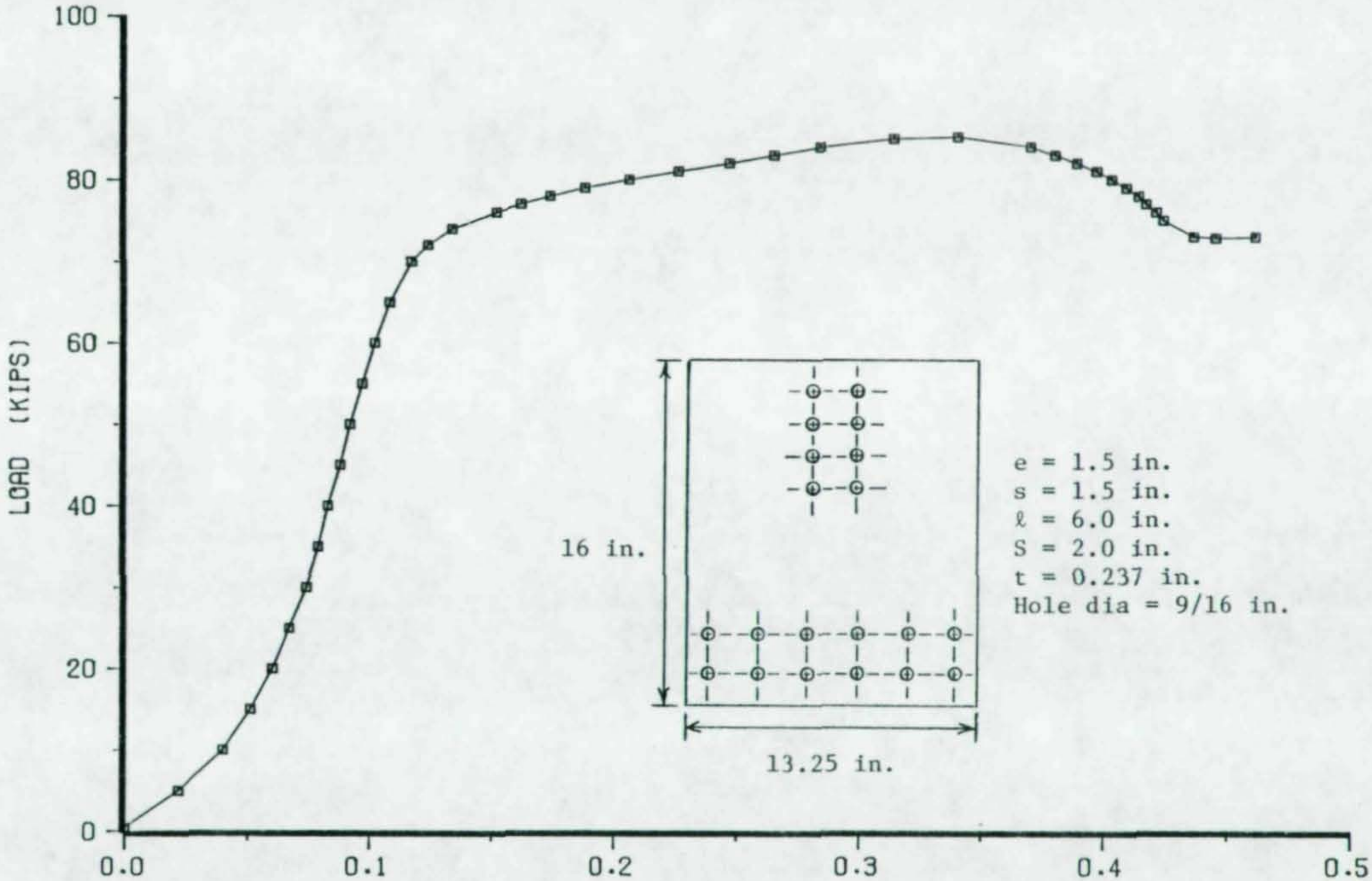

TEST PLATE 15. ULTIMATE STRENGTH = 85.2 KIPS.

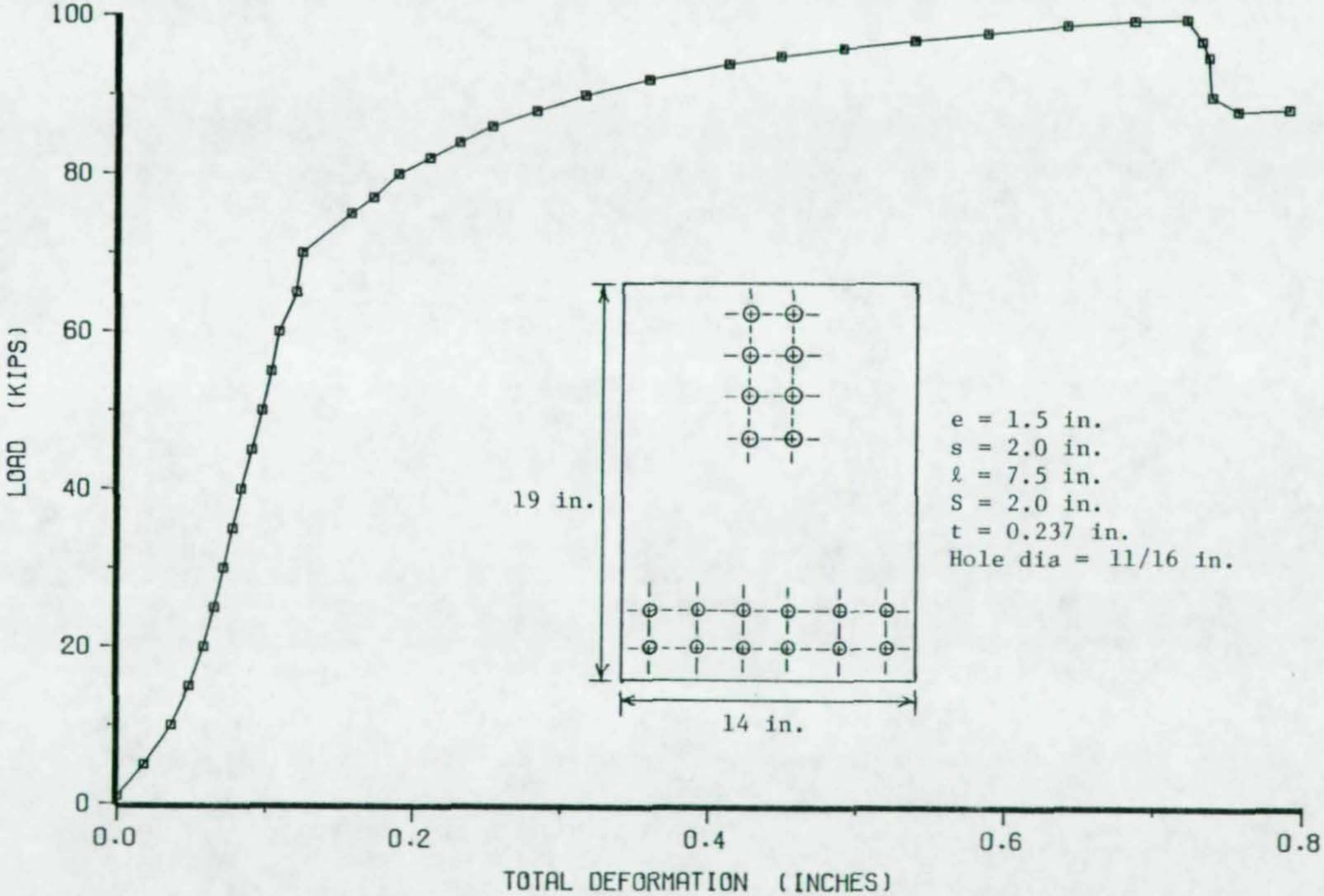

TEST PLATE 16. ULTIMATE STRENGTH = 99.8 KIPS.

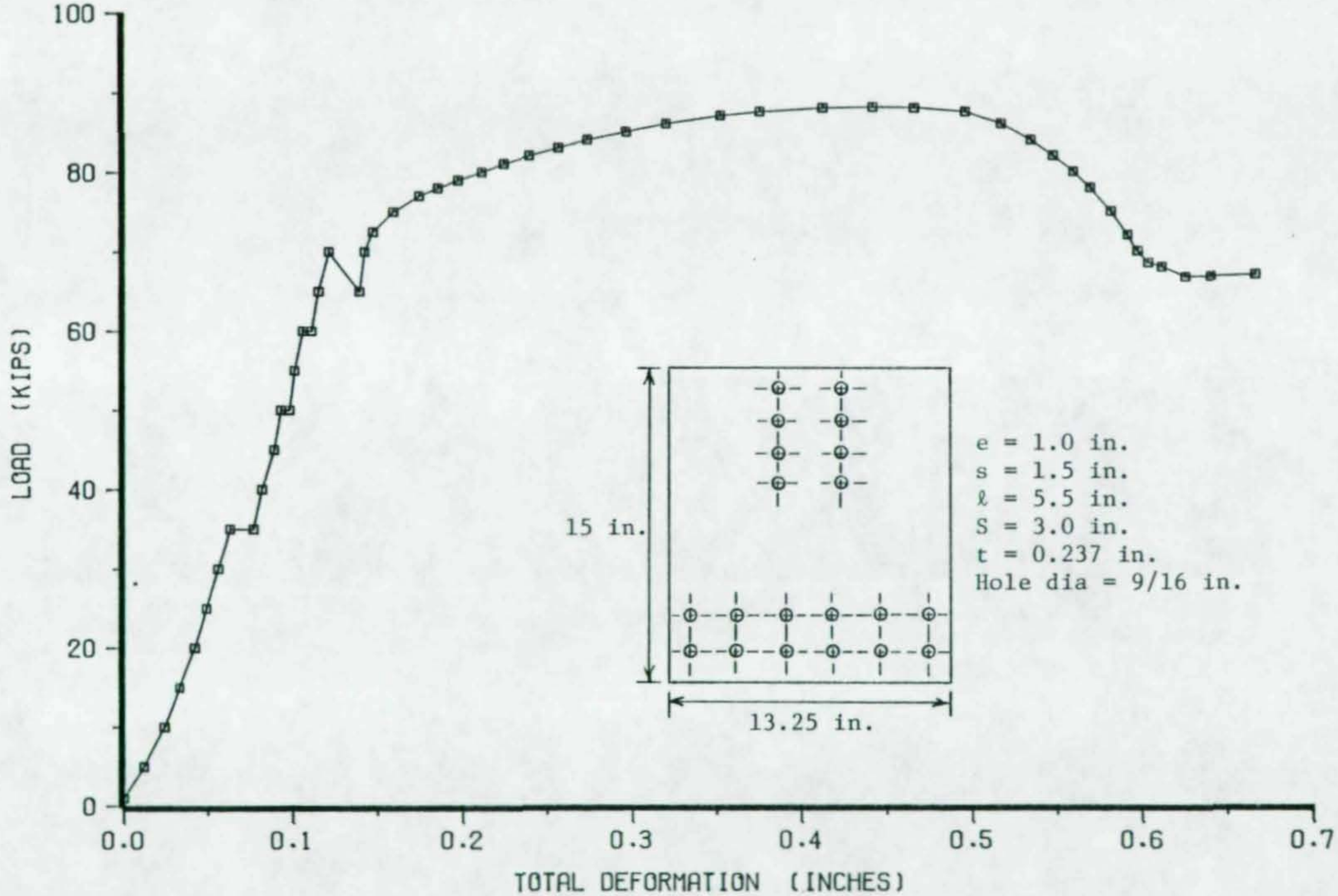

TEST PLATE 17. ULTIMATE STRENGTH = 88.1 KIPS.

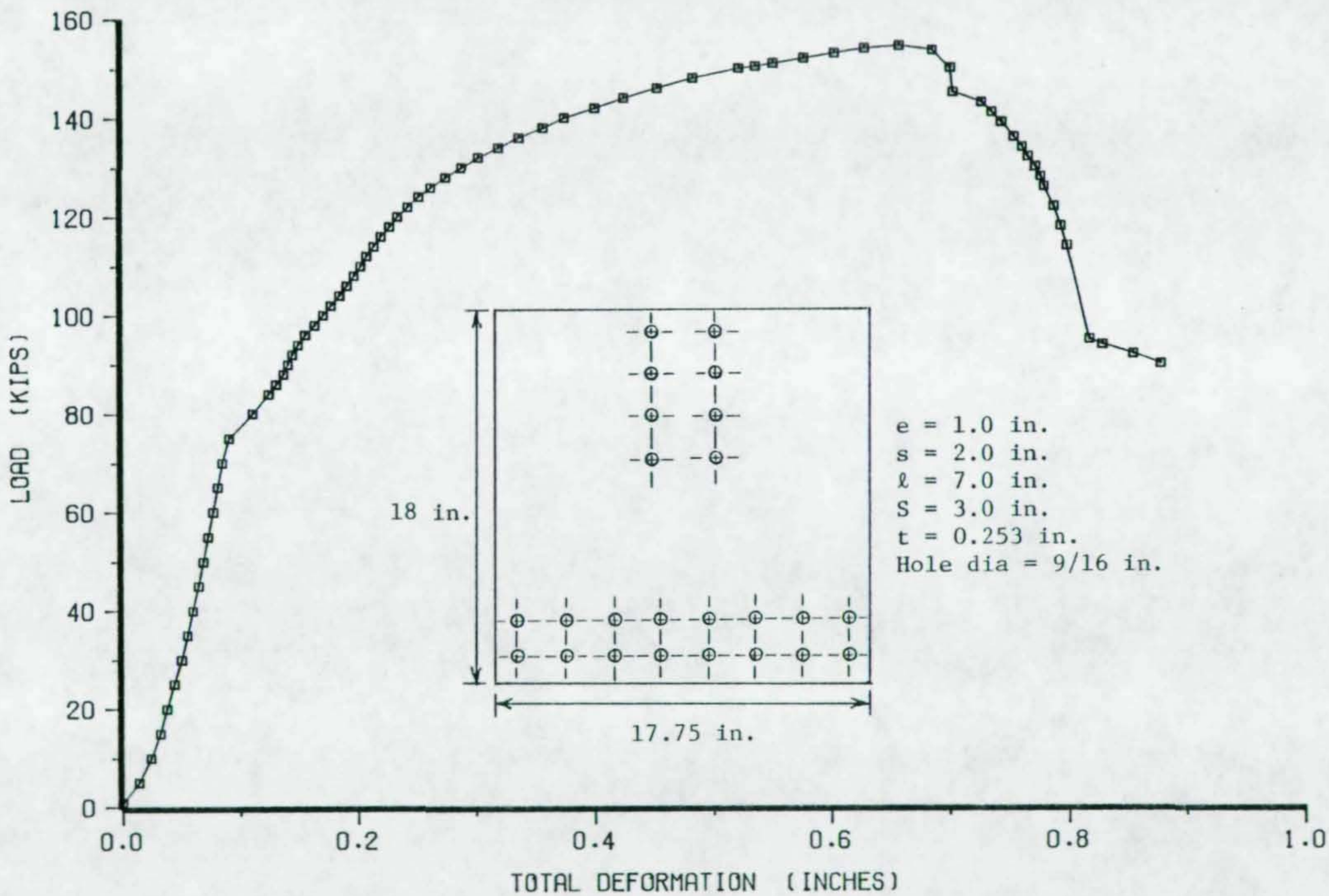

TEST PLATE 18. ULTIMATE STRENGTH = 154.5 KIPS.

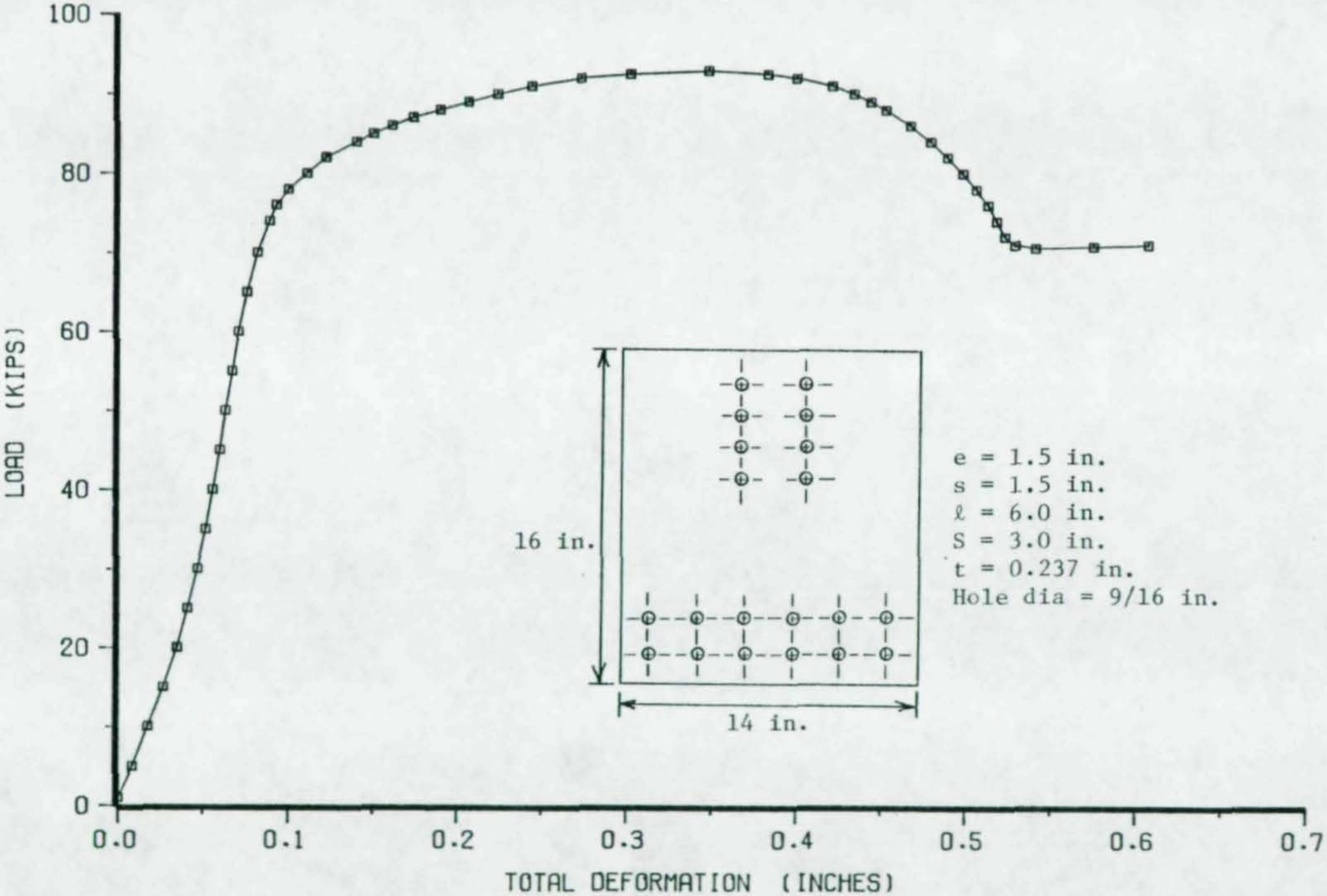

TEST PLATE 19. ULTIMATE STRENGTH = 92.9 KIPS.

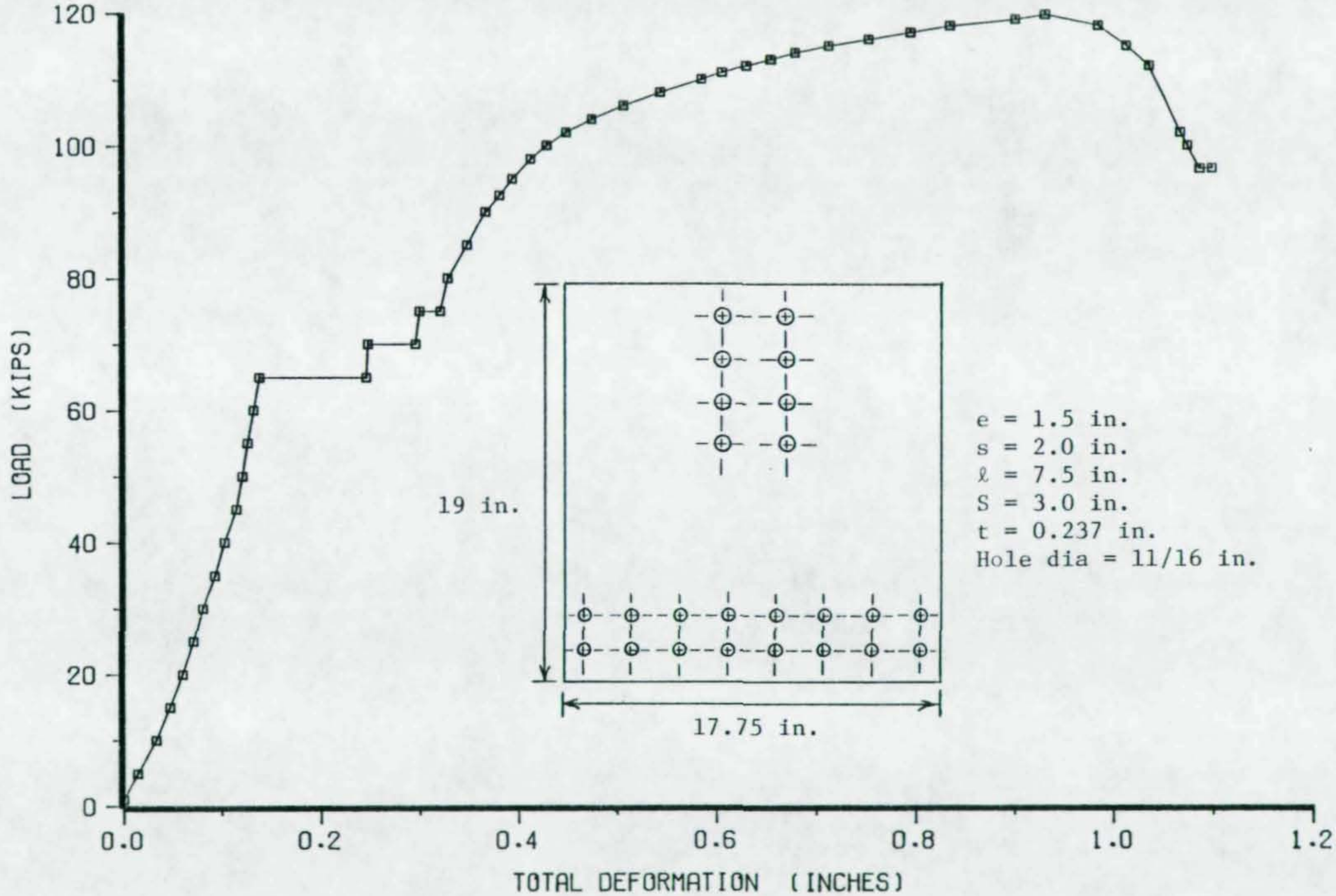

TEST PLATE 20. ULTIMATE STRENGTH = 119.7 KIPS.

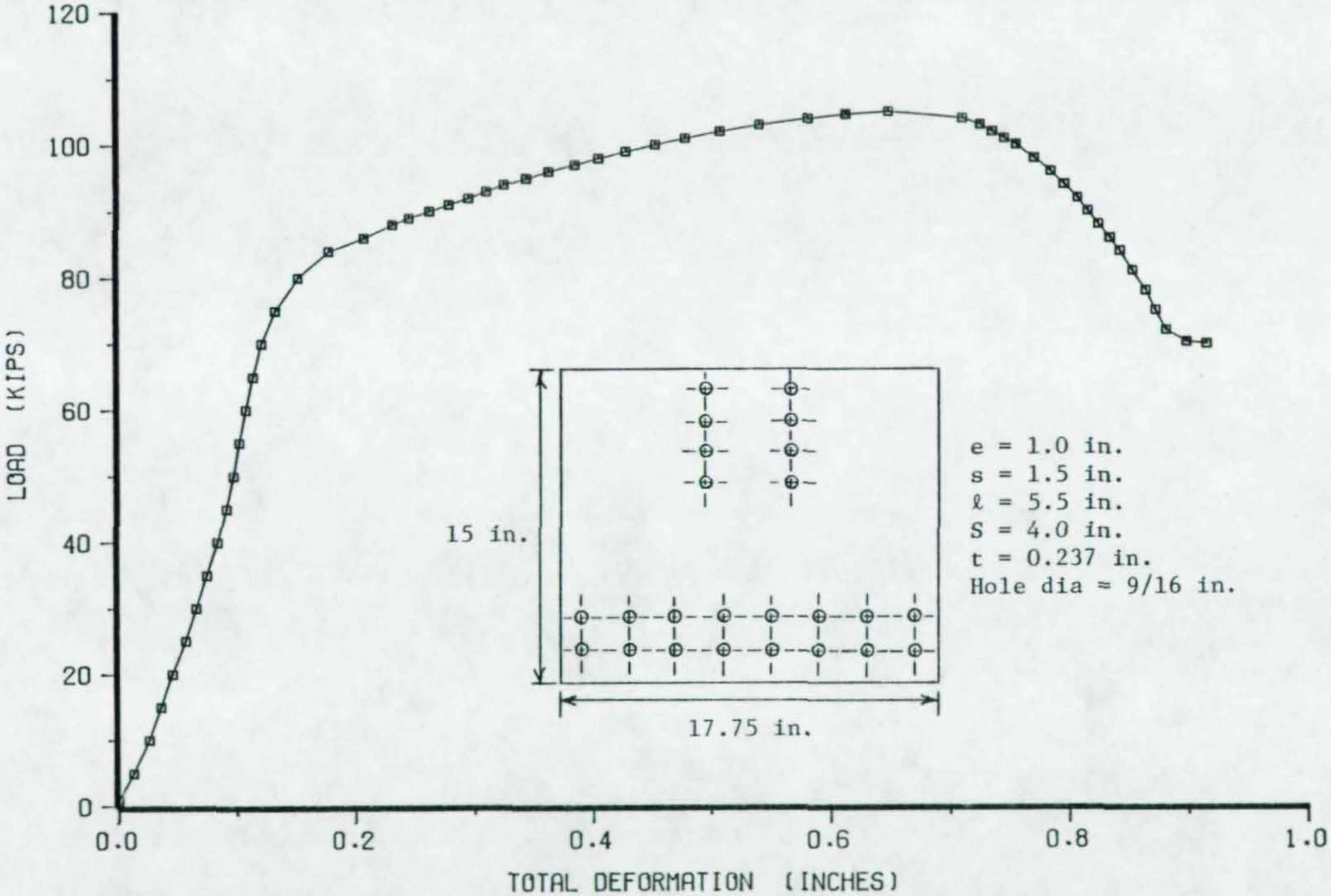

TEST PLATE 21. ULTIMATE STRENGTH = 105.0 KIPS.

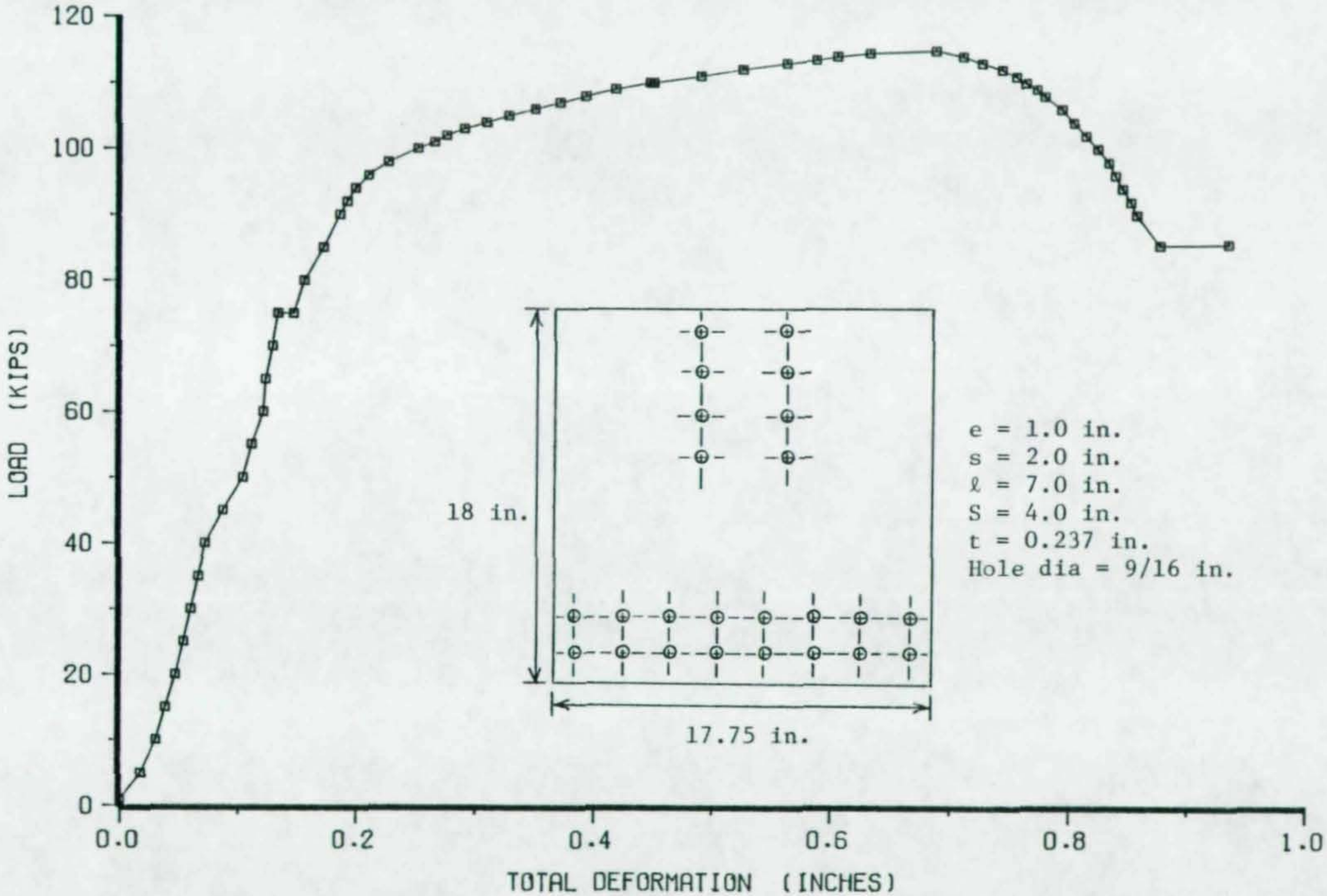

TEST PLATE 22. ULTIMATE STRENGTH = 114.9 KIPS.

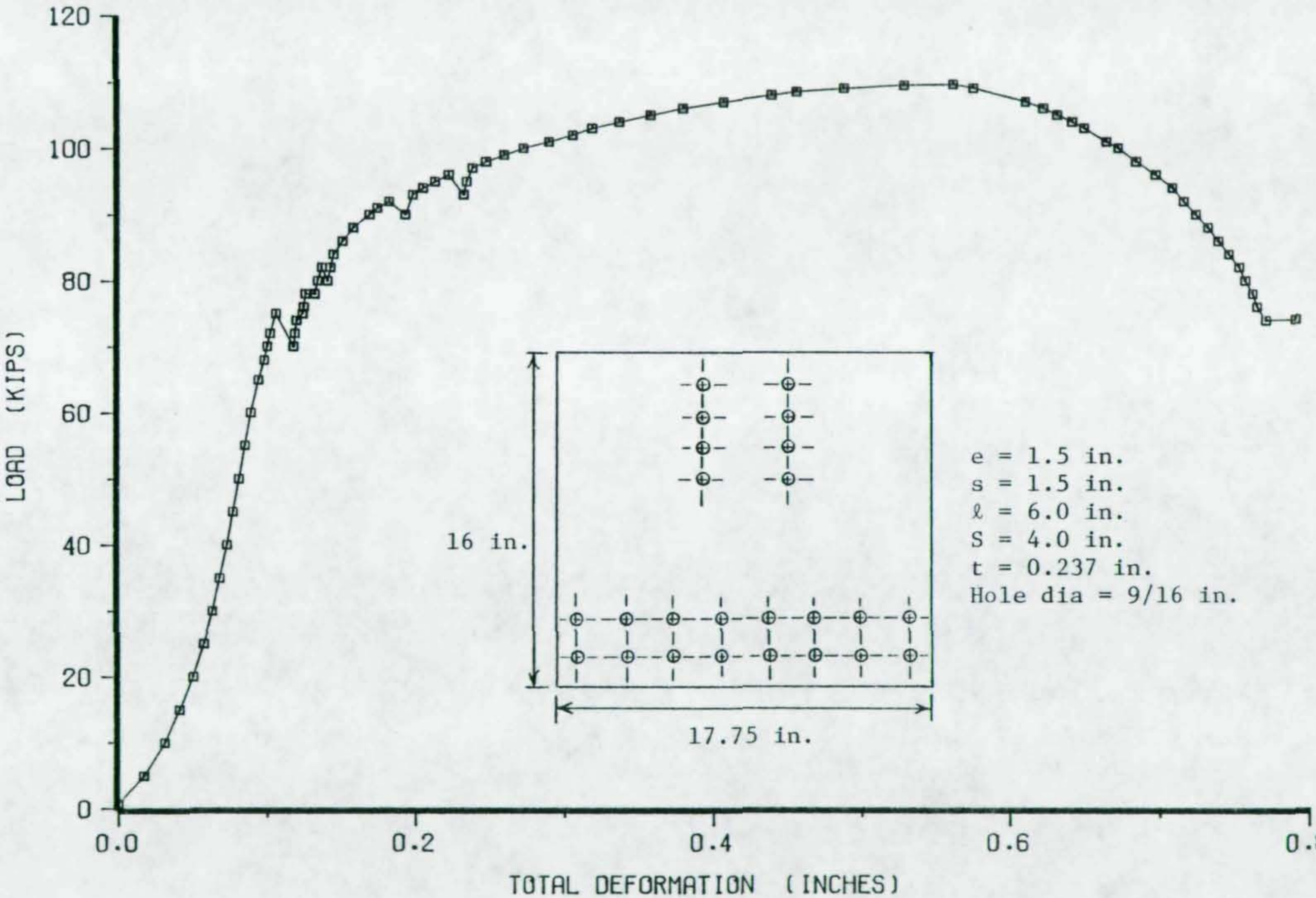

TEST PLATE 23. ULTIMATE STRENGTH = 109.6 KIPS.

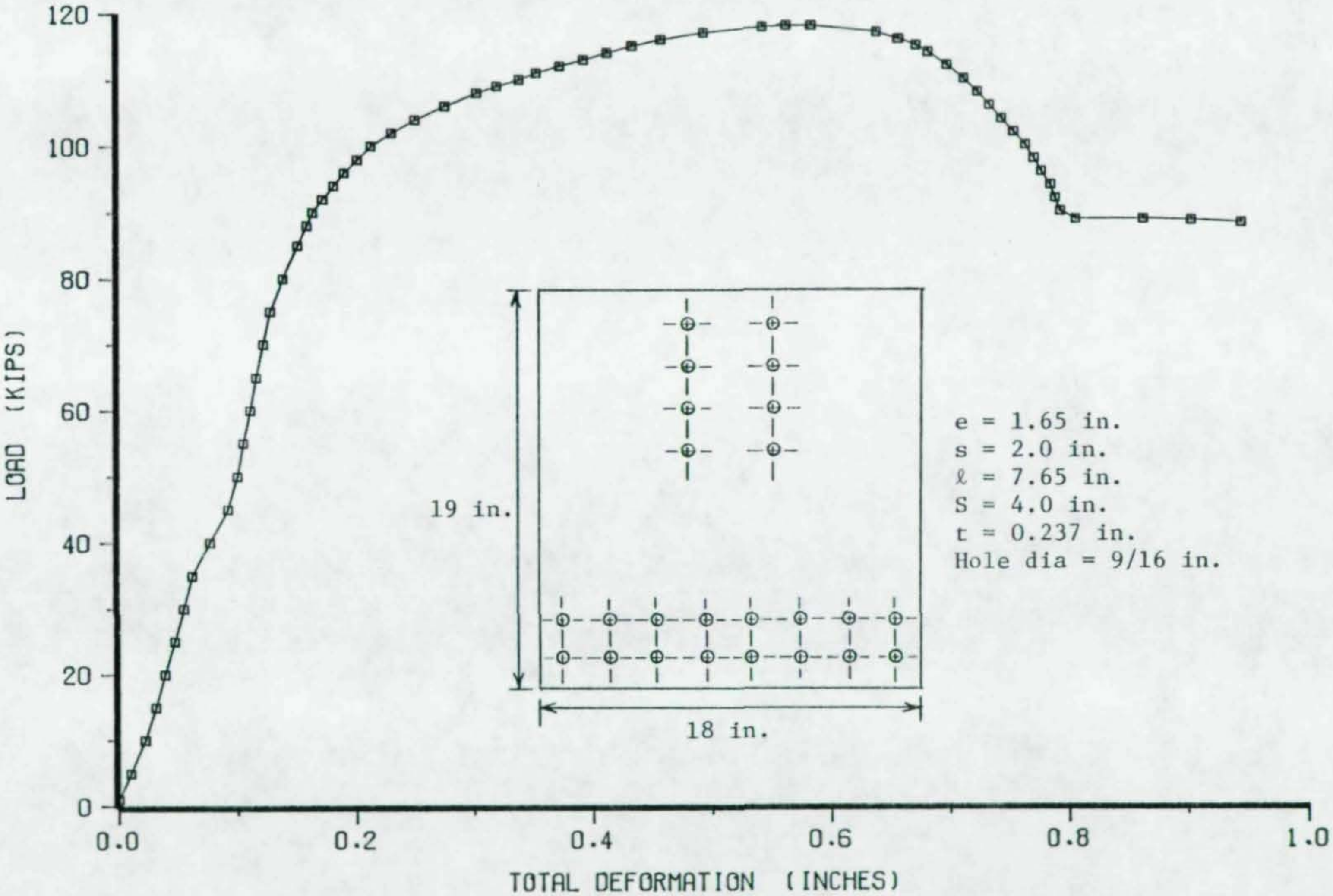

TEST PLATE 24. ULTIMATE STRENGTH = 118.0 KIPS.

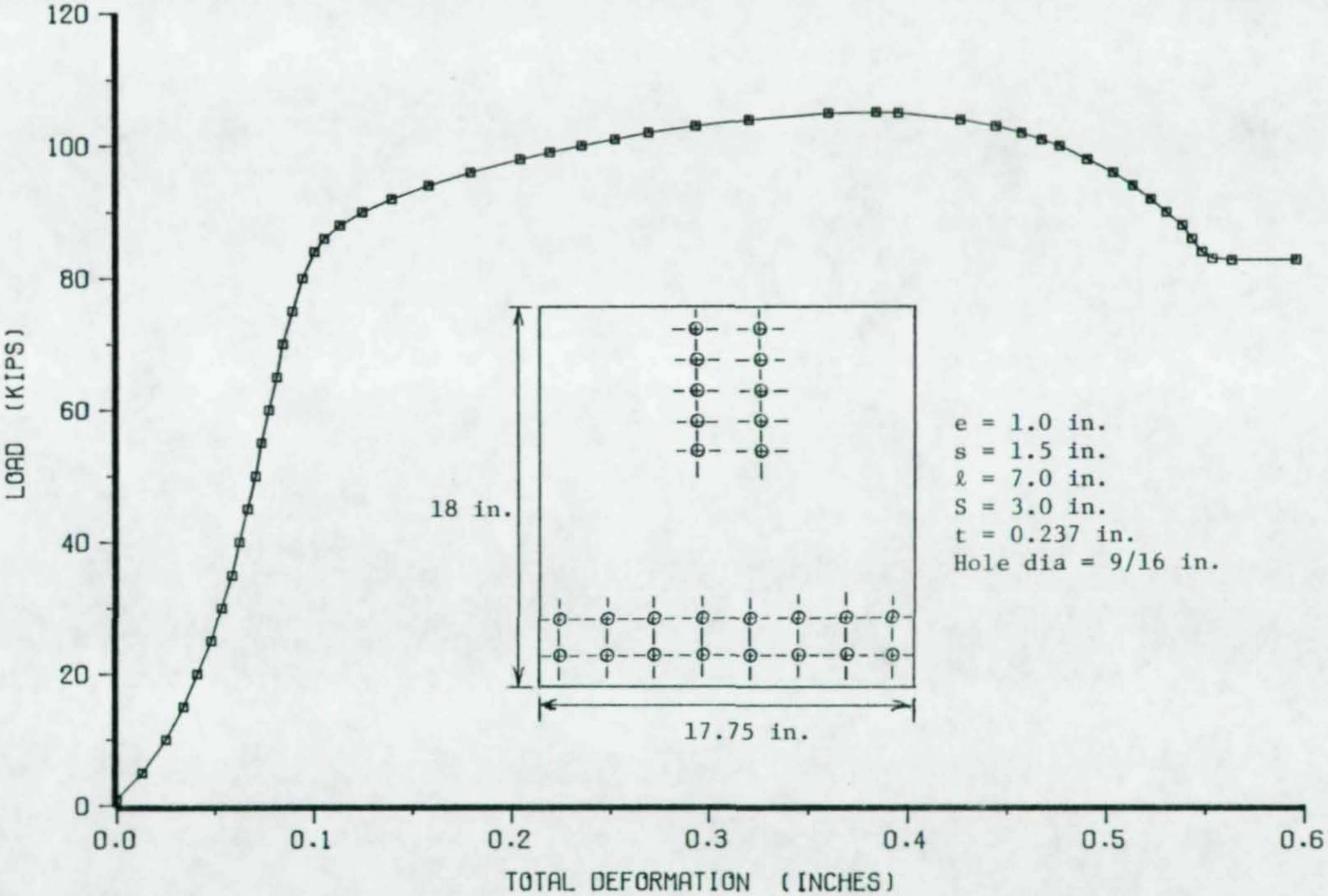

TEST PLATE 25. ULTIMATE STRENGTH = 105.1 KIPS.

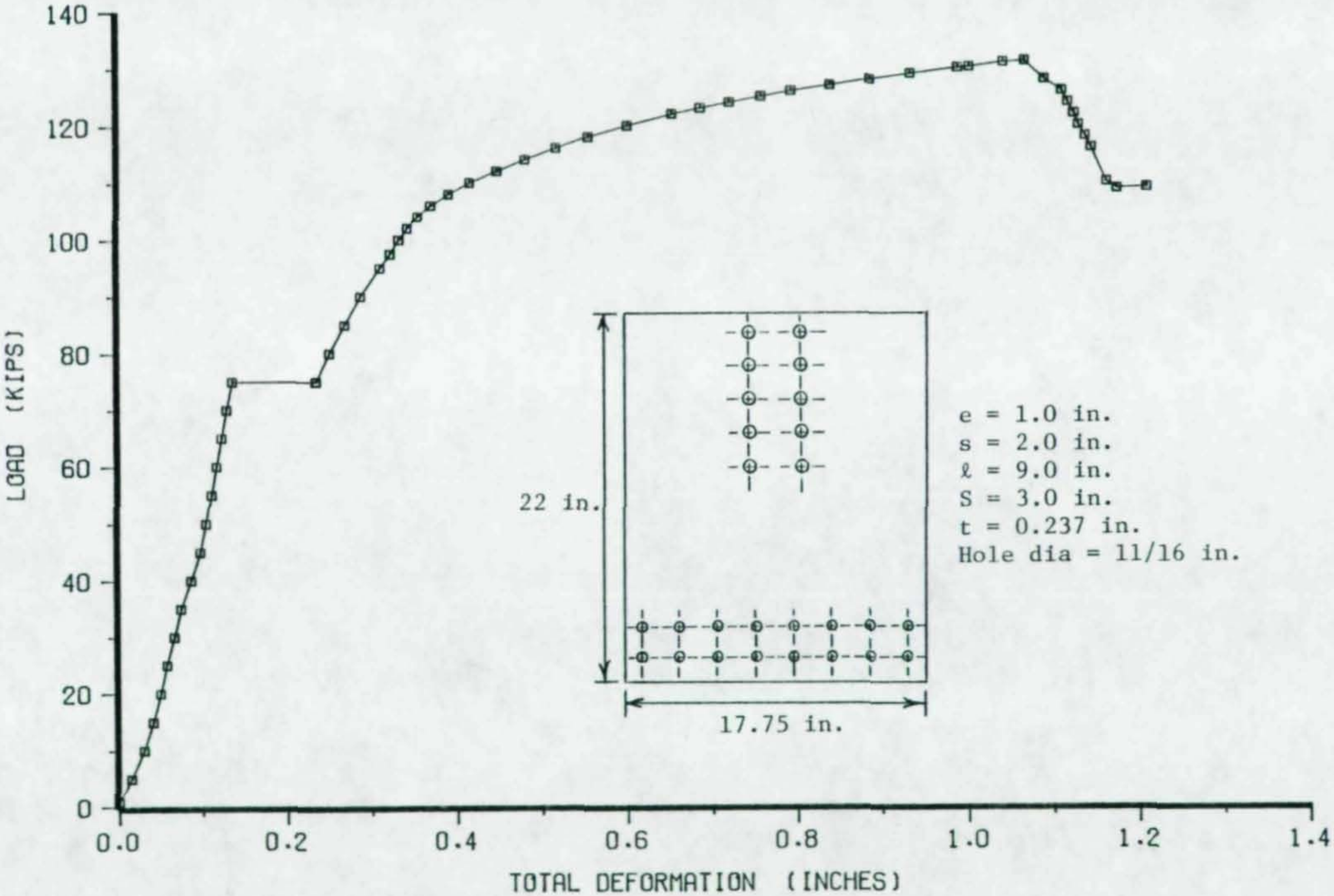

TEST PLATE 26. ULTIMATE STRENGTH = 131.2 KIPS.

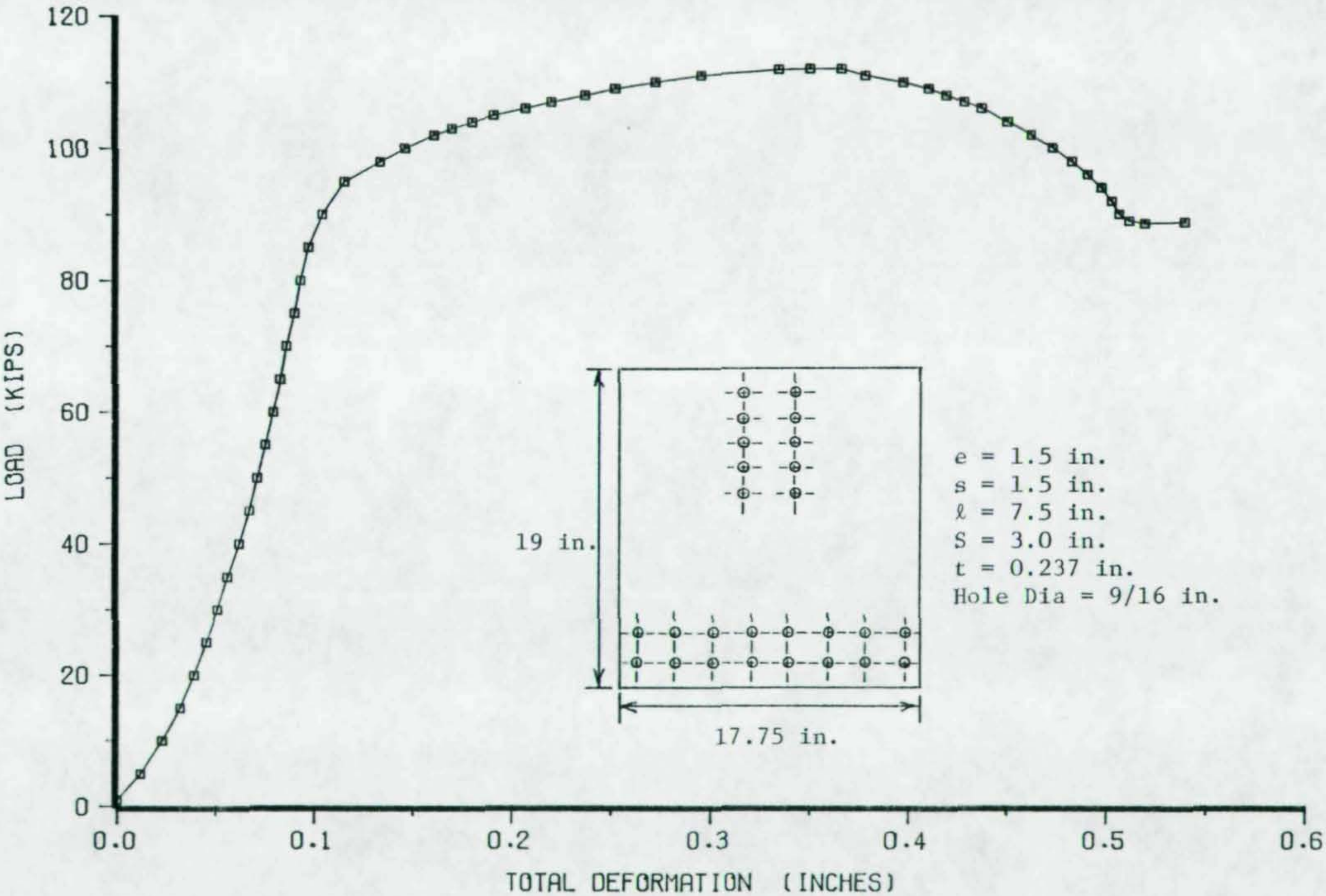

TEST PLATE 27. ULTIMATE STRENGTH = 112.0 KIPS.

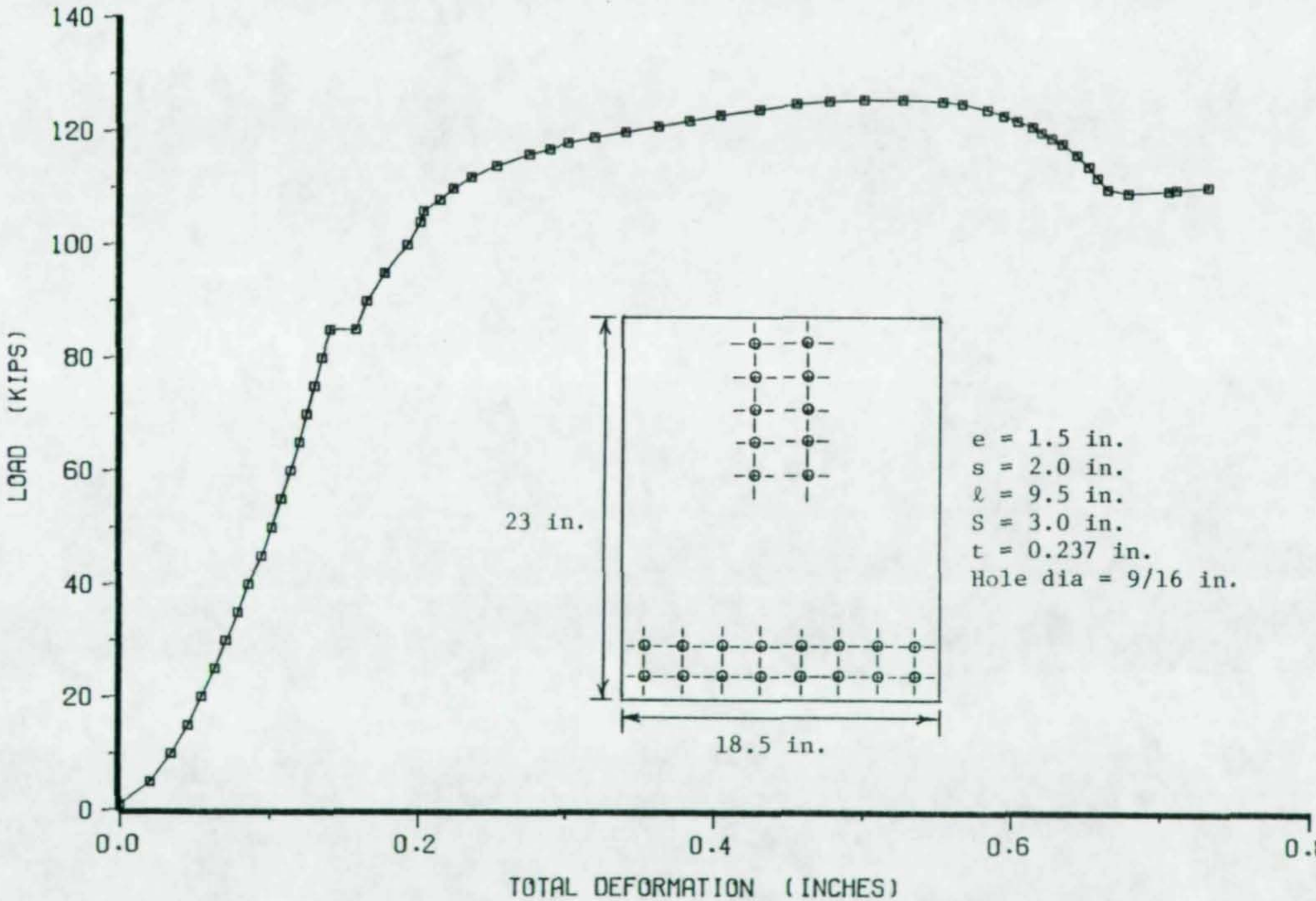

TEST PLATE 28. ULTIMATE STRENGTH = 125.7 KIPS.

APPENDIX B

PHOTOGRAPHS OF GUSSET PLATE TEST SPECIMENS AFTER TESTING FOR THE PRESENT STUDY

(Numbers in photos refer to gusset plate test number.)

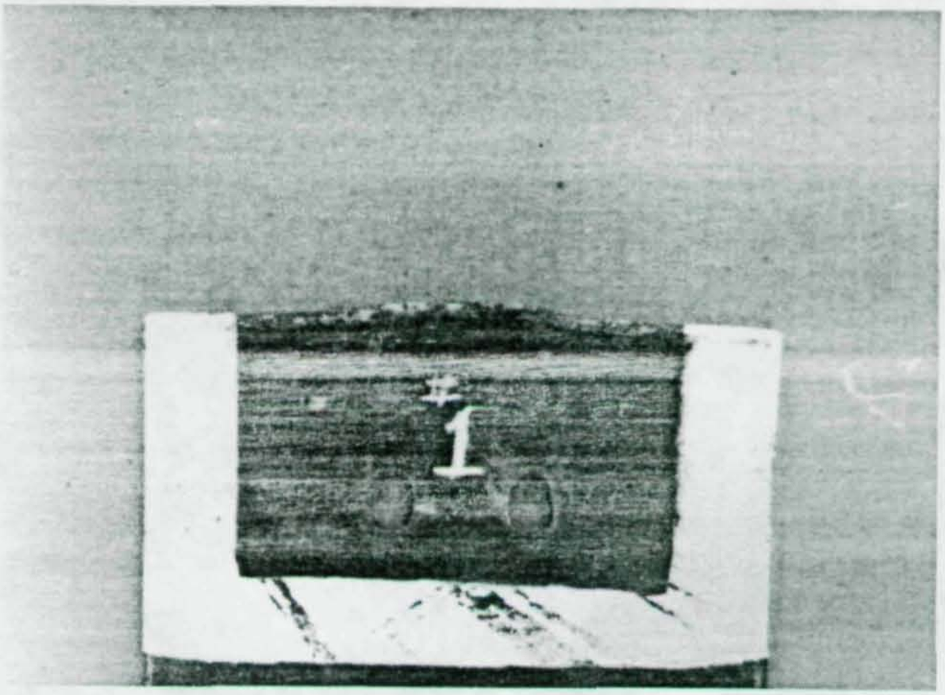
#
1

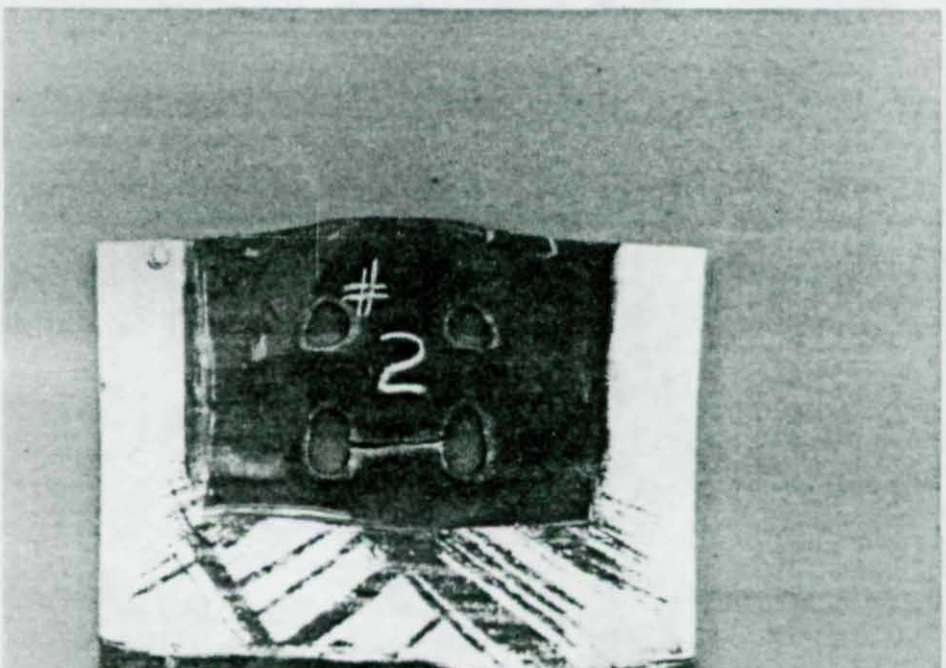
#
2

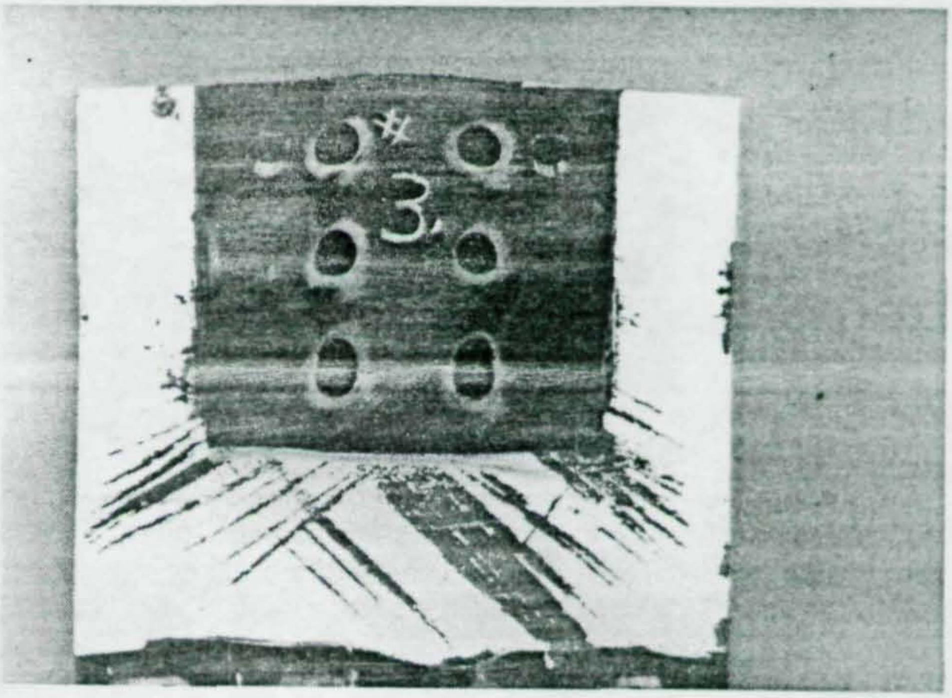
#3

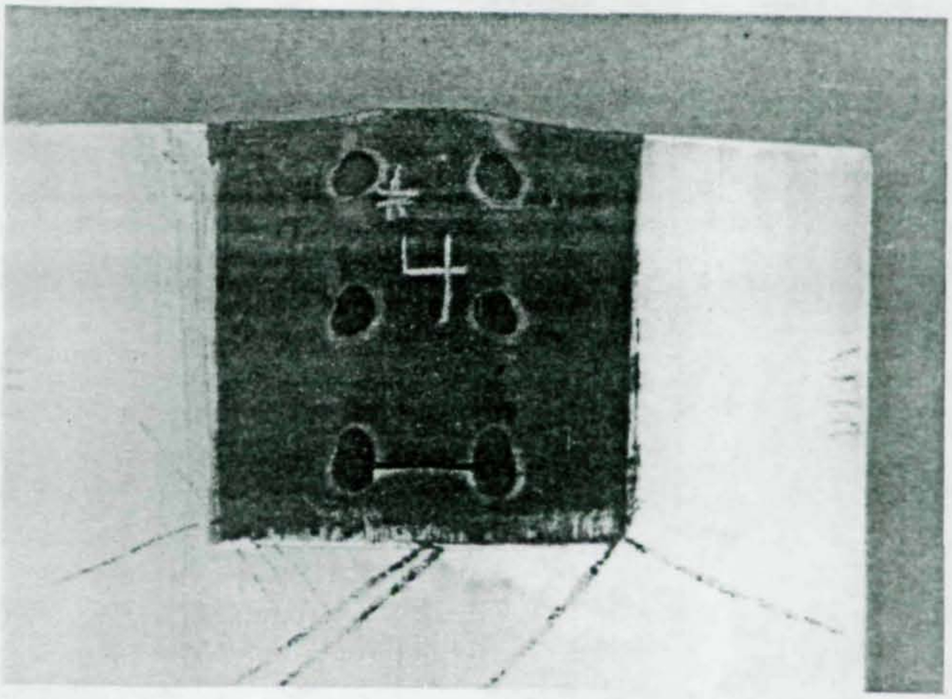
#4

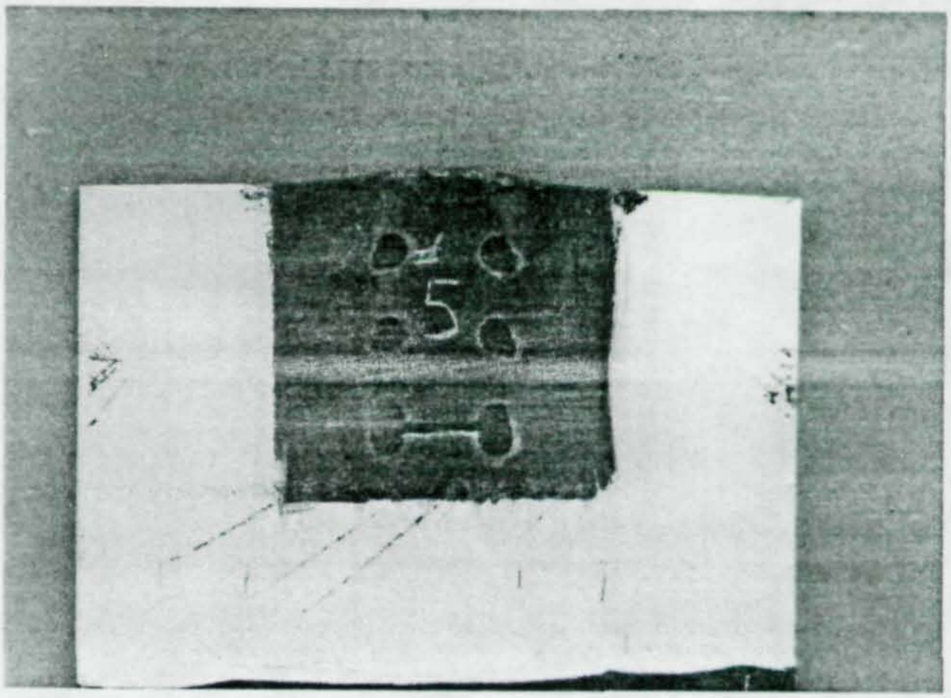
#5

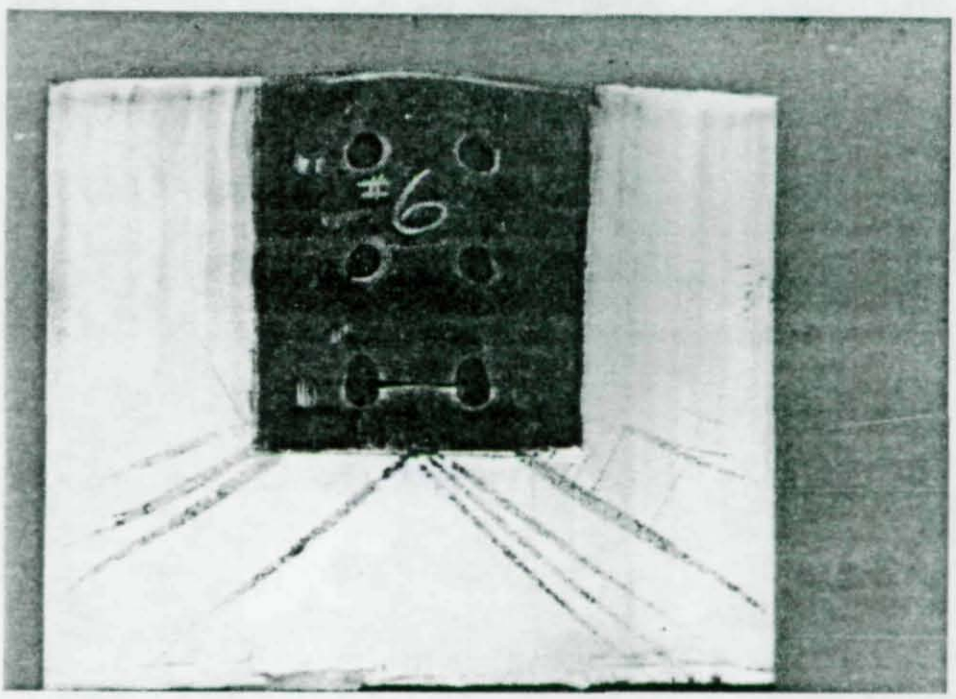
#6

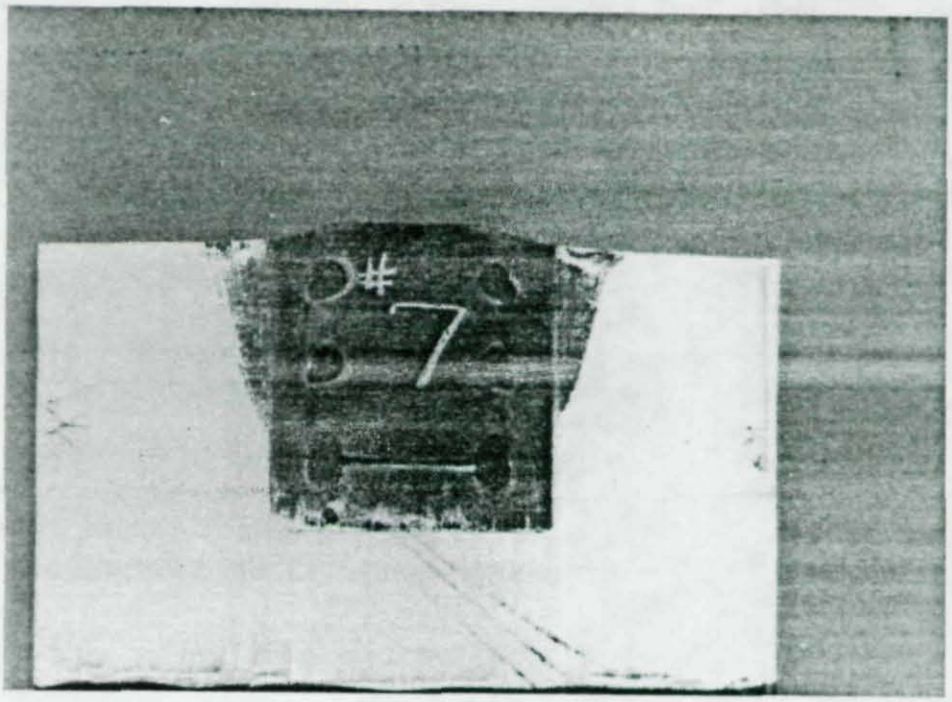
#7

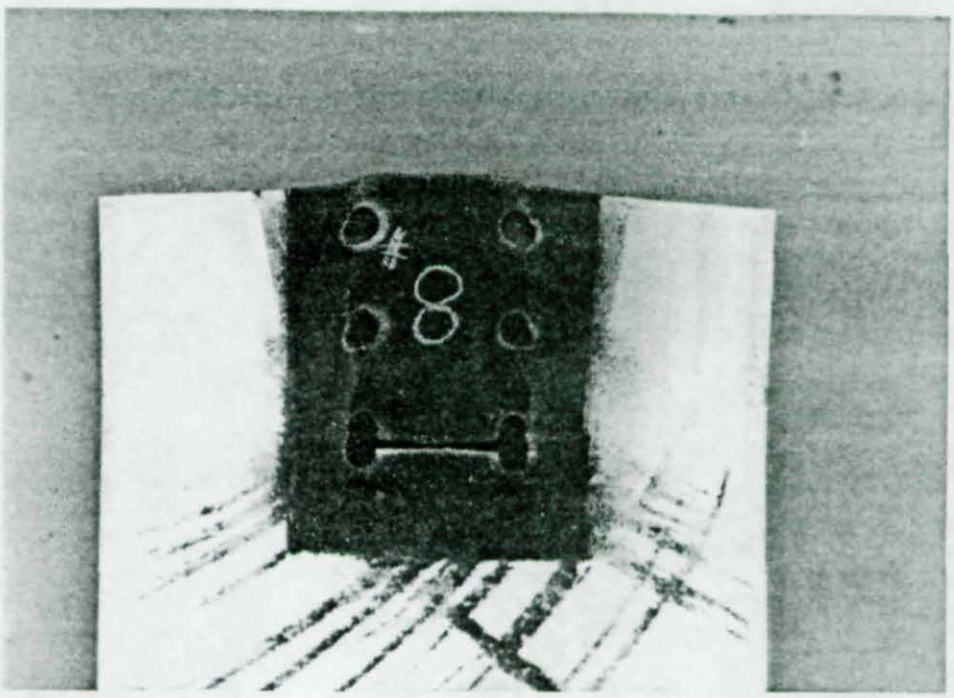
#8

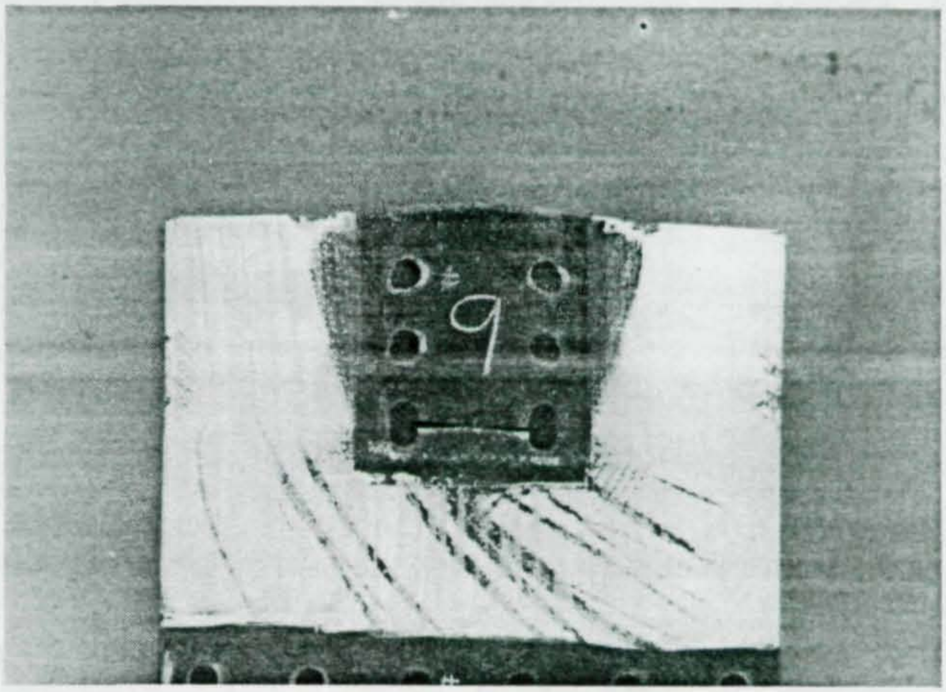
#9

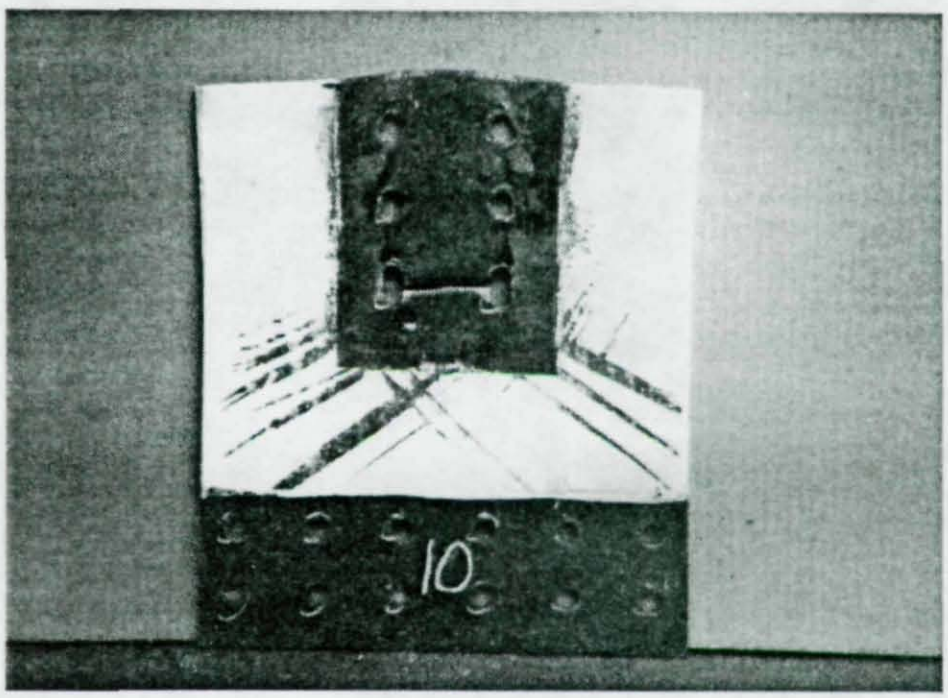
10

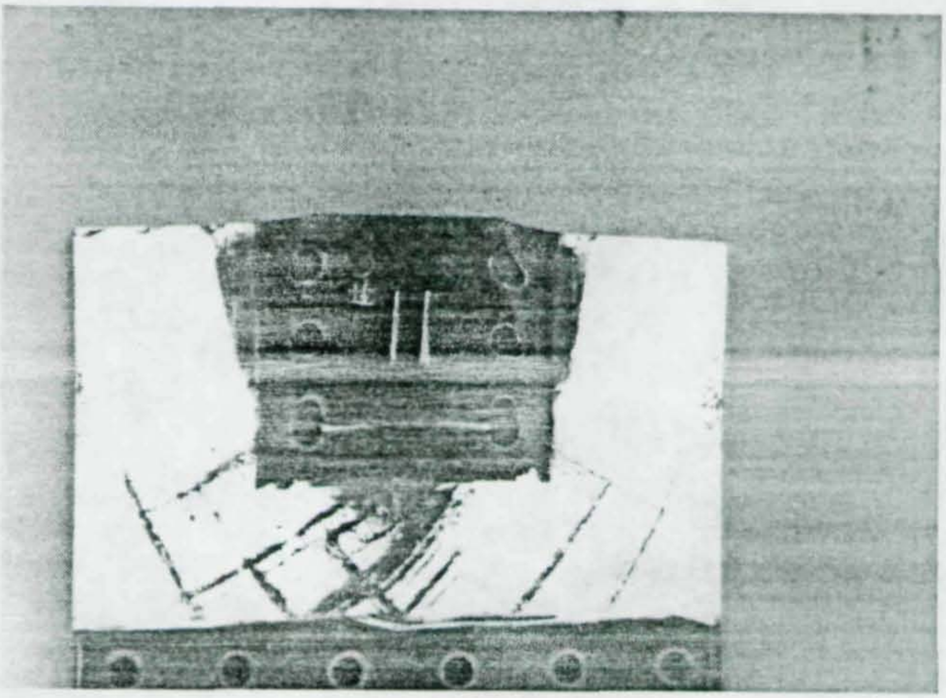
#11

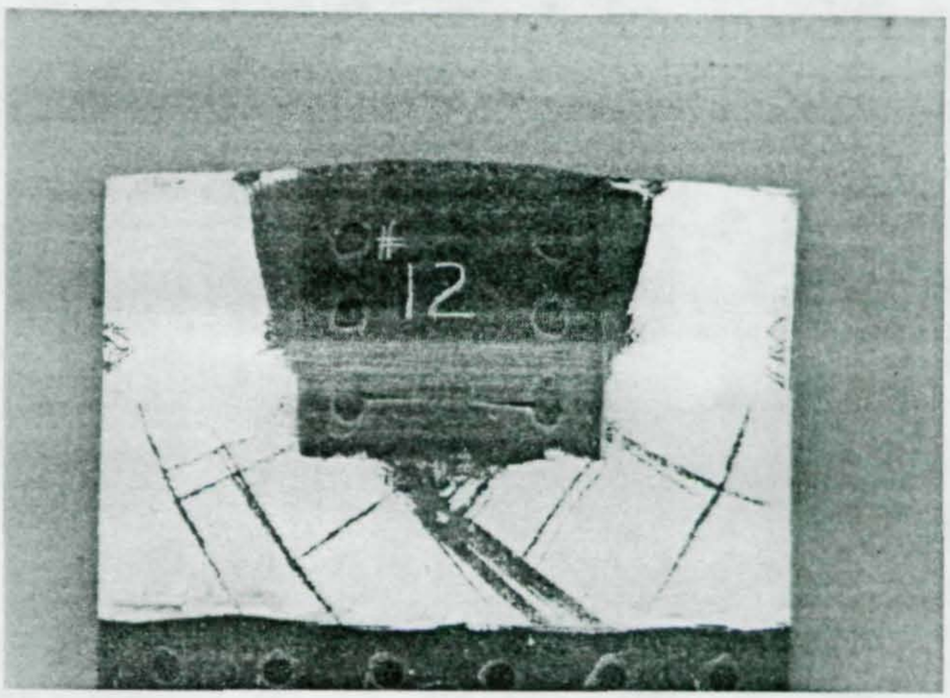
#12

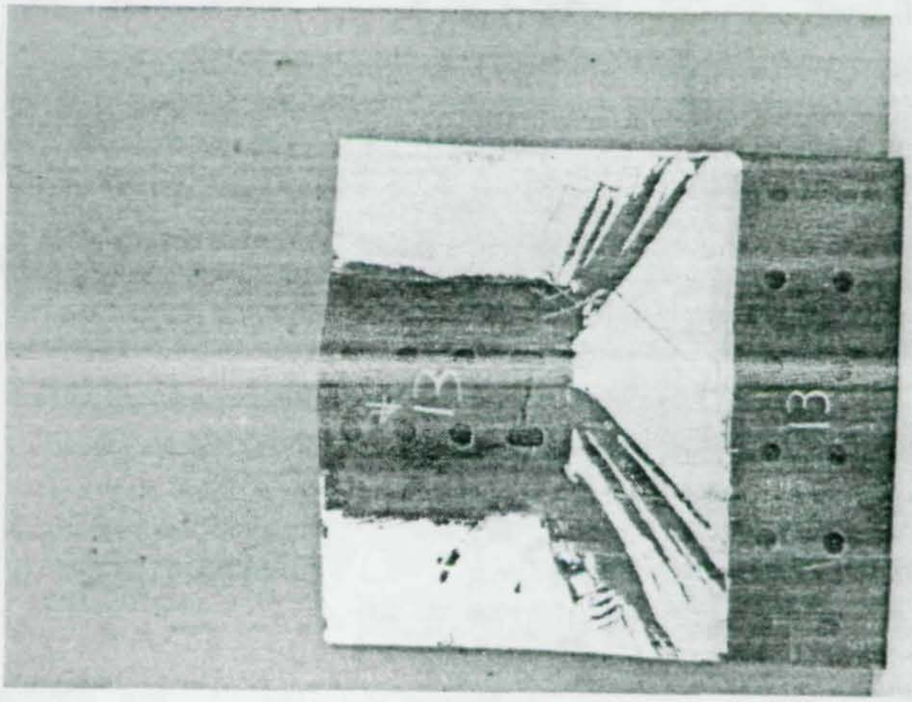
#13
13

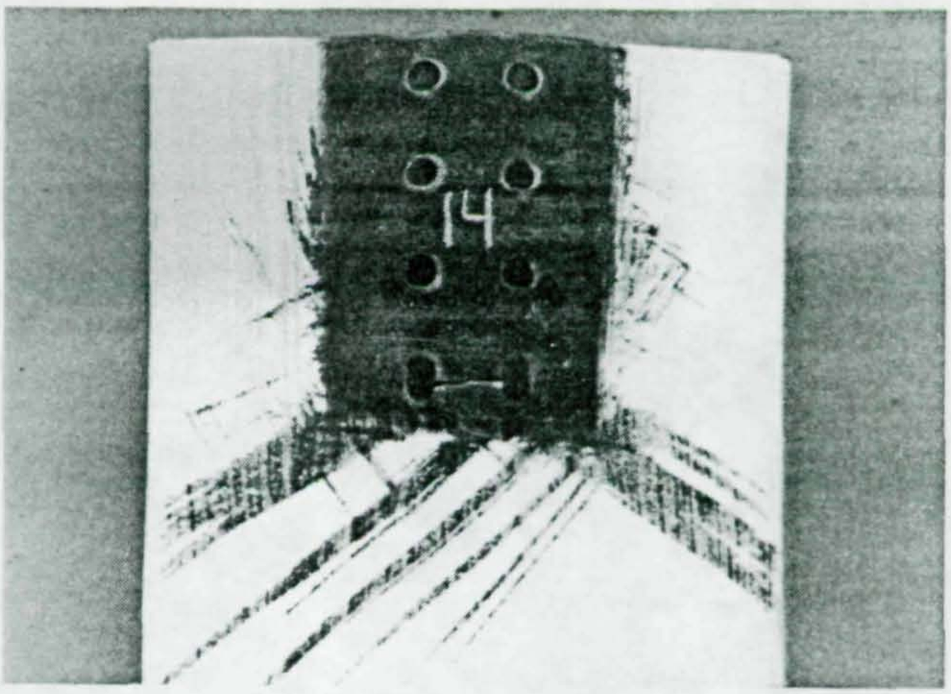
14

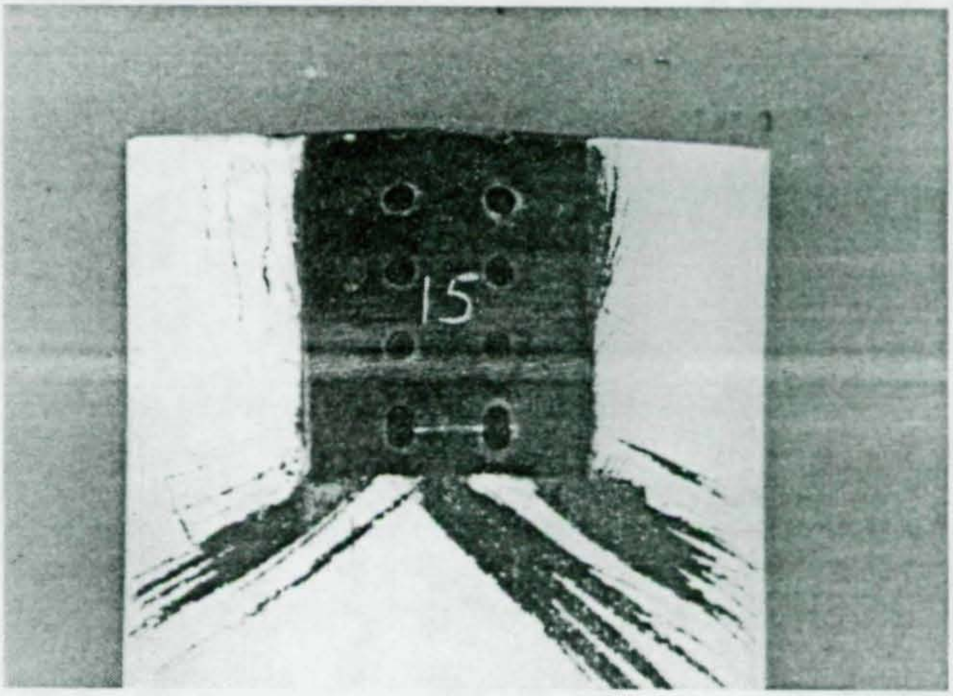
15

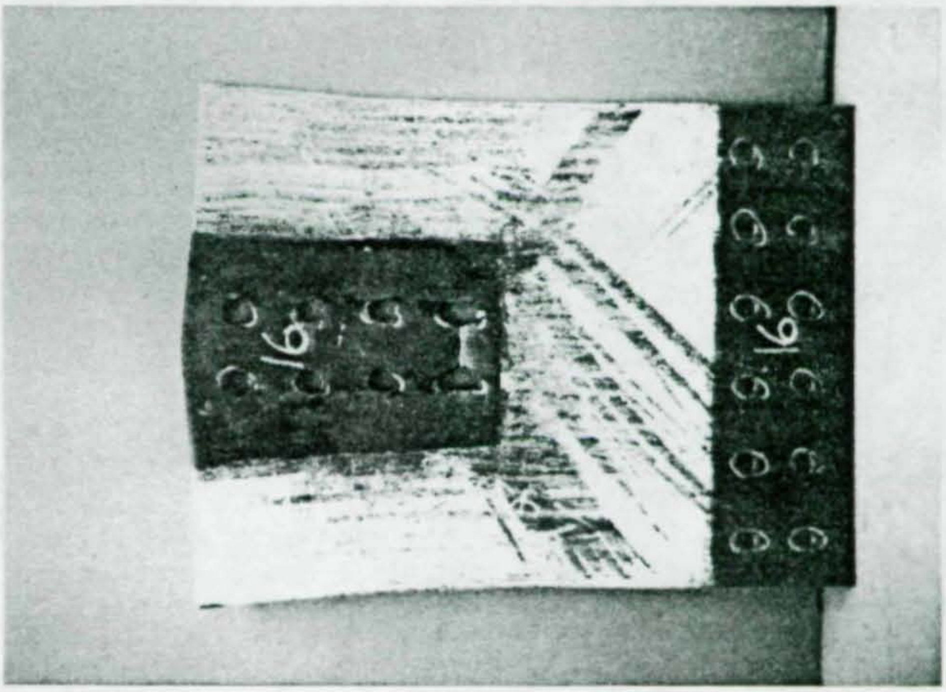
16

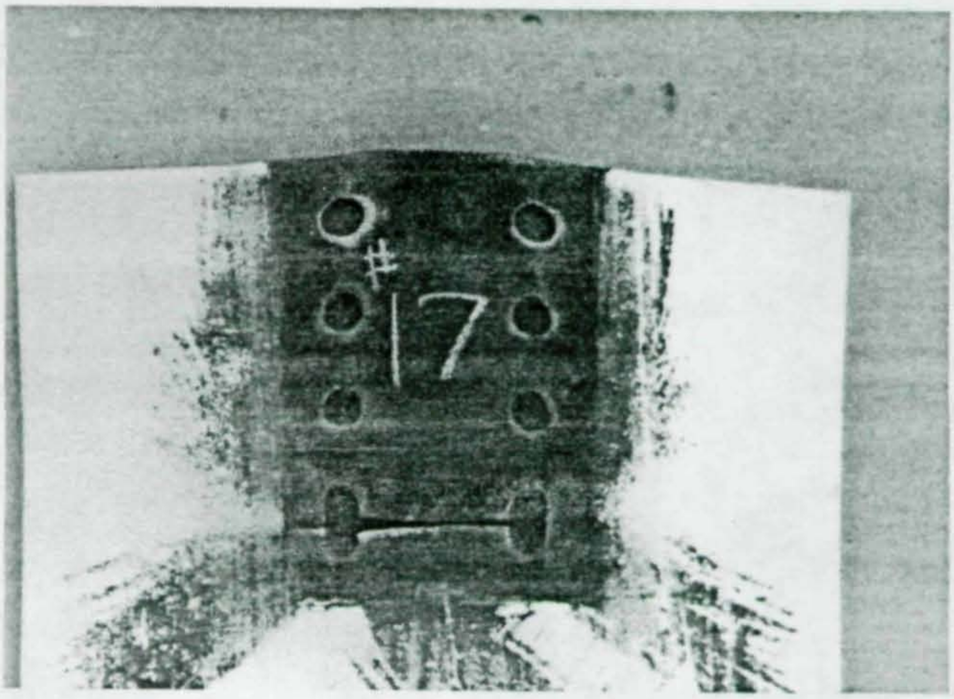
#17

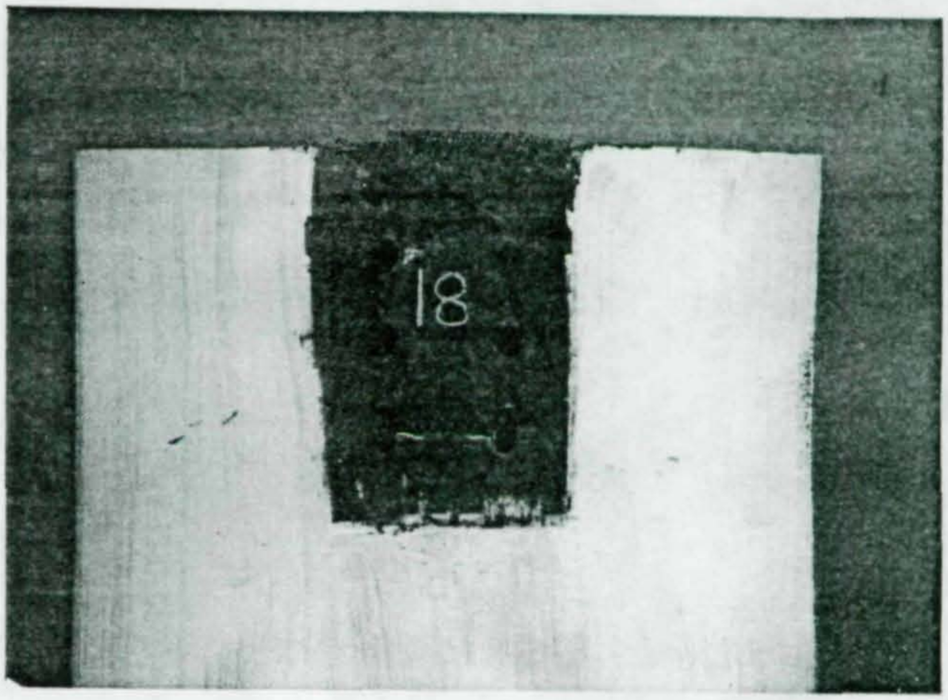
18

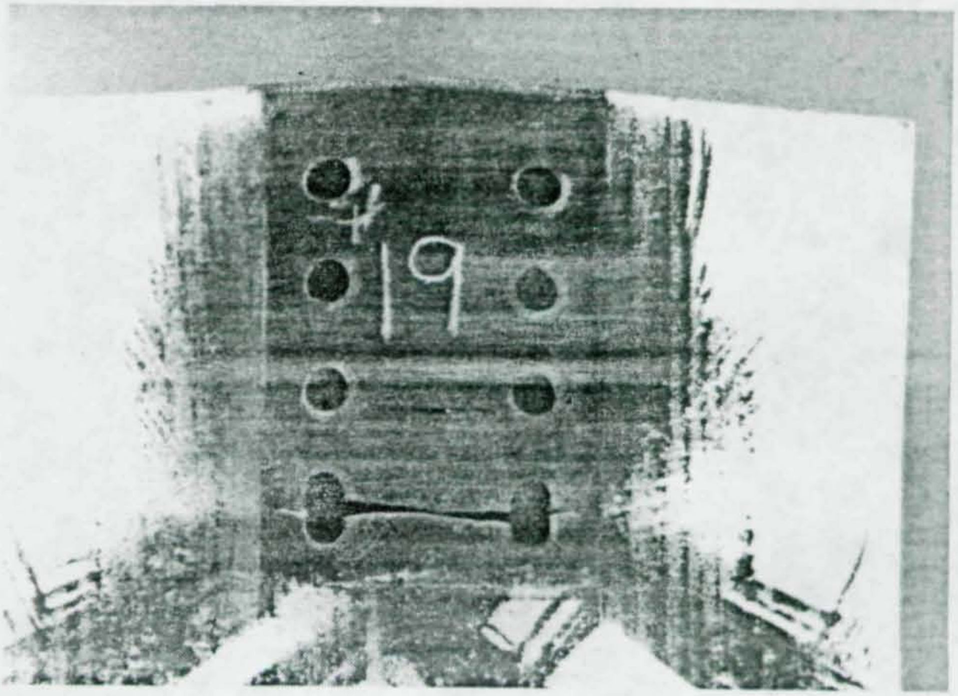
#19

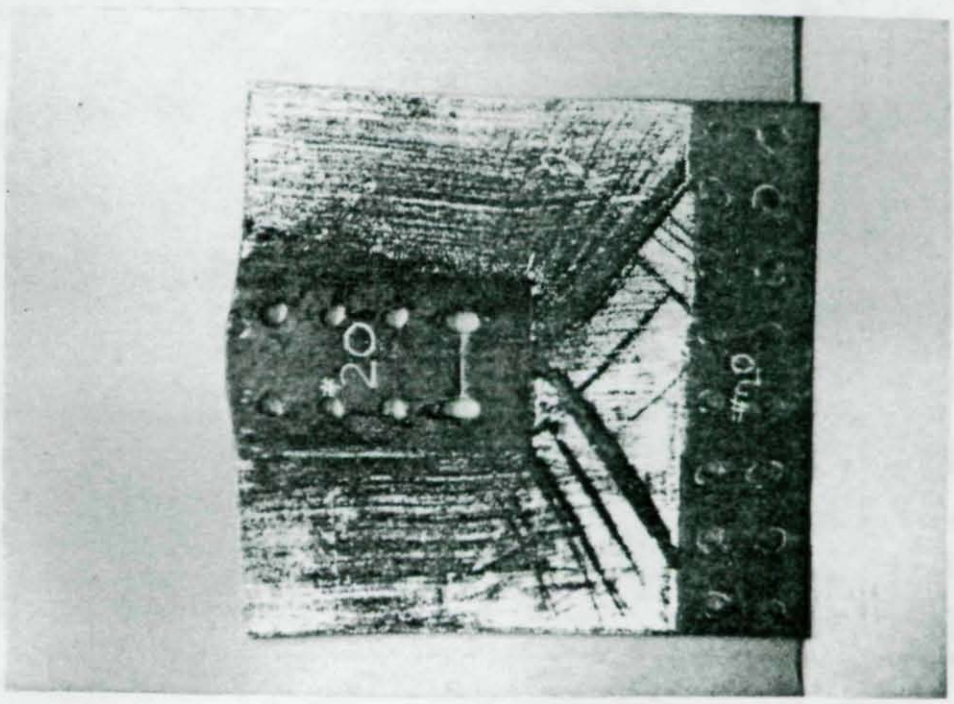
*20

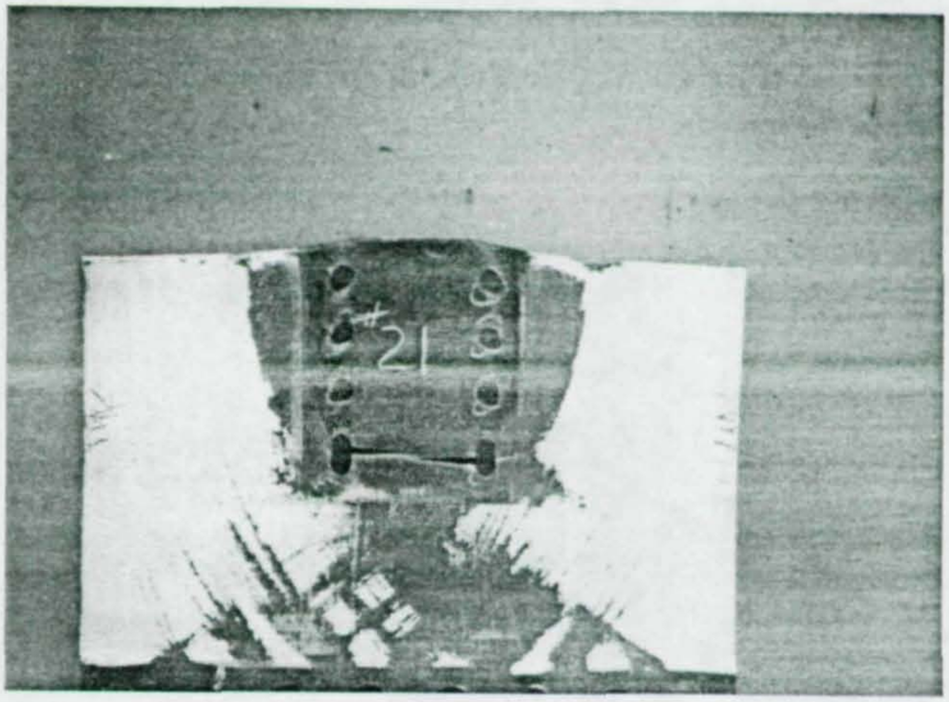
#21

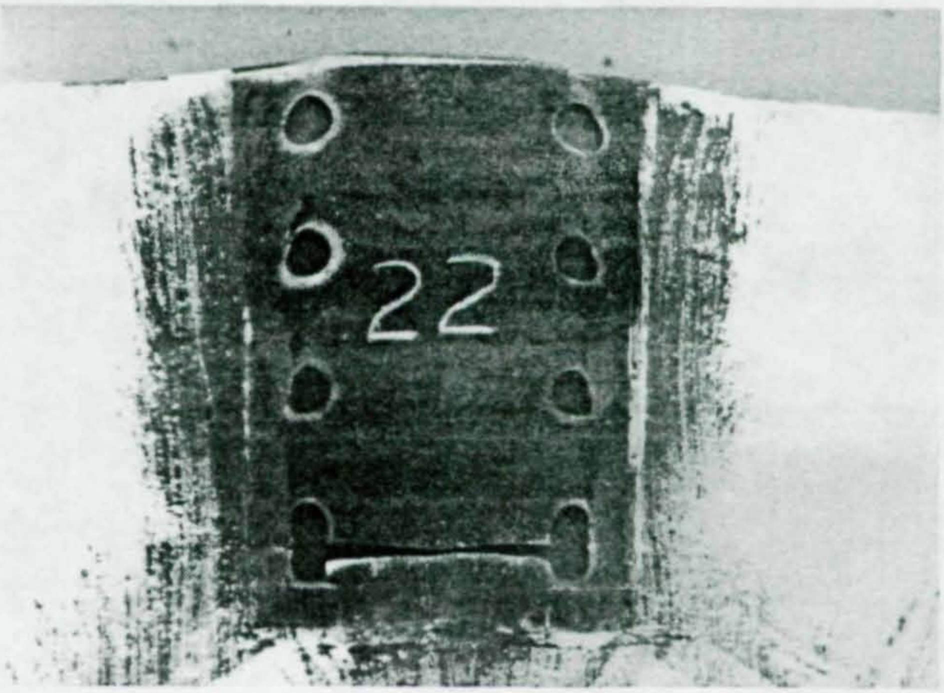
22

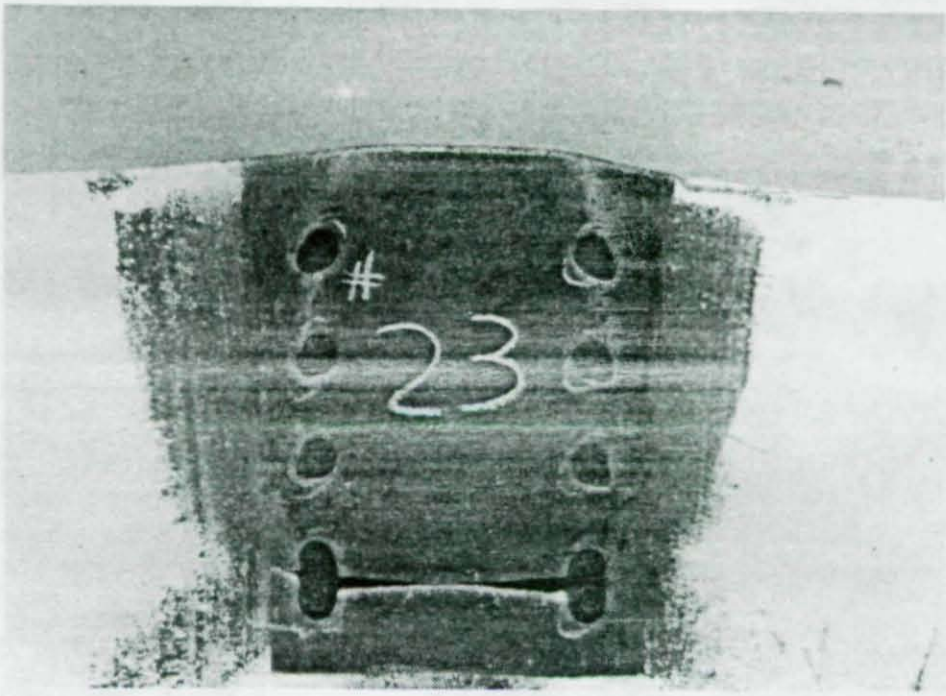
#
23

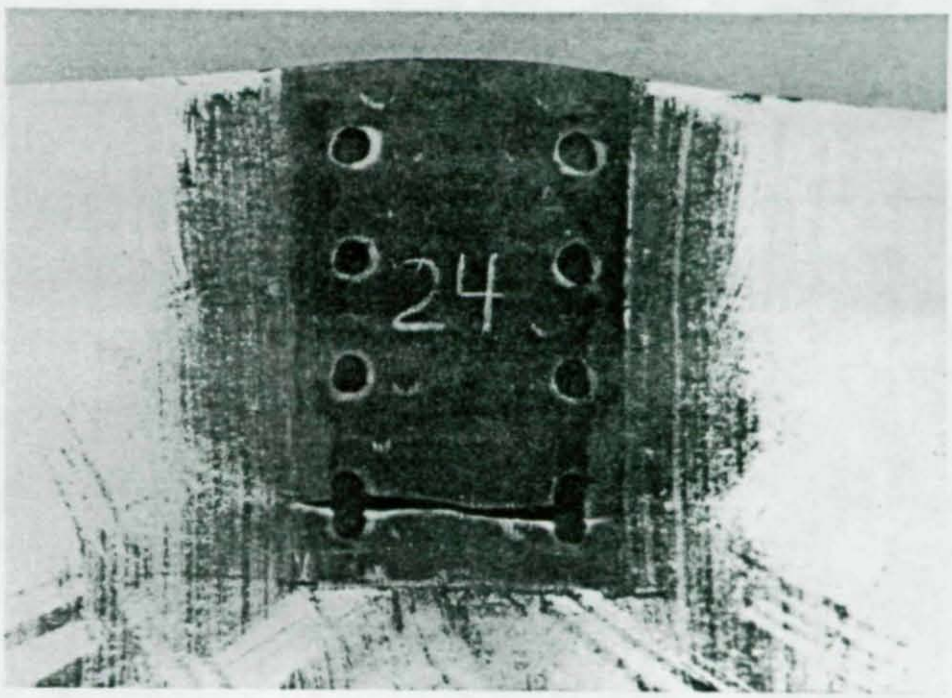
24

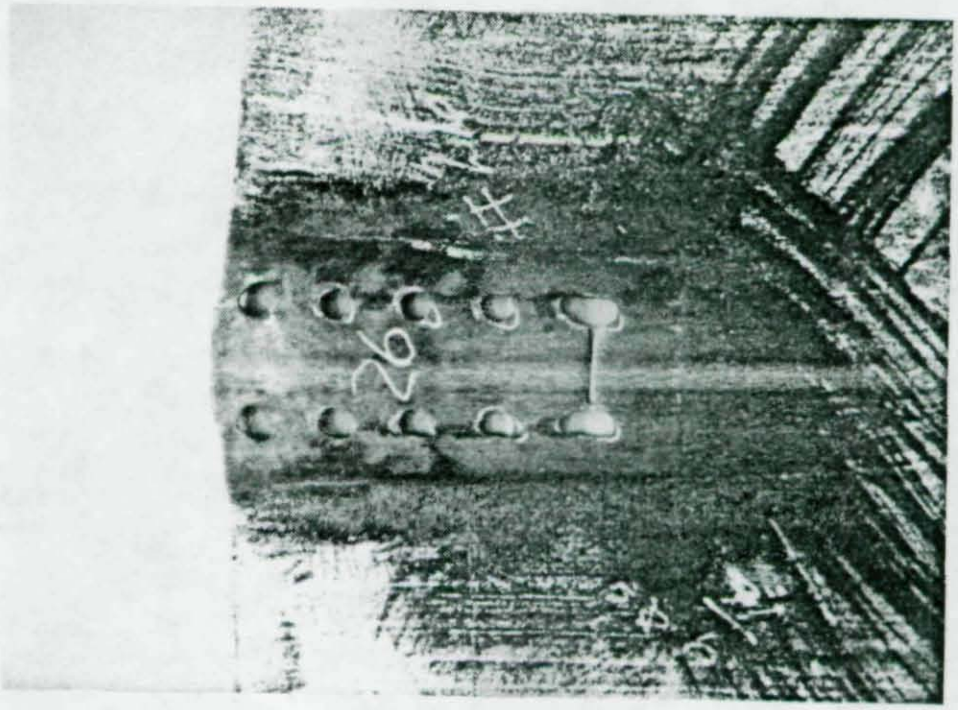
26

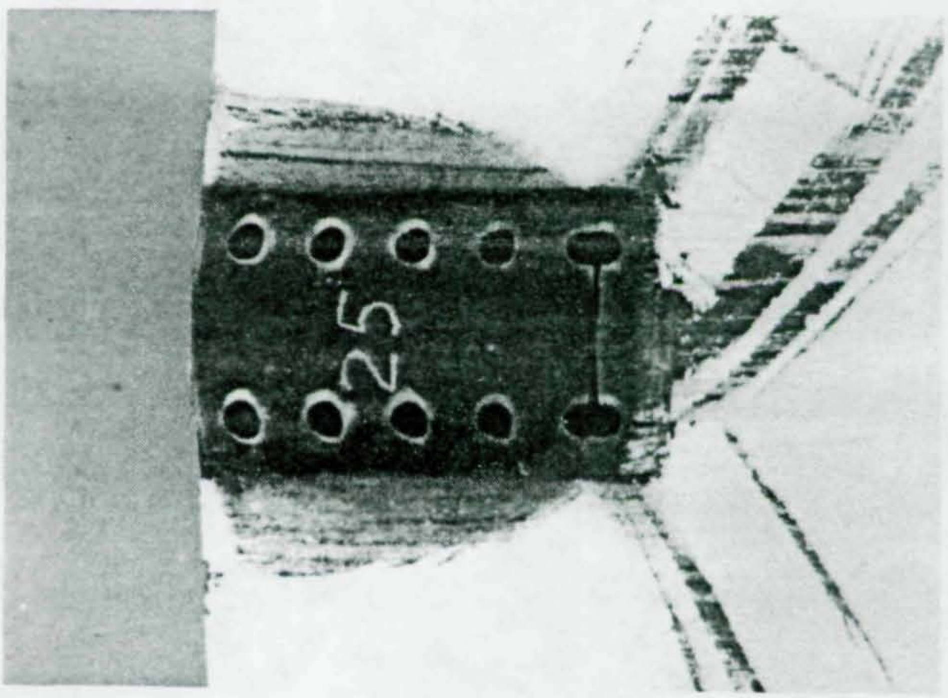
25

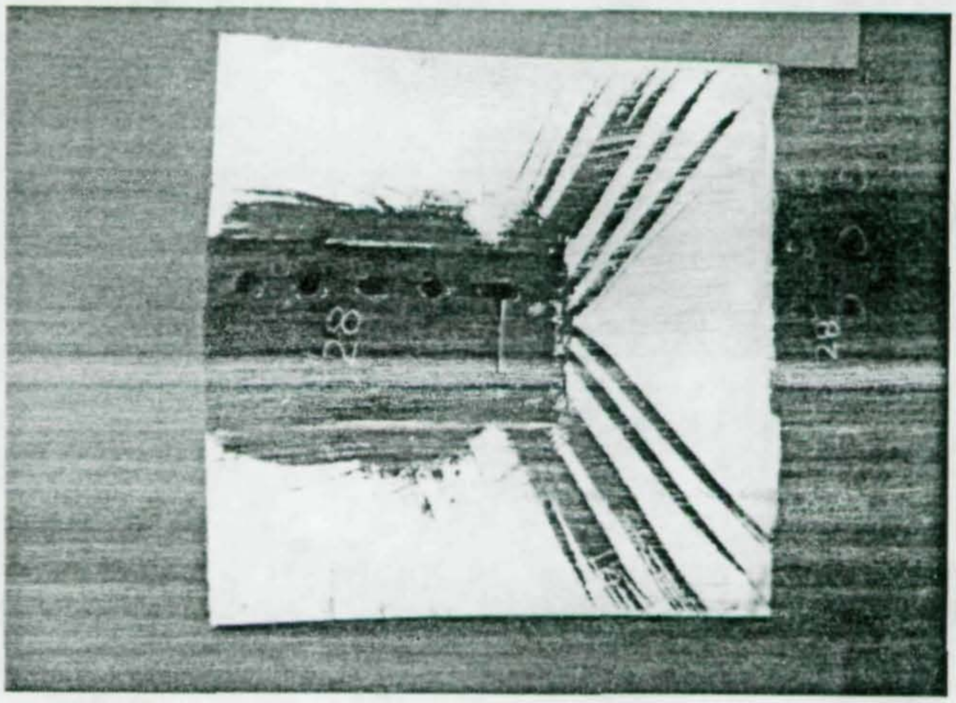

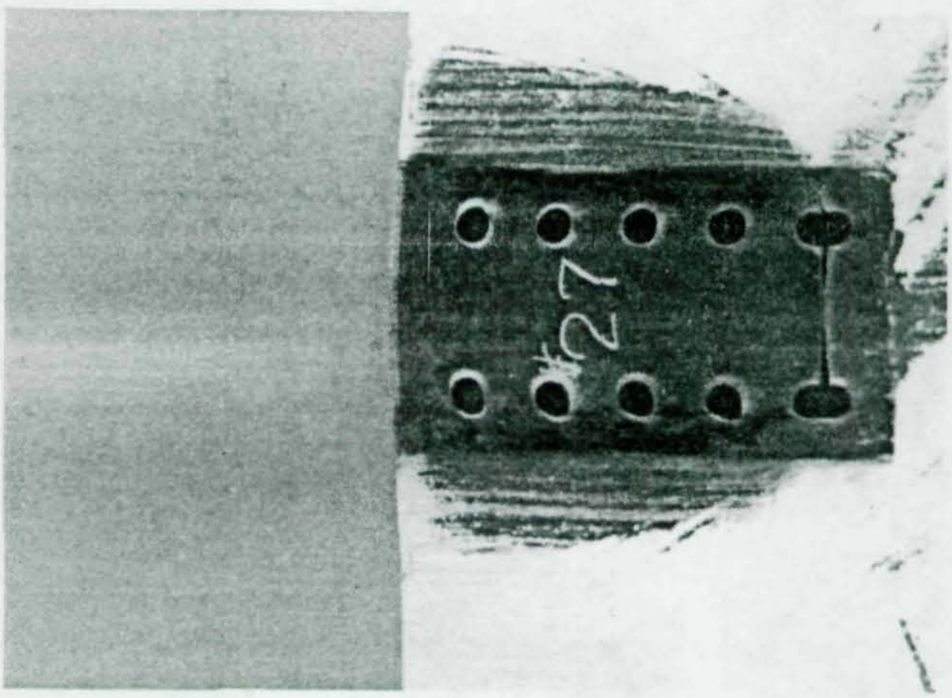

REFERENCES

1. Fisher, J. W. and Struik, J. H. A. Guide to Design Criteria for Bolted and Riveted Joints, John Wiley, New York, 1974.

2. Whitmore, R. E. Experimental Investigation of Stresses in Gusset Plates, University of Tennessee Engineering Experiment Station Bulletin 16, May 1952.

3. Irvan, W. G. Jr. Experimental Study of Primary Stresses in Gusset Plates of a Double Plane Pratt Truss, University of Kentucky Engineering Experiment Station Bulletin 46, December 1957.

4. Hardin, B. O. Experimental Investigation of the Primary Stress Distribution in the Gusset Plates of a Double Plane Pratt Truss Joint with Chord Splice at the Joint, University of Kentucky Engineering Experiment Station Bulletin 49, September 1958.

5. Birkemoe, P. C., Eubanks, R. A. and Munse, W. H. Distribution of Stresses and Partition of Loads in Gusseted Connections, Structural Research Series Report No. 343, Department of Civil Engineering, University of Illinois, Urbana, March 1969.

6. Vasarhelyi, D. D. "Tests of Gusset Plate Models," Journal of the Structural Division, ASCE, Vol. 97, ST2, February 1971, pp. 665-678.

7. Chesson, E. Jr. and Munse, W. H. "Behavior of Riveted Truss-Type Connections," ASCE Transactions, Vol. 123, 1958, pp. 1087-1128.

8. Chesson, E. Jr. and Munse, W. H. "Riveted and Bolted Joints: Truss-Type Tensile Connections," Journal of Structural Division, ASCE, Vol. 89, ST1, February 1963, pp. 67-106.

9. Bjorhovde, R. and Chakrabarti, S. K. Tests of Gusset Plate Connections, Research Report, Department of Civil Engineering and Engineering Mechanics, University of Arizona, Tucson, April 1983.

10. Struik, J. H. A. "Applications of Finite Element Analysis to Non-Linear Plane Stress Problems," Ph.D. Dissertation, Department of Civil Engineering, Lehigh University, Bethlehem, Pennsylvania, November 1972.

11. Rabern, D. A. "Stress, Strain, and Force Distribution in Gusset Plate Connections," M.S. Thesis, Department of Civil Engineering and Engineering Mechanics, University of Arizona, Tucson, April 1983.

12. Manual of Steel Construction, 8th Edition, American Institute of Steel Construction, Chicago, Illinois, 1980.

13. Steel Structures for Buildings -- Limit States Design, CSA Standard S16.1-1974, Canadian Standards Association, Rexdale, Ontario, December 1974.

14. Birkemoe, P. C. and Gilmor, M. I. "Behavior of Bearing Critical Double-Angle Beam Connections," Engineering Journal, AISC, Vol. 15, No. 4, Fourth Quarter, 1978, pp. 109-115.

15. Yura, J. A., Birkemoe, P. C., and Ricles, J. C. "Double Angle Beam Web Connections: An Experimental Study," Journal of the Structural Division, ASCE, Vol. 108, No ST2, February 1982, pp. 311-325.

16. Ricles, J. M. and Yura, J. A. "Strength of Double-Row Bolted-Web Connections," Journal of the Structural Division, ASCE, Vol. 109, No. 1, January 1983, pp. 126-142.

17. Richard, R. M., Rabern, D. A., Hormby, D. E., and Williams, G. C. "Analytical Models for Steel Connections," Behavior of Metal Structures, Proceedings of the W. H. Munse Symposium, Edited by W. J. Hall and M. P. Gaus, ASCE, May 17, 1983, pp. 128-155.

18. Annual Book of ASTM Standards, ASTM, Section 1, Vol. 01.04, Easton, Maryland, 1984.

19. Galambos, T. V. "Load and Resistance Factor Design," Engineering Journal, AISC, Third Quarter, 1981, pp. 74-82.

20. Galambos, T. V. and Ravindra, M. K. "Load and Resistance Factor Design for Steel," Journal of the Structural Division, ASCE, Vol. 104, No. ST9, September 1978, pp. 1337-1353.

21. Galambos, T. V. and Ravindra, M. K. "Properties of Steel for Use In LRFD," Journal of the Structural Division, ASCE, Vol. 104, No. ST9, September 1978, pp. 1459-1468.

22. Fisher, J. W. et al. "Load and Resistance Factor Design Criteria for Connectors," Journal of Structural Division, ASCE, Vol. 104, No. ST9, September 1978, pp. 1427-1441.

23. Proposed Load and Resistance Factor Design Specification for Structural Steel Buildings, American Institute of Steel Construction, Chicago, Illinois, September 1, 1983.